2013-01-25

Targeting the PI3K and Ras Signal Transduction Pathways in a Murine Model of Osteolytic Breast Cancer Metastasis

Bosma, Nicholas

UNIVERSITY OF CALGARY

"Targeting the PI3K and Ras Signal Transduction Pathways in a Murine Model of Osteolytic Breast Cancer Metastasis"

by

Nicholas Adam Joseph Bosma

A THESIS

SUBMITTED TO THE FACULTY OF GRADUATE STUDIES

IN PARTIAL FULFILMENT OF THE REQUIREMENTS FOR THE

DEGREE OF MASTER OF SCIENCE

DEPARTMENT OF BIOCHEMISTRY AND MOLECULAR BIOLOGY

CALGARY, ALBERTA

JANUARY 2013

Abstract

Bone metastasis frequently occurs in patients with advanced breast cancer, and leads to widespread bone destruction. Aberrant activation of the PI3K and Ras-MAPK pathways are consistently observed in high-grade metastatic breast cancers, making these pathways attractive targets for therapeutic intervention. Complex signal crosstalk between these pathways is implicated in cancer cell perpetuation; therefore, dual inhibition should theoretically provide maximal targeting. The PI3K and MEK inhibitors, PX866 and AZD6244 were employed to investigate the therapeutic potential in an *in vivo* model of MDA-MB-231-EGFP/Luc2 human breast cancer osteolytic metastases. PI3K inhibition did not directly affect bone-colonized cancer cells, however, it demonstrated an attenuation of bone loss, whereas MEK inhibition resulted in a significant reduction of both tumor growth and osteolysis. Simultaneous inhibition of PI3K and MEK resulted in a reduction of tumor growth, but paradoxically exhibited an exacerbation of bone damage. These findings suggest that MEK inhibition alone may be a valuable additional treatment for breast cancer osteolytic metastasis.

Preface

It is apparent that cancer cells have developed sophisticated mechanisms to sustain proliferative expansion and survival, even in the face of toxic stimuli. Therefore, strategies that target the aberrant molecular machinery of cancer cells will be essential for future therapeutics. Signal crosstalk in aberrantly activated signal transduction pathways is a prime example of this. Furthermore, in order to investigate the therapeutic potential of certain agents relevant to human malignancies, the specific micro-environment of the primary or metastatic niche also needs to be taken into consideration. Therefore, this study employed small-molecule inhibitors to target potential signal pathway crosstalk in an *in vivo* model that recapitulates many of the processes in osteolytic breast cancer metastasis. Systematic investigation into molecular mechanisms that govern cancer cell fate, and the development of more accurate *in vivo* models will be essential for the progression of effective treatment modalities.

Acknowledgements

This thesis would not have been possible without the guidance and support of several individuals who have contributed in one form or another. First and foremost, I would like to thank my supervisor Dr. Frank Jirik. His vast repository of knowledge and endless assistance and direction was a prominent reason for my success.

I would also like to acknowledge all of my lab members, as they all contributed to this work in one way or another. Everyone's contribution was invaluable.

Dr. Helen Buie helped with much of the microCT work, and was an extreme asset to the completion and success of this work.

I would also like to acknowledge Leona Barclay's vast contribution in the sectioning and staining of the majority of histology slides.

My committee members, Dr. Shirin Bonni and Dr. Steven Boyd also provided a tremendous amount of influence and supportive guidance through the learning process of this research.

Lastly, I would like to acknowledge the tremendous influence my family and friends provided throughout. They all taught me to strive for nothing but perfection. I would especially like to thank my parents and Laura Evans for their indispensable support that motivated my passionate ambition for success.

Dedication

I would like to dedicate the work of this thesis to the memory of my grandmother and grandfather, who passed away from breast cancer and pancreatic cancer, respectively. Having experienced the detrimental power that cancer delivers has been a profound influence in my desire to uncover effective strategies for therapeutic opportunities.

They will be forever missed, but never forgotten.

Table of Contents

List of Figures and Illustrations

List of Symbols, Abbreviations and Nomenclature

Symbol	Definition
µCT	Micro-computed tomography
Akt	Acutely transforming retrovirus AKT8 in rodent T cell lymphoma
BLI	Bioluminescence imaging
BMD	Bone mineral density
BMP	Bone morphometric protein
BS	Bone surface
BSA	Bovine serum albumin
BV	Bone volume
CK17	Cytokeratin 17
CK5	Cytokeratin 5
ConnD	Connectivity density
CSF-1	Colony stimulating factor-1
CTR	Calcitonin receptor
CtTh	Cortical thickness
DMEM	Dulbeco's modified Eagle's medium
EDTA	Ethylenediaminetetraacetic acid
EGF	Epidermal growth factor
EGFP	Enhanced green fluorescent protein
EGFR	Epidermal growth factor receptor
EMT	Epithelial-mesenchymal transition
ER	Estrogen receptor
ERK	Extraceullar-regulated kinase
EtOH	Ethanol
FACS	Fluorescent activated cell sorting
FBS	Fetal bovine serum
FOXO	Forkhead homeobox type O
G-CSF	Granulocyte colony-stimulating factor
GDP	Guanosine diphosphate
GNEF	Guanine nucleotide exchange factor
GEP	Gene expression profile
GM-CSF	Granulocyte macrophage colony-stimulating factor
GPCR	G-protein coupled receptor
GSK-3β	Glycogen synthase kinase-3 beta
GTP	Guanosine triphosphate
HA	Hydroxyapatite
HER2	Human epidermal growth factor receptor-2

HRP	Horseradish peroxidase
IC	Intracardiac
IGF-1	Insulin-like growth factor-1
IHC	Immunohistochemistry
IL-8	Interleukin-8
IL-11	Interleukin-11
IP10	Interferon gamma-induced protein-10
Luc2	Luciferase2
MAPK	Mitogen activated protein kinase
MCP-1	Monocytic chemotactic protein-1
MEK	Mitogen-activated protein kinase/extracellular signal-regulated kinase kinase
MMP9	Matrix metalloproteinase 9
mTOR	Mammalian target of rapamycin
NFκB	Nuclear factor κ B
OPG	Osteoprotegerin
PA	Phosphatidic acid
PBS	Phosphate buffered saline
PCR	Polymerase chain reaction
PDGF	Platelet derived growth factor
PDK1	Phosphoinositide-dependent kinase-1
PGE_2	Prostaglandin E_2
PH	Pleckstrin homology (domain)
PI	Propidium iodide
PI3K	Phosphatidylinositol 3-kinase
PIP_2	Phosphotidylinositol 4,5-bisphosphate
PIP_3	Phosphotidylinositol 3,4,5-trisphosphate
PLD	Phospholipase D
PR	Progesterone receptor
PTEN	Phosphatase and tensin homolog deleted on chromosome 10
PTH	Parathyroid hormone
PTHrP	Parathyroid hormone related protein
RANKL	Receptor activator of nuclear factor κ B ligand
RIPA	Radioimmunoprecipitation assay buffer
ROI	Region of interest
SDF1	Stromal cell-derived factor 1
SEM	Standard error of the mean
SOS	Son-of-sevenless
SRE	Skeletal related event
TbN	Trabecular number
TbSp	Trabecular separation
TbTh	Trabecular thickness

TGFα	Transforming growth factor α
TGFβ	Transforming growth factor β
TN	Triple-negative
TRAP	Tartrate resistant acid phosphatase
TRK	Tyrosine receptor kinase
TSC1/2	Tuberous sclerosis complex protein 1/2
TUNEL	Terminal dUTP nick end-labeling
TV	Total volume
Wnt	Wingless int-1
ZFN	Zinc finger nuclease

Epigraph

We shall not cease from exploration, and the end of all our exploring will be to arrive where we started and know the place for the first time.

- T.S. Eliot

Chapter One: **Introduction**

1.1 Breast cancer

Based on recent global statistics breast cancer is the most prevalent type of cancer in females, accounting for 23% of total new cancer cases. Furthermore, breast cancer is the leading cause of cancer related deaths in females worldwide at approximately 14%. In general, breast cancer is more common to Western countries, such as Western/Northern Europe, Australia/New Zealand, and North America, however, the incidence is increasing in less developed countries as well, such as in Africa and Asia [1].

1.1.1 Breast cancer subtypes

Breast cancer is a heterogeneous disease, and can be categorised by a variety of different methods, such as histological staining, clinical parameters and gene expression profiles. At least 18 different subtypes have been classified using histological methods [2]. More recently, molecular profiling has generated at least 5 subtypes, including luminal A, luminal B, HER2 positive, basal-like and normal breast-like [3] **(Figure 1-1)**. Luminal tumors arise in the cells that line the ducts and glands and generally grow slower, whereas basal-like tumors arise in the deep tissue of the ducts and glands and frequently grow much quicker [4]. These two subtypes demonstrate a distinct pattern of immunohistochemical staining that correlates with luminal and myoepithelial (basal) tissue origin. However, recently, strong evidence suggests that basal-like tumors likely arise from luminal progenitors and not from basal stem cells [5]. This finding has important implications, as the cell of origin of a tumor is crucial to understanding cancer progression, and therefore holds valuable prognostic and therapeutic indications. Although

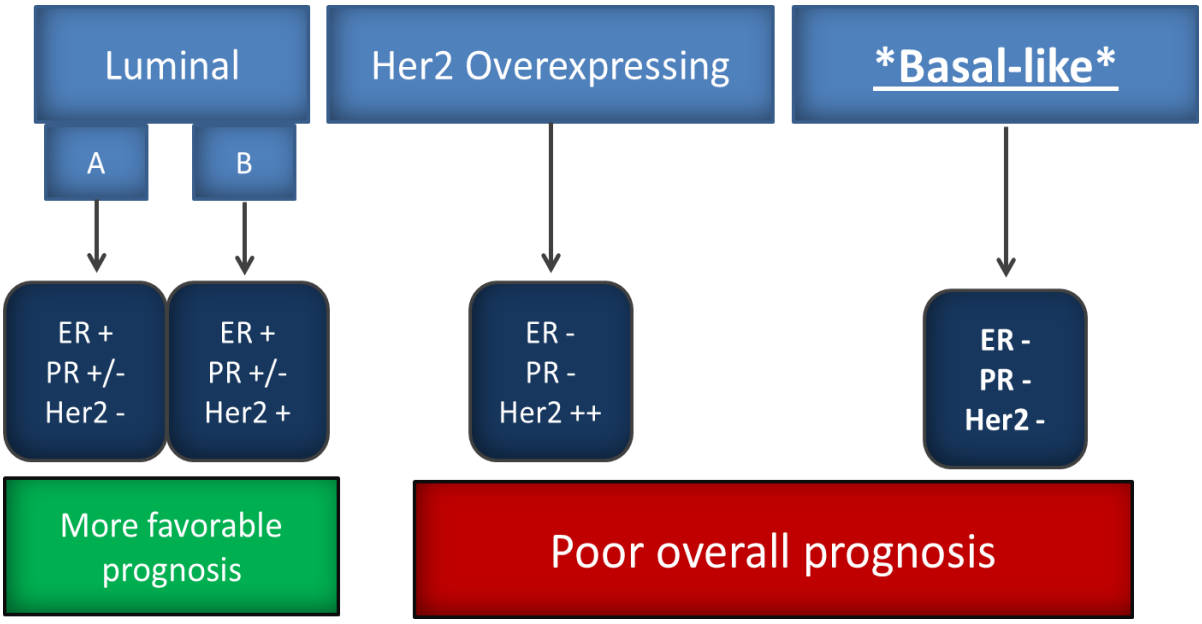

Figure 1-1. Breast cancer subtypes based on molecular classifications.

Breast cancer is a heterogeneous disease that can be classified into distinct subtypes, based on molecular profiling. Luminal types of breast cancer are further sub-classified into types A and B, with a key identifying feature of the absence or presence of the HER2/neu receptor, respectively. Clinically, this type is associated with a much more favorable prognosis using conventional therapeutic approaches, such as chemotherapy. As the name implies the HER2/neu overexpressing type of breast cancer harbor an overexpression of the receptor, and generally lack the ER and PR. This type is generally associated with a poor prognosis; however, there has been some success in targeting the overexpressed Her2 receptor. Lastly, the basal-like subtype is generally synonymous with a triple-negative profile that lacks hormonal receptors. This type is also associated with a poor prognosis, and also relatively difficult to target therapeutically due to the absence Her2, ER, and PR. Abbreviations: ER = estrogen receptor, PR = progesterone receptor.

molecular subtyping of breast cancers [6-9] doesn't entirely correlate with immunohistochemical classifications [10-12], genetic profiling still provides strong evidence for the effective use of therapeutic modalities and for determining patient prognosis. The major molecular distinctions that were identified to characterize the different subtypes were dependent on the presence or absence of hormone receptors, estrogen receptor (ER), progesterone receptor (PR) and the human epidermal growth factor receptor-2 (HER2/neu), in addition to other biomarkers, such as cytokeratin epithelial markers and Ki67 as a measure of mitotic index [11].

The luminal A subtype is considered the most common, accounting for 50-60% of total cases, and is generally characterized by the expression of the ER, variable expression of the PR, and absence of the HER2/neu receptor. Additionally, luminal A subtypes demonstrate low proliferation, based on Ki67 mitotic index, and low histological grade. The luminal B subtype accounts for 10-20% of cases, and similarly express the ER and PR, but also frequently express the Her2/neu and the epidermal growth factor receptor (EGFR). This subtype also demonstrates a more aggressive phenotype and higher mitotic index than the luminal A subtype [13], however there has been some clinical success in targeting the estrogen receptor with tamoxifen [14].

As the name implies the HER2/neu subtype demonstrates an overexpression of the HER2 receptor, and generally lacks the expression of ER and PR. HER2 tumors are also characterized by high proliferation, high histological grade and generally a poor overall prognosis. However, there has been substantial success in the last decade with the use of anti-Her2 treatments to target the amplified receptor, both in the initial stage and late metastatic disease [13, 15, 16].

Basal-like subtypes of breast cancer represent 10-20% of all cases and, as the name implies, express genes present in normal breast myoepithelial cells, such as cytokeratins CK5 and CK17 and EGFR. An additional major characteristic is the absence of receptors present in

other subtypes (ER, PR, and HER2/neu), and therefore basal-like cancers are generally referred to as the "triple-negative" (TN) subtype [13]. The absence of these receptors is a major reason for the difficulty in targeting basal-like triple negative breast cancers. The primary form of therapeutic intervention involves chemotherapy, and although relatively sensitive due to the inherently high mitotic index [17], early metastatic relapse is a frequent occurrence when compared to non-triple-negative breast cancers [18]. Basal-like triple-negative breast cancers have a high frequency of p53 mutations [19], which may be one explanation for their apparent aggressiveness and lack of response to standard treatment modalities. The MDA-MB-231 breast cancer cell line used in our investigations is of the basal-like triple-negative subtype, based on the absence of hormonal receptors, as well as presence of other markers, such as elevated EGFR expression and a high Ki67 mitotic index. Additionally, the MDA-MB-231 cell-line harbors a p53 mutation, and also demonstrates considerable invasive and metastatic capacity.

1.2 Breast cancer bone metastasis

It is increasingly evident that certain types of cancers are associated with a distinct metastatic profile that is representative of an elevated propensity to colonize distant sites in the body. These characteristics result in various cellular programs that permit intravasation, survival in the blood stream, and eventual colonization and growth in specific micro-environments. Thus, breast cancer is frequently observed to metastasize to distinct distant organs, such as the bone, lung, liver and brain [20, 21]. Interestingly, there is now ample evidence implicating the expression of several chemokine receptors, such as CXCR3, CXCR4, CCR4, CCR5, and CCR7 with organ-specific metastasis [22]. For example, high levels of CXCR4 are highly implicated in the effective homing of breast cancer cells to the SDF-1 producing bone microenvironment, and

survival of cancer cells in the bone-marrow [23]. Bone is the most frequent site of metastatic colonization in advanced breast cancer, occurring in up to 70% of patients [24]. Despite recent advances in screening, a significant proportion of women initially present with advanced breast cancer. Associated micrometastases, especially within the bone often initially go undetected [25], owing to the unique characteristics of that microenvironment. Once tumors metastasize to bone they are usually incurable, with only 20% of breast cancer patients remaining alive at 5 years following detection [24, 26].

The consequences of developing bone metastasis are devastating, including severe pain, hypercalcemia, pathological fractures, as well as nerve and spinal cord compression syndromes [27]. There are a number of reasons for bone being a frequent site of metastasis, including the permissive nature of the fenestrated structure of bone marrow sinusoid capillaries, allowing cancer cell infiltration [21]. Also the highly mineralized and growth factor rich bone microenvironment is an ideal site for tumor growth and survival. In fact, insulin-like growth factors (IGFs), transforming growth factor β (TGFβ), fibroblast growth factors (FGFs), platelet-derived growth factors (PDGFs), and bone morphogenetic proteins (BMPs) present within the bone matrix are able to promote the growth of bone-colonized cancer cells [28].

In order to effectively investigate specific types of primary cancers, or their associated metastases, it is necessary to include the contextual cues of the accompanying microenvironment. This is becoming increasingly achievable with the development of mouse models that more closely recapitulate human disease. In fact, a comparison of established breast cancer cell lines, such as the widely used MDA-MB-231 cells and primary tumors taken from human patients, have demonstrated a similar poor-prognosis transcriptional signature, as well as a distinct organ-specific metastatic potential [29].

1.2.1 Current therapies for osteolytic metastasis

Skeletal metastases demonstrate a difficult target for therapeutic intervention, owing to the complex nature of the bone microenvironment and the associated relationship that tumors cells establish with resident bone cells. Currently, treatment options are limited and are palliative at best.

Presently, management options include analgesia, radiation therapy, surgery and systemic therapy. Analgesia simply represents a form of pain control in an attempt to reduce poor quality of life resulting from tumor-induced skeletal-related events [30]. Similarly, radiation therapy and surgery are primarily used as a palliation for painful bone metastasis, for example, to reduce osteolysis and prevent pathological fractures, respectively, while controlling tumor burden to some degree [25, 30]. Systemic therapy includes conventional cytotoxic chemotherapy, as well as administration of bisphosphonates. The latter treatment represents a specific anti-resorptive strategy owing to their propensity to be absorbed into the inorganic matrix of bone. The drug is subsequently internalized by activated osteoclasts, whose function they inhibit [31]. Within the context of bone metastasis, bisphosphonates represent a treatment that targets an important subset of the stromal cell population, thereby reducing the production of local growth factors that effectively promote the growth of the tumor [32]. Zoledronic acid (Zoledronate) is a relatively effective bisphosphonate that has been shown to delay the onset of first skeletal related events (SREs), as well as an ability to reduce the total number of SREs in patients with bone metastases [33-35]. However, this form of treatment is known to have toxic side effects, such as nephrotoxicity, induction of hypocalcemia, and osteonecrosis of the jaw [34]. Furthermore, breast cancer cells have demonstrated potent inhibition of bisphosphonate-induced osteoclast apoptosis, ultimately rendering this treatment ineffective [36]. As the currently available

treatments are primarily palliative and controversial with regard to their universal benefit, there is a critical need for more effective therapeutic options that can target breast cancer cells within the bone microenvironment.

1.3 Bone remodelling in normal and cancer cells

In healthy individuals, there is a fine homeostatic balance that is responsible for the proper maintenance of bone architecture. Normal bone-remodeling is carried out by the coordinated actions of bone-depositing osteoblasts, and bone-resorbing osteoclasts, in order to sustain appropriate bone function and structural integrity **(Figure 1-2)**. An imbalance between the activities of these cells can lead to disproportionate bone formation, or bone loss, as seen in osteopetrosis, or osteoporosis, respectively.

Osteolytic breast cancer metastasis leads to widespread bone destruction by effectively altering normal bone remodelling such that it favors bone resorption by osteoclasts. This results from sophisticated and complex autocrine and paracrine loops between cancer cells and resident bone cells that lead to a mutual promotion of tumor growth and extensive bone destruction. Tumor-stromal cell interactions thus constitute an important consideration that dictates cancer cell fate and the efficacy of treatments. Therefore, it is essential that pre-clinical examination of potential therapeutics targeting osteolytic metastasis be studied in tumors located within the bone microenvironment.

1.3.1 Osteoclasts

Osteoclasts are tissue-specific cells derived from the differentiation of precursor monocyte/macrophage cells. Pre-osteoclasts fuse together to form multi-nucleated, post-mitotic

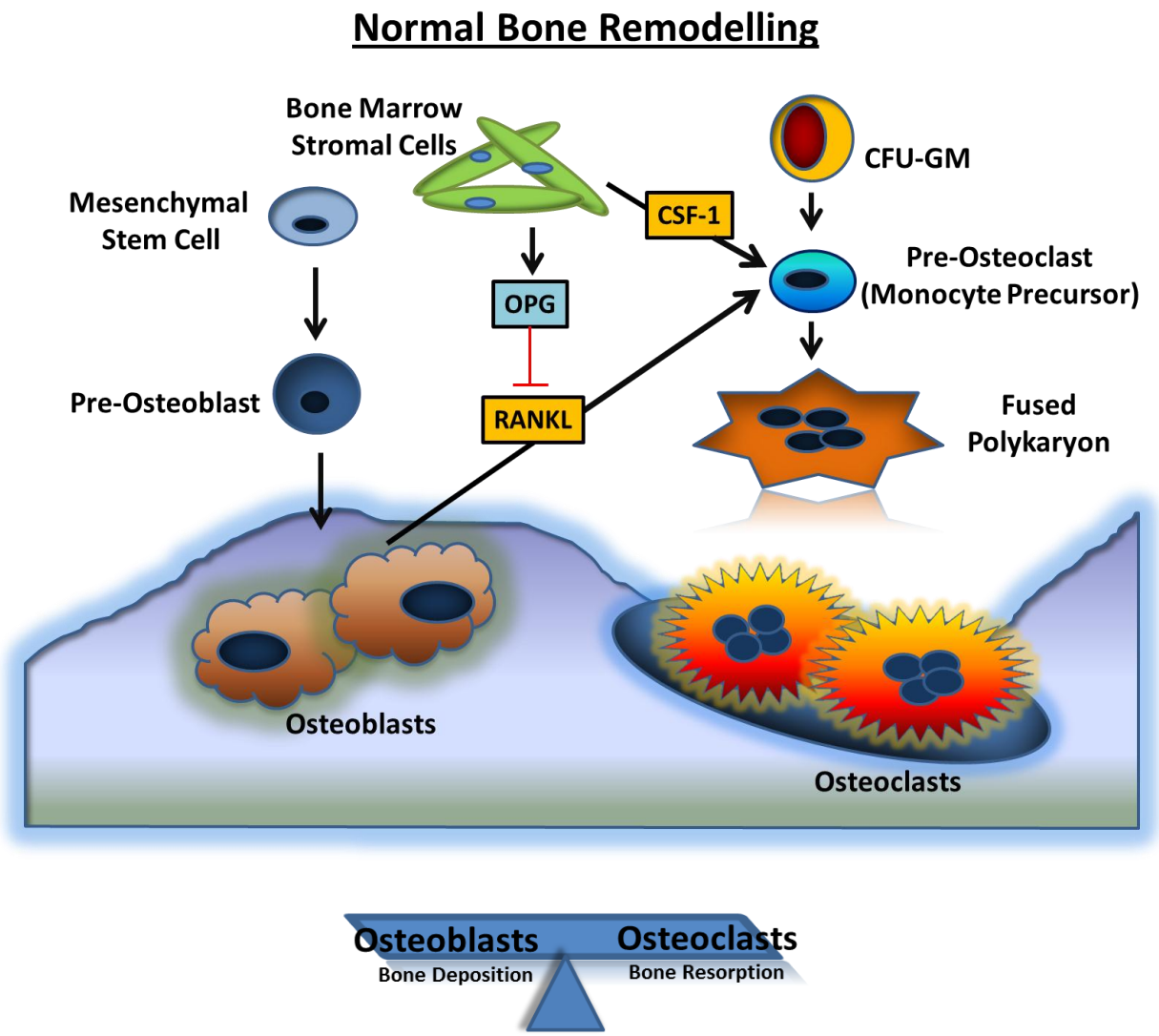

Figure 1-2. Normal bone remodelling.

Many cells within the bone microenvironment are responsible for regulating the homeostatic balance between bone deposition and bone resorption. Osteoblasts are derived from mesenchymal stem cells, which undergo terminal differentiation through the influence of cytokines and growth factors, such as PTH and BMPs. Mature osteoblasts, in conjunction with bone marrow stromal cells are critical for osteoclastogenesis through their expression of RANKL, and CSF-1. Negative regulation of osteoclastogenesis is supplied by OPG, a decoy receptor for RANKL. Osteoclasts are derived from monocytic precursors, and upon activation and differentiation fuse together, becoming multinucleated. Mature osteoclasts that hold the capacity to resorb bone express the markers TRAP, CTR, Cathepsin K, and the β_3 integrin. Abbreviations: PTH = Parathyroid Hormone, BMPs = bone morphogenetic proteins, RANKL = receptor activator of nuclear factor κ B ligand, CSF-1 = colony stimulating factor-1, OPG = osteoprotegerin, TRAP = tartrate resistant acid phosphatase, CTR = calcitonin receptor.

mature osteoclasts [37]. Two hematopoietic factors are primarily required for this differentiation; these include the TNF-related cytokine RANK ligand (RANKL), and the growth factor, macrophage colony-stimulating factor (CSF-1 or M-CSF). Together, these factors induce the expression of genes that generate the osteoclast lineage, including TRAP (tartrate resistant acid phosphatase), cathepsin K, calcitonin receptor, and the $\alpha v\beta_3$ integrin [38]. Other factors, such as prostaglandin E_2 (PGE_2) and parathyroid hormone related protein (PTHrP) can stimulate osteoclastogenesis indirectly by inducing the expression of RANKL by osteoblasts. [37]. Factors such as IL-8 [39] and IL-11 [40] can also induce osteoclast maturation directly.

Following the appropriate signals and stimulation, mature osteoclasts undergo internal structural changes that prepare the cell to begin bone resorption, such as actin cytoskeletal rearrangement and the formation of a sealed tight junction between the bone surface and the basal membrane. It is now clear that the αvβ3 integrin is essential for osteoclast recognition of bone and is a key mediator of the adhesive and resorptive function of osteoclasts [41]. Once there is an interaction, the enclosed space between osteoclasts and the bone surface becomes acidified through a vacuolar H^+ ATPase [42]. Osteoclasts then release cathepsin K into the acidified region, which degrades type I collagen [43], and subsequently liberates other matrix-associated factors. Interestingly, invasive breast cancer cell lines, including the MDA-MB-231 cells used in this study, also show high expression levels of αvβ3 integrin [44] and is likely another explanation for the colonization preference to bone, and also the observed close proximity of tumor and osteoclast cells in the bone microenvironment.

1.3.2 Osteoblasts

In contrast to osteoclasts, osteoblasts are derived directly from mesenchymal stem cells.

Their differentiation from progenitor cells is primarily controlled by growth factors within the bone microenvironment, including Wnts, BMPs, PTH [45, 46] and others. In fact, an approved treatment for osteoporosis is the daily administration of PTH, however, enthusiasm for its use in bone metastases is tempered by the observed increase incidence in osteosarcomas seen in rats treated with PTH [32]. The differentiation of osteoblasts is less well understood than osteoclasts, however, a critical transcription factor for this process is known to be Runx-2, as mice that lack this gene do not develop bones [47]. It is also known that early precursors produce alkaline phosphatase, and more differentiated osteoblasts produce osteocalcin and calcified bone matrix.

Interestingly, osteoclast differentiation and maturation is under the control of immature osteoblasts through the expression of membrane-bound RANKL [48]. Intuitively, this is a logical relationship, as coupling the opposing functions of bone formation and destruction generates regulatory mechanisms that can support the structural requirements of bone, as well as the physiological demands of the body, such as release of Ca^{2+} into the blood stream.

Bone-colonized cancer cells are able to induce the expression of osteoblast RANKL through the secretion of factors, such as PTHrP [27], which subsequently enhance osteoclastogenesis. This is one approach that allows cancer cells to effectively tip the balance to favor osteoclast activity within the bone, leading to widespread destruction. Interestingly, it has also been reported that enhanced apoptosis of mature osteoblasts occurs following bone-colonization of MDA-MB-435 breast cancer cells, and that conditioned media *in vitro* prevents differentiation of pre-osteoblast cells with bone-depositing capacity [49]. These observations demonstrate the important role of osteoblast cells in producing and maintaining a pro-osteolytic imbalance. It also highlights the need for treatments that not only target bone-colonized cancer

cells, but are also able to induce net bone formation by skewing the balance towards mature bone depositing osteoblasts.

1.4 The 'vicious cycle' of bone metastasis

The 'vicious cycle' can be considered a multi-faceted relationship between cancer and resident bone cells that leads to profound tumor expansion and an imbalance of normal bone remodelling. This relationship can be presumed to begin with the specific recruitment, homing and initial survival of cancer cells in the bone microenvironment, by mechanisms such as those involving the SDF-1/CXCR4 axis [23], followed by tumor propagation. Once colonized, cancer cells in the bone produce factors that directly or indirectly modulate the generation and/or activity of osteoblasts, and osteoclasts **(Figure 1-3)**. As previously mentioned, these factors, such as PTHrP and PGE_2 can induce osteoblast expression of RANKL. Additionally, cancer cells can secrete factors that directly induce the maturation of osteoclasts, such as CSF-1, granulocyte-macrophage colony-stimulating factor (GM-CSF), IL-11 and IL-8 [50-52]. The increased presence of bone resorbing osteoclasts is primarily responsible for the osteolytic lesions that occur. Cancer cell secretion of factors, such as monocytic chemotactic protein-1 (MCP-1) or interferon gamma-induced protein-10 (IP-10) is highly implicated in the recruitment of pre-osteoclast monocyte precursor cells [53]. Once recruited to the bone, osteoclasts become differentiated into mature cells with resorptive capacity. Furthermore, it has been demonstrated that MDA-MB-231 cells exert potent and direct anti-apoptotic effects on mature osteoclasts [54], thereby maximizing the destructive potential of the 'vicious cycle.' Bone resorption, in turn, releases latent growth factors from the bone matrix, such as PDGF, IGF-1 and 2, FGF-1 and 2, BMPs and TGF-β [32]. These factors, and particularly TGFβ, further stimulate colonized breast

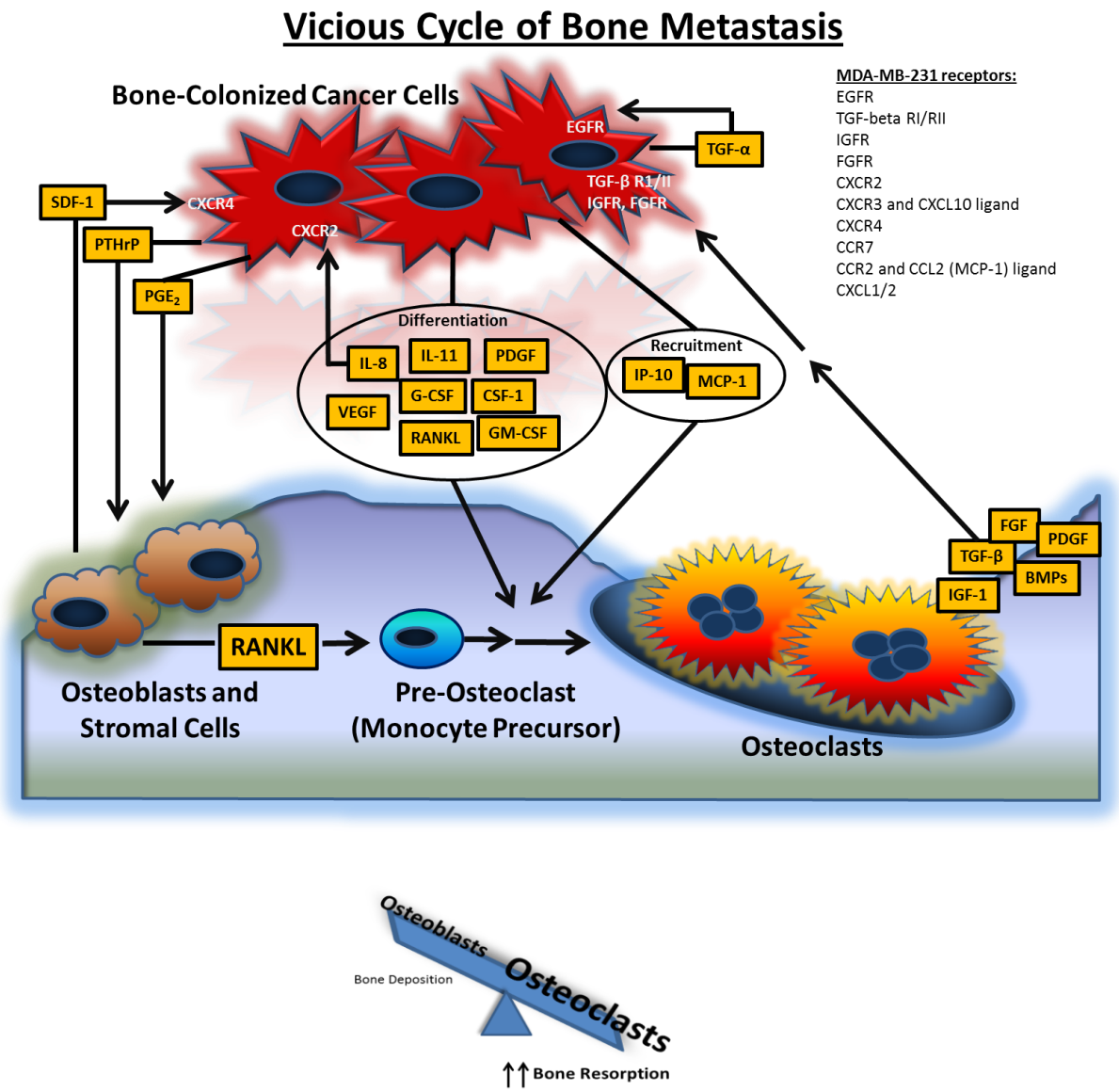

Figure 1-3. The 'vicious cycle' of bone metastasis.

The presence of colonized breast cancer cells in the bone microenvironment results in an imbalance of bone deposition and bone resorption, ultimately favoring the generation and function of bone-resorbing osteoclasts. This can occur either indirectly through the secretion of factors that induce osteoblast expression of RANKL, leading to osteoclastogenesis, or through the secretion of factors that can act directly on monocytic osteoclast precursor cells. Once activated, osteoclasts degrade the bone, releasing latent matrix factors, such as IGF-1 and TGFβ, that can act on cancer cells to promote their growth. Abbreviations: IGF-1 = insulin-like growth factor-1, TGFβ = transforming growth factor-beta.

cancer cells by directly promoting expansion, and indirectly, by inducing cancer cell secretion of osteoclastogenic factors [55], thereby completing the 'vicious cycle' of bone metastases. The establishment of this paracrine relationship generates a scenario where tumor growth progresses concomitantly with bone destruction.

1.5 Signaling pathways implicated in breast cancer bone metastasis

1.5.1 The phosphatidylinositol 3-kinase (PI3K) pathway

Class I PI3Ks are heterodimers, found in four isoforms, that are further divided into two subclasses. Class IA (PI3K-α, PI3K-β, and PI3K-δ) heterodimers consist of a catalytic subunit p110 (α, β, δ) and regulatory subunit p85 (α or β) and are activated via receptor tyrosine kinases (RTKs). Class IB PI3Ks (PI3K-γ) consist of a catalytic subunit p110 (γ) that is associated with one of two regulatory subunits, p101 and p84, that is activated through G-protein-coupled receptors (GPCRs). PI3K functions to phosphorylate the phosphoinositide PIP_2 to PIP_3. PIP_3 propagates downstream intracellular signaling through the recruitment and direct binding of various proteins containing pleckstrin-homology (PH) domains, such as PDK1 and AKT. The phosphorylation and activation of AKT by PDK1 and the mTOR complex mTORC2 at threonine308 and serine473, respectively, generates a cascade of downstream signaling that affects growth and protein synthesis (mTOR/S6), cell survival (BAD), cell cycle progression (FOXO), glucose metabolism (GSK3), among others **(Figure 1-4)** [56].

1.5.1.1 PI3K signaling in (breast) cancer

Studies have established the central role for the PI3K signaling pathway in diverse cellular functions such as metabolism, growth, survival, motility and cancer progression [56], and is

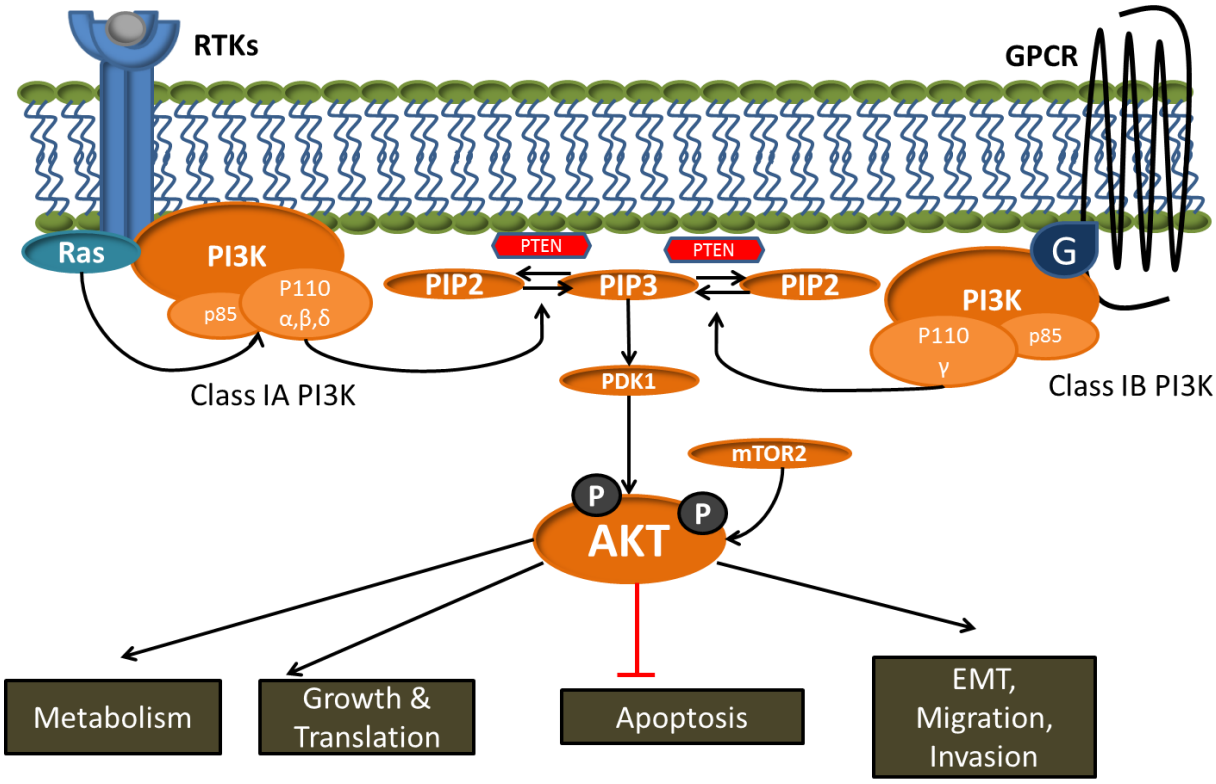

Figure 1-4. The phosphatidylinositol 3-kinase (PI3K) pathway.

PI3K functions to convert PIP_2 to PIP_3. Class IA PI3K is activated through ligand binding to RTKs. Upon receptor activation, p85 binds to phosphorylated tyrosine residues, which activates the catalytic subunit p110 (α, β, δ) which converts PIP_2 to PIP_3. Class IB PI3K act similarly, however are activated by GPCRs, and generate PIP_3 from the p110 γ catalytic subunit isoform. Ras is also able to act upstream, and activate p110 catalytic activity resulting in PIP_3 generation. PIP_3 subsequently propagates downstream intracellular signaling through the recruitment and direct binding of various proteins containing PH domains, such as PDK1 and AKT. The phosphorylation and activation of AKT by PDK1 and the mTOR complex mTORC2 at threonine308 and serine473, respectively, results in multiple downstream effects such as growth and inhibition of apoptosis. Abbreviations: RTKs = receptor tyrosine kinases, PIP2 = phosphatidylinositol 4,5-bisphosphate, PIP3 = phosphatidylinositol 3,4,5-triphosphate, GPCRs = G-protein coupled receptors, PH = pleckstrin-homology.

currently considered among the most commonly activated pathways in human cancer [57]. PI3K can be aberrantly activated by multiple routes, such as mutational activation or amplification/over-expression of PI3K isoforms, loss of PTEN tumor suppressor activity, oncogenic Ras signaling, and activation of many cell surface receptors (eg. IGFR, HER2/neu, EGFR) [58]. Mutational activation of the PI3K p110α catalytic subunit (PIK3CA) gene has an incidence of 32% of colorectal, 36% of endometrial, 40% of ovarian, and 30% of breast cancers, among others [58]. Although less frequent, aberrant activation of PI3K signaling can occur as a result of PTEN mutations that are estimated to occur in up to 14% of prostate, 9% of colorectal, and 6% of breast cancers [58]. Infrequently, AKT can also undergo mutational activation, as seen in 5% of thyroid, and 3% of breast cancers [58]. Furthermore, as discussed in greater detail below, PI3K can also be activated through upstream signaling of the Ras pathway, either through mutational activation, such as in KRAS, HRAS, or NRAS mutations, or alternatively through receptor and signaling amplification, such as with EGFR. The latter form is especially dependent on the presence of cytokine and growth factors within the microenvironment that can activate Ras pathway signaling. For example, 70-80% of breast carcinomas demonstrate EGFR overexpression [59], and this appears to be primarily responsible for the hyperactivation of the Ras pathway seen in breast cancer patients [60].

PI3K-α and PI3K-β are ubiquitously expressed, while the PI3K-δ and PI3K-γ isoforms are largely restricted to cells of hematopoietic origin [61]. Although not a central theme of our study, targeting all PI3K isoforms with a pan-PI3K inhibitor holds the potential of attenuating aberrant PI3K signaling in cancer cells, as well as in resident bone-marrow and recruited stromal-cells.

1.5.2 The Ras-MAPK pathway

There are three *ras* genes comprising four Ras isoforms (H-Ras, N-Ras, K-Ras4A and K-Ras4B) that function as molecular switches near the apex of a complex signaling network cascade. Although there is some redundancy between these isoforms, there is evidence that they exhibit specific roles, most notably in oncogenic signaling [62]. For example, K-Ras was shown to be the most potent inducer of the transformed phenotype, when compared to N-Ras and H-Ras [63]. Ras proteins are GTPases, that in their GDP-bound state are inactive and become activated upon GDP dissociation and replacement with the more abundant GTP. This is achieved through guanine nucleotide exchange factors (GNEFs), such as son-of-sevenless (Sos). Activated GTP-bound Ras phosphorylates and stimulates the Raf kinase, which goes on to activate a second protein kinase, MAPK/ERK kinase (MEK1/2). MEK, in turn, phosphorylates and activates a third set of protein kinases, the extracellular signal-regulated kinases (ERK1/2), which results in the regulation of proliferation, differentiation, cytoskeletal rearrangement, and anti-apoptotic processes. For example, activated ERK has the ability to activate many downstream targets **(Figure 1-5)**, such as c-MYC, ELK-1, and NF-κB that are responsible for the expression of genes associated with proliferative and anti-apoptotic signals, such as Cyclin D1, and Bcl2 [64]. Mutations of any of the Ras isoforms results in these proteins being predominantly GTP-bound, and therefore in the constitutively activated state [65].

1.5.2.1 Ras-MAPK signaling in (breast) cancer

Aberrant activation of the Ras pathway occurs in approximately 30% of all human cancers [66], making it one of the most frequently activated pathways in cancer. The Ras pathway has been implicated in promoting cell proliferation, differentiation, survival, motility

and invasion [62]. Similar to PI3K signaling, the Ras pathway can be aberrantly activated through multiple mechanisms, such as activating mutations at the level of Ras or downstream effectors, such as Raf.

KRAS mutations are a frequent occurrence in certain types of cancers, such as pancreatic (~90%), and thyroid (~60%) tumors [67]. Breast cancer displays a lower frequency of KRAS activating mutations, estimated at approximately 5% [68], and has led to the notion that Ras signaling does not play an important pathogenetic role in this cancer. However, as previously mentioned a very large proportion of patients present with an overexpression of EGFR and subsequent Ras pathway hyperactivation, which likely plays a role in breast cancer invasion, development, growth [68], and resistance to conventional chemotherapeutic approaches [69]. In fact, more than 50% of patients demonstrate hyperactivation of the Ras-MAPK pathway and this has also associated with an overall shortened survival [60]. The importance of EGFR signaling within the context of breast cancer bone metastasis is apparent, as demonstrated by several studies. For example, an autocrine/paracrine loop has been implicated in invasion [70], and survival of bone-colonized breast cancer cells due to macrophage secretion of EGF ligand, and subsequent tumor cell secretion of CSF-1, leading to an induction of Ras signaling in both cell types [71]. Furthermore, it was determined that inhibition of EGFR-Ras signaling can induce cancer cell necrosis and also decrease paracrine secretion of CSF-1 and MMP9, factors that are highly implicated in the support of the tumor-bone microenvironment [71].

The MDA-MB-231 breast cancer cell line used in this study harbors an overexpression of EGFR and a mutant K-Ras that leads to aberrant Ras pathway activation. Although not central to our study, the Ras signaling pathway has also been implicated in osteoclast survival and differentiation [72, 73], and therefore targeting components within this pathway hold the strong

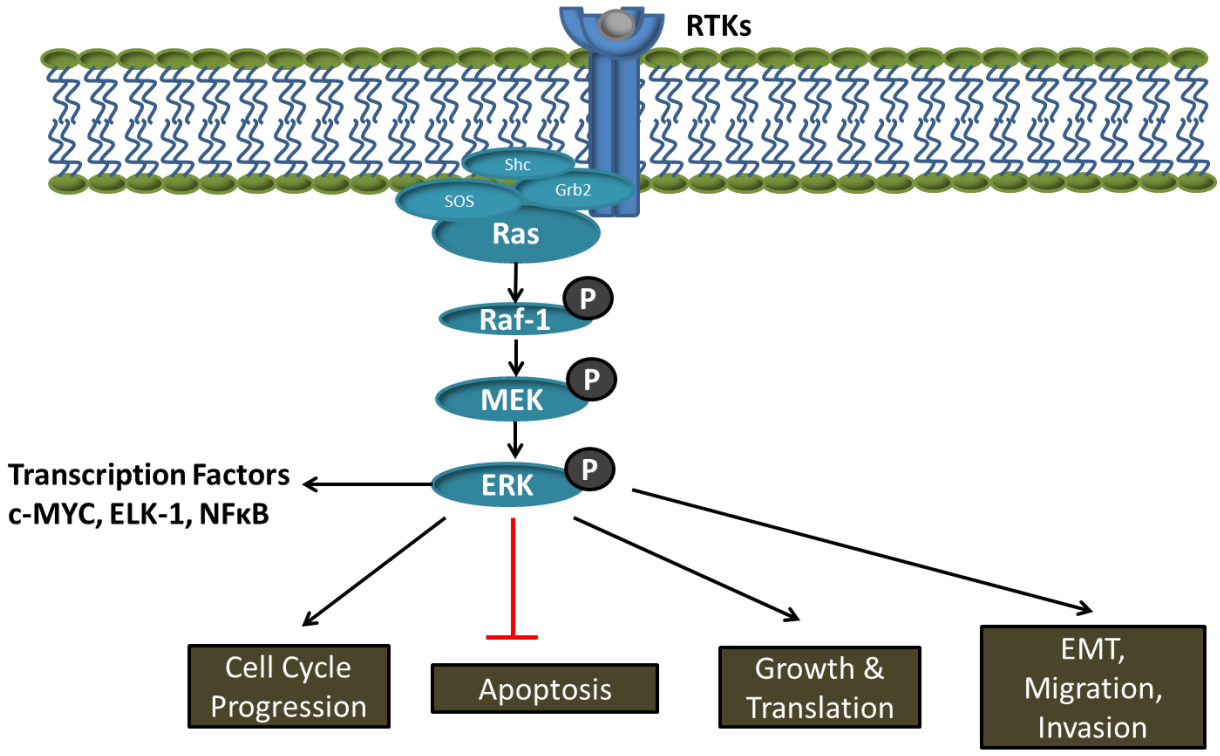

Figure 1-5. The Ras-MAPK pathway.

The Ras-MAPK pathway is activated upon RTK ligand binding. Upon RTK activation, Grb2 binds phosphorylated tyrosine residues, and subsequently binds Sos, which is a guanine nucleotide exchange factor (GNEF). Shc is an adaptor protein, which is proposed to help in the interaction between Grb2 and Sos. Activated Sos then promotes the removal of GDP, and binding of GTP to Ras. Activated GTP-bound Ras phosphorylates and stimulates Raf kinase activity, which goes on to phosphorylate MEK, whose kinase activity phosphorylates and activates ERK. Activated ERK promotes the regulation of many processes, such as proliferation, growth and the inhibition of apoptosis. Abbreviations: Sos = sons of sevenless, GNEF = guanine nucleotide exchange factor, RTK = receptor tyrosine kinase, GDP/GTP = guanine nucleotide di/tri-phosphate.

potential to prevent/limit tumor growth, as well as to attenuate osteoclast activity in the context of osteolytic metastasis.

1.5.3 PI3K and Ras pathway crosstalk and survival mechanisms

Cancer cell reliance on the PI3K and Ras signal transduction pathways is supported by extensive experimental and clinical investigation. Adding further complexity, there is substantial evidence that multiple levels of crosstalk exist between these two pathways [74].

As previously mentioned, Ras can activate PI3K. Early investigations demonstrated that Ras directly binds the PI3K p110 catalytic subunit, providing a direct link between these pathways [75]. However, it is becoming increasingly evident that there is interconnectedness between these pathways at multiple levels **(Figure 1-6)**. For example, it was demonstrated that AKT can inactivate Raf, an antagonistic mechanism thought to have evolved to ensure survival of cells [76]. Furthermore, several studies have established a feedback loop, in which inhibition of the common downstream effector mTOR can lead to activation of upstream AKT and ERK [77, 78]. Interestingly, there are multiple levels of downstream convergence of these pathways, such as the activation of the translational machinery (eIF4E and S6), NFκB, and inhibition of pro-apoptotic BAD [74], among others. These convergences and pathway crosstalk have the potential to demonstrate feedback loops upon inhibition, or alternatively to induce downstream signal amplification in the context of simultaneous pathway activation. In fact, inhibiting only one of these pathways can result in signal amplification of an alternate pathway in a compensatory fashion [79], suggesting that simultaneous inhibition of both pathways may be necessary to completely ablate downstream effects **(Figure 1-7)**. Recently, a group reported an analysis of a large panel of breast cancer cell lines and xenograft models with a basal-like gene

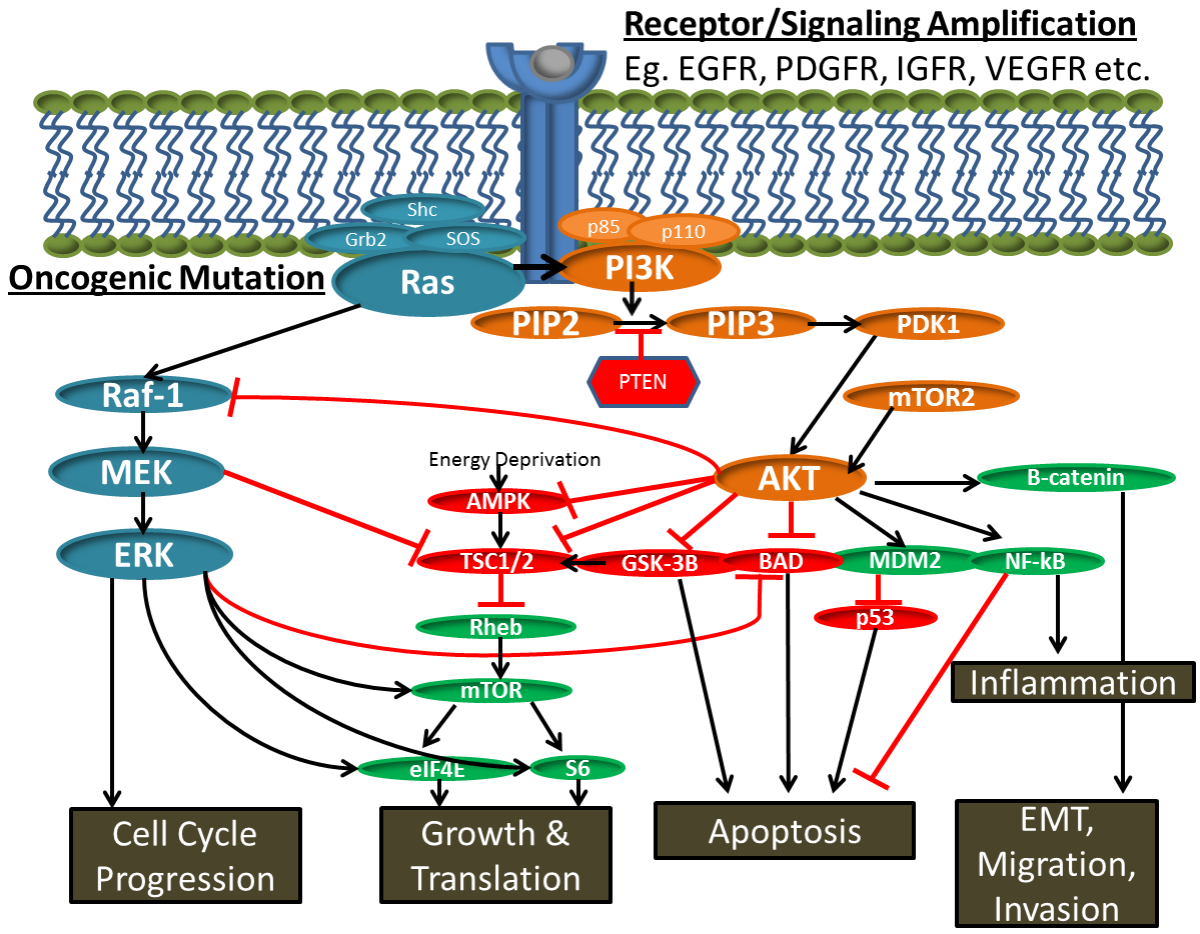

Figure 1-6. Signaling crosstalk between Ras and PI3K pathways.

There are multiple levels of crosstalk between the PI3K and Ras signal transduction pathways. Ras can act upstream of PI3K to propagate downstream activation of AKT and other molecules. Additional levels of crosstalk can occur downstream, such as with AKT and Raf, MEK and TSC1/2, and ERK on multiple PI3K effector proteins, among others. Aberrant activation of either or both pathways, through receptor and signaling amplification, or oncogenic mutations can therefore lead to complex pathway crosstalk, regulating such processes as apoptosis, growth and translation.

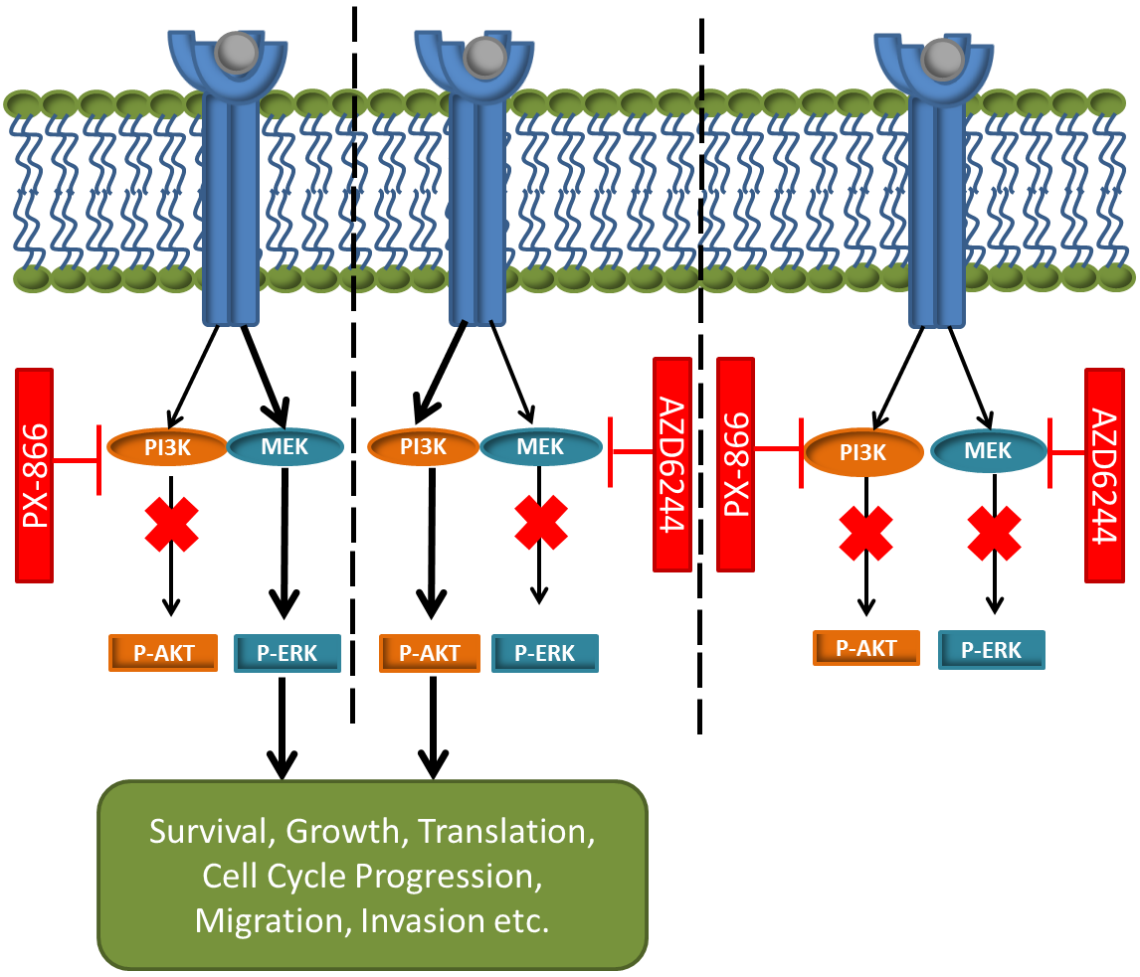

Figure 1-7. Signal transduction pathway crosstalk survival mechanisms.

Due to the extensive crosstalk between the PI3K and Ras signal transduction pathways, inhibition of one pathway alone can result in signal amplification of the alternate pathway in a compensatory fashion. This has led to the notion that single-agent inhibition may lead to therapeutic resistance, and therefore simultaneous inhibition of both pathways may be necessary to completely ablate all downstream signaling, thereby effectively preventing cancer cell growth and/or survival.

expression that exhibited a profound Ras-like transcriptional program at baseline, and were correspondingly sensitive to MEK inhibition with small molecule inhibitors. The importance of these pathways is further demonstrated by the fact that loss of the PTEN tumor suppressor (that leads to upregulation of the PI3K-AKT pathway) is associated with a resistance to MEK inhibitors and continued cell survival. This indicates that both of these pathways are responsible for generating survival cues, even in the presence of MAPK pathway inhibition [80]. It was also observed that in the presence of wild-type PTEN, inhibition of the MAPK pathway leads to feedback activation of the PI3K-AKT pathway in an EGF-dependent manner [79]. This latter finding provides evidence of the importance of extracellular environmental stimuli in the form of cytokines and growth factors. The interconnectedness of the PI3K and Ras-MAPK pathways, and their apparent importance in basal-like breast cancers, encourages investigation into pathway crosstalk survival mechanisms in specific microenvironments, such as in osteolytic metastasis.

1.6 Small-molecule inhibitors in pre-clinical and clinical use

The detrimental consequences of systemic chemotherapy and other conventional treatment options has led to an intense investigation into alternative therapies that attempt to more specifically target cancer cells. The discovery of aberrant signaling pathway activation in specific subtypes of different cancers has led to the notion that certain pathways demonstrate important avenues in the perpetuation and longevity of tumors. The more recent creation of small-molecule inhibitors for the use of targeting specific cancer cell signaling pathways has generated an exciting new opportunity for more effective and individualized treatment. There are currently countless small-molecule inhibitors in pre-clinical and clinical trials. This study employed two small-molecule inhibitors that target either the PI3K or the MEK component of

the Ras signal transduction pathway, and that are currently in clinical trials for several different cancers with promising results.

1.6.1 Small-molecule PI3K inhibitor: PX866

There are currently a diverse number of PI3K inhibitors under investigation that have shown varying results. Effectiveness is generally predicted by transcriptional-gene signatures that are associated with addiction to the PI3K pathway. PI3K inhibitors can be subdivided into isoform-specific or pan-PI3K inhibitors. For example, targeting the p110α and p110β isoforms, which are ubiquitously expressed and that often show mutational activation in breast cancers, has the potential to specifically target such cancer cells. Similarly, targeting the p110δ and p110γ isoforms, that are restricted to hematopoietic lineages, is a more effective means for targeting bone marrow-derived stromal cells within the bone microenvironment (as in the context of skeletal metastases). Conversely, the use of a pan-PI3K inhibitor holds the capacity to inhibit multiple cell types. Some examples of different PI3K inhibitors in clinical trials include the dual PI3K/mTOR inhibitor, NVP-BEZ235 [81], the pan-PI3K inhibitors, GDC-0941 [82] and PX866 [83], the p110δ isoform specific inhibitor, CAL-101, and Akt inhibitor, MK-2206 [84].

PX866 **(Figure 1-8)**, the small-molecule inhibitor employed in this study, is a pan-PI3K inhibitor, that effectively targets all p110 isoforms (α, β, δ, γ), with an IC_{50} of 14 nM, 57 nM, 131 nM, and 148 nM, respectively, therefore demonstrating the most potent inhibition of the α and β isoforms [85]. PX866 has demonstrated improved PI3K pathway inhibition with minimal toxicity, as compared to the original wortmannin analogue. It is also unique in that it provides irreversible inhibition of PI3K through the generation of a covalent bound complex. This permits effective low *in vivo* dosing of 2-4 mg/kg and once daily administration [85, 86]. Pre-clinical

PX866

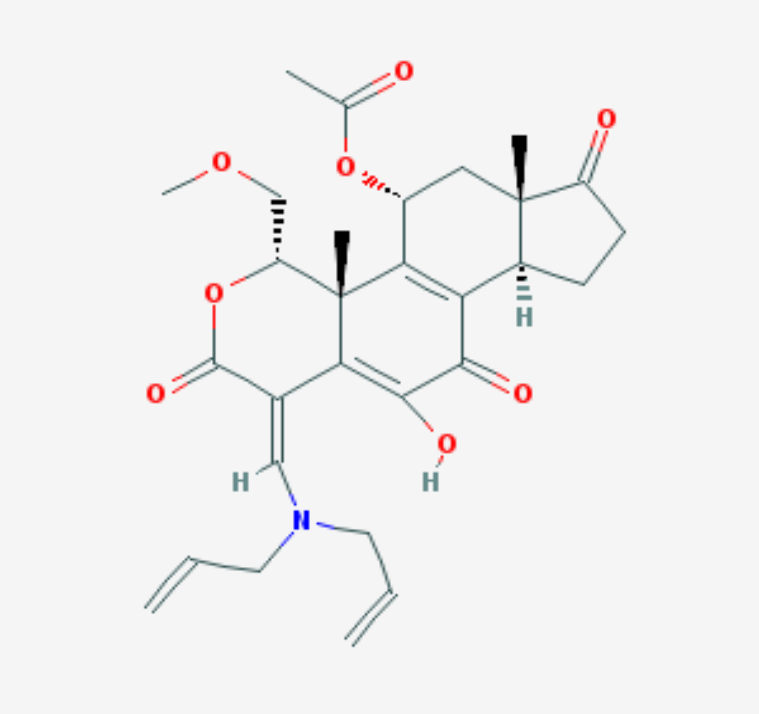

Figure 1-8. The PI3K inhibitor PX866.

Owing to the unique structure, PX866 generates a covalently-bound complex, making it the only irreversible PI3K inhibitor in development. PX866 is a pan-PI3K inhibitor that can effectively inhibit all isoforms, including the Class IA α, β, δ, and Class IB γ isoforms.

studies have reported an effective anti-tumor effects with the administration of PX866 in xenograft models of human glioblastoma [87], ovarian, colon [86], and lung cancers [88]. Phase I trials using PX866 have been completed and currently there are numerous phase II trials underway investigating effects of this agent against prostate, glioblastoma multiforme, non-small cell lung cancer, and colorectal cancer (clinicaltrials.gov). Furthermore, this compound has been shown to be well-tolerated, with minimal toxicity, and has led to prolonged disease stabilization in patients with advanced incurable cancers [89].

1.6.2 Small-molecule MEK inhibitor: AZD6244

Currently there are no potent and selective inhibitors against Ras, Raf or ERK, and therefore the development of small-molecule inhibitors targeting MEK1/2 may demonstrate the most optimal way to inhibit Ras-MAPK signaling. Additionally, because ERK can elicit many diverse downstream effectors and processes, targeting the upstream MAPK/ERK (MEK) kinase may prove to be an effective means to inhibit important signal inputs from multiple levels of signaling.

There are numerous MEK inhibitors in pre-clinical and clinical trials, and these have demonstrated varying results and efficacies. For example, CI-1040 was the first MEK inhibitor in human trials and initially demonstrated low toxicity and tolerance in phase I trials, however due to low efficacy reported in phase II trials, development was stopped [90]. Other MEK inhibitors such as PD098059 and U0126 demonstrate effective means to study the role of the MAPK pathway in carcinogenesis, however, demonstrate low solubility and bioavailability and therefore are restricted to *in vitro* investigation. A second generation CI-1040 MEK inhibitor, named AZD6244 (ARRY-142886/Selumetinib) [91], has exhibited effective oral bioavailability

AZD6244

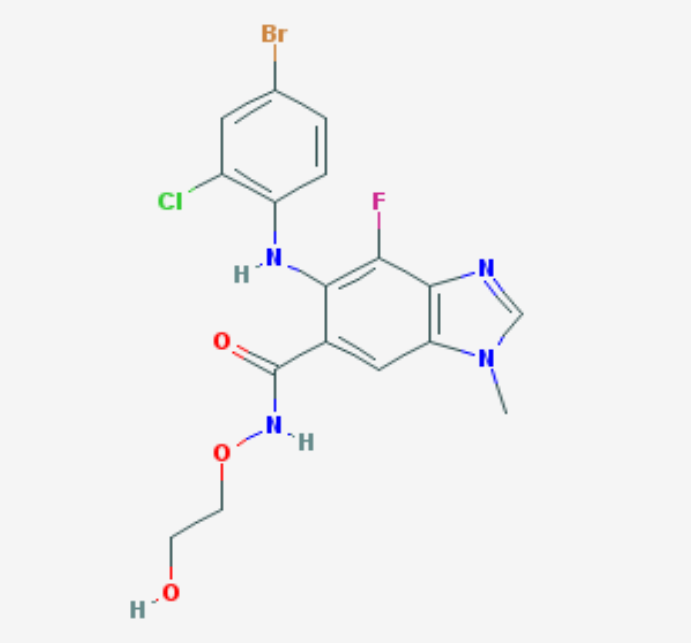

Figure 1-9. The MEK inhibitor AZD6244.

The AZD6244 compound is an ATP-noncompetitive, selective and potent inhibitor of MEK1/2, which prevents Ras-mediated ERK activation. The compound has shown efficacy in various pre-clinical and clinical studies.

and tolerance, and is currently in phase II clinical trials, with more than 40 trials underway (clinicaltrials.gov). AZD6244 **(Figure 1-9)** is a potent and selective, ATP-noncompetitive inhibitor against MEK1/2, demonstrating an IC_{50} of approximately 14 nM. In fact, concentrations of AZD6244 tested against more than 40 different kinases consistently showed selective inhibition of MEK1/2 [92]. Pharmacokinetic studies in mice have demonstrated AZD6244 to effectively inhibit downstream ERK activation at concentrations as low as 10 mg/kg, which are consistent with concentrations administered in clinical trials [93]. Furthermore, pre-clinical reports have shown that AZD6244 demonstrates anti-proliferative and apoptosis induction in several xenograft tumor models, such as colorectal [94], and lung cancer [95], as well as the *in vitro* sensitivity of a panel of breast cancer cell lines [96]. This drug has also been well tolerated in conjunction with chemotherapeutic compounds [94], indicating the potential for combinatorial treatment.

1.7 Thesis overview

As described in more detail below, this thesis concerns an investigation of the effects of PI3K and MEK inhibition on the breast cancer cell line MDA-MB-231-EGFP/Luc2, both *in vitro* and *in vivo*. Additionally, the small molecule inhibitors used, were administered to healthy mice in order to delineate the potential effects of PI3K and/or MEK inhibition on normal bone development. The Xenogen/Caliper bioluminescence imaging system allowed us to quantify tumor growth via the luciferase reporter expressed by the MDA-MB-231-EGFP/Luc2 tumor cells, as a function of photon emission or flux. Micro-computed tomography (μCT) technology allowed evaluations of bone integrity.

1.7.1 Pre-clinical in vivo model of breast cancer bone metastasis

Although *in vitro* and subcutaneous *in vivo* experiments have been useful, much more relevant knowledge can be gained when tumor micro-environments are also taken into consideration. Therefore, this study utilized a model of breast cancer bone metastasis that portrays many of the mechanisms and processes involved in human disease, including cell survival in the circulation, extravasation, colonization at an appropriate microenvironment [21, 97-100], and development of osteolytic lesions through recruitment of stromal components, such as osteoblasts, osteoclasts, macrophages and blood vessels.

1.7.2 Intracardiac injection and xenogen bioluminescence imaging

Our lab has previously established a pre-clinical murine model of breast cancer metastasis based on the introduction of the MDA-MB-231-EGFP/Luc2 cells into the arterial circulation via their intracardiac (IC) injection into nude-beige athymic (NIH-III) mice. Although these cells generate soft tissue metastases, they are particularly prone to developing bone metastases, the primary focus of this study. Thus, following successful injection, mice almost invariably develop unilateral or bilateral knee metastases within the first 2 weeks as seen using bioluminescence imaging. All mice were imaged twice a week (on days 7, 10, 14, 17 and 21), with daily administration of the different inhibitors beginning on day 14 **(Figure 1-10)**. Bioluminescence detection technology allowed us to monitor tumor progression and follow responses to therapeutic treatments non-invasively in real time over the 21 day experimental period.

Variability can occur when performing an intracardiac injection. This can be due to the level of technical skill required, with each injection having a variable level of success, ultimately determining the numbers of cells that enter the arterial circulation. This could theoretically

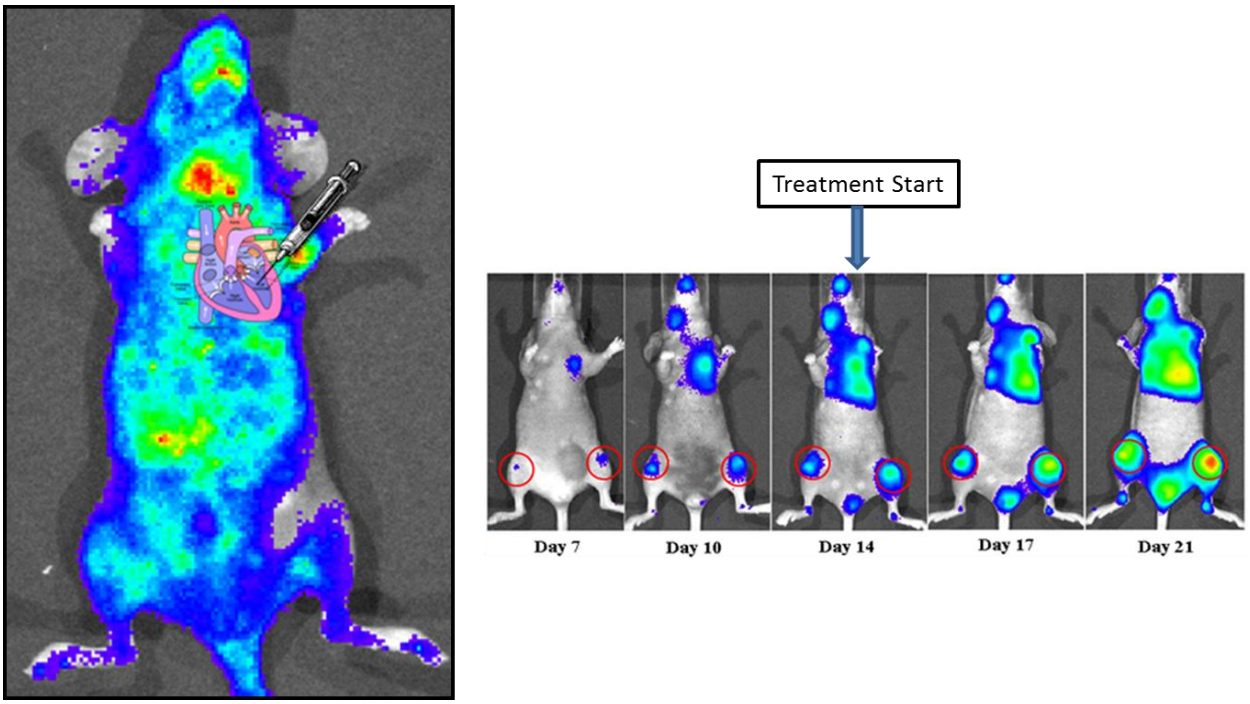

Figure 1-10. Intracardiac injection of MDA-MB-231-EGFP/Luc2 cells: an *in vivo* model of breast cancer bone metastasis.

Injection of MDA-MB-231-EGFP/Luc2 cells into the left ventricle of NIH-III mice results in the frequent establishment of bone metastases. Upon successful injection, an immediate scanning with the Xenogen bioluminescence imaging system reveals full body bioluminescence, indicating a systemic distribution of cancer cells. Successful survival in the blood stream, extravasation, and colonization in the bone microenvironment leads to the establishment of bone metastasis that can be visualized in the first week post IC injection. Tumor progression is monitored throughout the experiment in real-time to assess the effects of different treatments. Abbreviations: IC = Intracardiac.

generate variable levels of metastases due to unequal levels of circulating metastatic cells that could potentially extravasate out of the circulation and colonize at an appropriate site. However, it has been demonstrated that nearly all cells injected by this route are unable to survive and there are only a few cells that are consistently capable of extravasating and colonizing the bone microenvironment to initiate tumor propagation [49]. Therefore, the large numbers of cells injected mean that the level of success of an intracardiac injection does not have a profound effect on the numbers of metastases obtained. However, to reduce any potential variation, only those mice that generated significant knee metastases by day 14, as assessed by Xenogen bioluminescence imaging, were used in the treatment studies. Similarly, if a mouse generated metastases in both knees, only the largest bioluminescence signal was followed for the remainder of the study.

1.7.3 Evaluation of bone integrity using μCT

μCT allows for a quantitative measurement of tumor-induced bone loss. This technology is a non-destructive method to image and quantify complex 3D structures, such as the distal femur and proximal tibia, which is the focus of this study **(Figure 1-11)**. Upon sacrifice on day 21, vehicle-treated controls and drug-treated mice legs were harvested in fixative and scanned with μCT technology. Multiple parameters were measured to evaluate and assess bone integrity including bone mineral density, connectivity density, trabecular number, bone surface and trabecular separation.

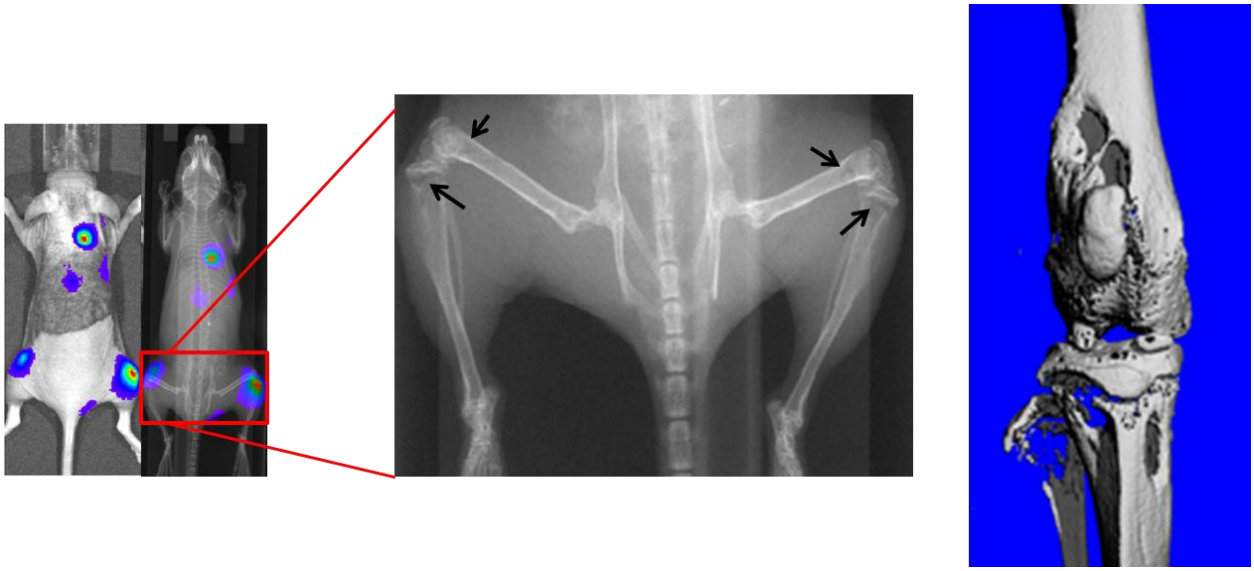

Figure 1-11. µCT as a measure of bone integrity.

µCT was used to generate 3D reconstructed images of bone and also evaluate different bone parameters, such as BMD, in order to determine a qualitative and quantitative measure of bone integrity. Generated bone (knee) metastases, as assessed by bioluminescence imaging can be compared to µCT quantification in order to assess the effect of treatment modalities, such as PX866 PI3K inhibition and/or AZD2644 MEK inhibition, as employed in this study. Arrows are demonstrating sites of radiographically visible tumor-induced osteolytic lesions (middle image). Abbreviations: BMD = bone mineral density.

1.7.4 Hypothesis and aims

1.7.4.1 Main hypothesis

Targeting the PI3K and Ras signal transduction pathways, using small-molecule inhibitors, will effectively target metastatic bone-colonized MDA-MB-231-EGFP/Luc2 cells, and a subsequent alleviation of tumor-induced bone destruction.

1.7.4.2 AIM 1: Investigate the effects of PI3K inhibition on MDA-MB-231 cells *in vitro* and on established bone metastases *in vivo*

The PI3K pathway is one of the most highly mutated pathways in human cancer, with a profound incidence in breast cancer, estimated in upwards of 40% patients [67, 101]. There have been promising results observed in pre-clinical breast cancer studies [102, 103], however these investigations involve the use of *in vitro* cell culture experiments, or subcutaneous *in vivo* models that fail to incorporate the important extracellular cues of the stromal-microenvironment. Additionally, PI3K inhibitors in clinical trials are showing promise in breast cancer patients [83], however, there are no studies currently examining their use in patients with osteolytic breast cancer metastasis.

Owing to the importance of the PI3K pathway in tumorigenesis, there have been considerable efforts in developing small-molecule pathway inhibitors. PX866, developed by Oncothyreon, currently in phase II clinical trials, is a unique irreversible pan-PI3K inhibitor that was employed in this study to determine the effects of PI3K pathway inhibition in an *in vivo* model of breast cancer bone metastasis. It was anticipated that PI3K inhibition with PX866 would reduce the levels of MDA-MB-231-EGFP/Luc2 cytokine and growth factor secretion, thereby diminishing stimulation of ‘the vicious cycle’ of bone metastasis. Furthermore, PX866

was hypothesized to directly reduce the growth of bone-colonized MDA-MB-231EGFP/Luc2 cells due to inhibition of signaling pathway activation from extracellular factors within the bone microenvironment.

1.7.4.3 AIM 2: Investigate the effects of MEK inhibition on MDA-MB-231 cells *in vitro* and on established bone metastases *in vivo*

Activating Ras mutations, as seen in the MDA-MB-231 cell line (KRAS) are infrequent in breast cancer (~5%) [68], however, there is considerable evidence that the Ras pathway is a prominent avenue during breast cancer progression. For example, breast cancer frequently demontrates an amplification of cell surface receptors (eg. EGFR, HER2/Neu), that upon stimulation with extracellular factors, activates the Ras pathway and promotes tumorigenesis [60, 69, 104]. In fact, upwards of 50% of patients demonstrate hyperactive aberrant expression of the Ras-MAPK pathway and is also associated with resistance to chemotherapeutic drugs [66], and an overall shortened survival [60].

Due to the importance of Ras pathway activation in many cancers, including breast cancer, small-molecule inhibitors have been under development. AZD6244, a potent and selective, ATP-noncompetitive inhibitor against MEK1/2, was developed by Array Biopharma/Astrazeneca. This drug has demonstrated significant suppression of tumor growth in an *in vivo* MDA-MB-231 breast cancer subcutaneous model [105]. Furthermore, phase I clinical studies of AZD6244 in breast cancer patients showed a significant reduction in the levels of p-ERK and Ki-67 mitotic indices [106], and is currently undergoing phase II clinical trials [92, 94].

For our study, it was anticipated that AZD6244 would reduce MDA-MB-231-EGFP/Luc2 cytokine and growth factor secretion, thereby diminishing stimulation of ‘the vicious cycle’ of

bone metastasis. Furthermore, AZD6244 was hypothesized to directly reduce the growth of bone-colonized MDA-MB-231-EGFP/Luc2 cells.

1.7.4.4 AIM 3: Investigate the effects of simultaneous PI3K and MEK inhibition on MDA-MB-231 cells *in vitro* and on established bone metastases *in vivo*

Emerging impressions regarding anti-cancer treatments suggest single agent therapeutic approaches are often ineffective due to the complex interactions of multiple signal transduction pathways. Therfore combinatorial treatment is a focus of current research. For example, in an MDA-MB-231 breast cancer subcutaneous xenograft model, PI3K or MEK inhibition alone showed a modest to significant effect on tumor growth, respectively, whereas combinatorial treatment demonstrated tumor regression [80]. Due to sophisticated signaling crosstalk survival mechanisms, simultaneous targeting of the Ras and PI3K pathways is an example of a potentially effective anti-cancer treatment. Interestingly, activation of the PI3K pathway following MEK inhbition [80, 107], or activation of the Ras pathway following PI3K inhibition can lead to resistance [103], likely due to multilevel pathway crosstalk [79]. Further investigation of potential therapeutic benefit targeting the Ras and PI3K pathways is warranted, notably, in the context of tumor-stromal interactions, such as in the microenvironment of osteolytic breast cancer metastases.

Simultaneous inhbition of PI3K and MEK with PX866 and AZD6244 small molecule inhibitors, respectively, was expected to exhibit maximal targeting of bone-colonized MDA-MB-231-EGFP/Luc2 cells and potentially induce a cytotoxic effect and tumor regression.

1.7.4.5 AIM 4: Investigate the effects of PI3K and/or MEK inhibition in normal healthy mice

Because the systemic administration of drugs induces pleiotropic effects on many different cells throughout the body, it was important to examine the effects of PI3K and/or MEK inhibition in the absence of osteolytic breast cancer metastases. Furthermore, because bone-colonized breast cancer cells establish paracrine relationships with resident stromal cells, it was important to investigate if signal pathway inhibition would have any direct effects on cells within the bone microenvironment, such as osteoblasts and/or osteoclasts. The PI3K and Ras pathways are known to be important regulators of osteoblasts and osteoclasts, and therefore PX866 and/or AZD6244 may alter normal bone remodelling. For example, blockade of either of these pathways has demonstrated a significant inhibition of osteoclastogenesis, cell survival, and resorptive function [108, 109]. Studies have also demonstrated crosstalk mechanisms between Ras/Raf and PI3K in osteoclasts to promote differentiation/survival, with simultaneous pathway inhibition resulting in synergistic osteoclast apoptosis [73, 110].

PX866 or AZD6244 administration in healthy mice is anticipated to enhance bone deposition through the reduction of bone resorptive osteoclasts, with simultaneous inhibition of both pathways exhibiting an additive effect.

Chapter Two: **Materials and Methods**

2.1 Cell culture

The human breast cancer cell line, MDA-MB-231, was kindly provided by Dr. T. Guise (University of Virginia, Charlottesville) and confirmed to be free of pathogenic murine viruses and *Mycoplasma spp.* by PCR testing at Charles River Laboratories (Wilmington, MA). The MDA-MB-231 cells were previously transfected by a member of our laboratory, with a plasmid expressing an EGFP-Luc2 fusion gene. Cells were grown in Dulbecco's modified Eagle medium (DMEM; Invitrogen, Grand Island, NY or Sigma, St. Louis, MO) and supplemented with 10% fetal bovine serum (FBS) (Invitrogen, Grand Island, NY), 100 U/mL penicillin, 100 μg/mL streptomycin (Invitrogen, Grand Island, NY) at 37^{o}C in a 5% CO_2 humidified incubator. For selection purposes, transfected MDA-MB-231-EGFP/Luc2 cells were also cultured in media containing 0.8 Geneticin (Invitrogen, Grand Island, NY).

2.2 Inhibitors

PX866 was kindly provided by Oncothyreon for experiments used *in vitro* and *in vivo* in the MDA-MB-231 tumor studies. For *in vivo* experiments in normal mice without tumors, PX866 was purchased from Active Biochem (Maplewood, NJ). AZD6244 used in all *in vitro* and *in vivo* tumor studies was purchased from Axon Medchem (Netherlands), whereas for *in vivo* experiments with normal mice without tumors, AZD6244 was purchased from Active Biochem (Maplewood, NJ). ABT-263 was also purchased from Active Biochem (Maplewood, NJ). Camptothecin was purchased from Sigma (St, Louis, MO).

2.3 Cell viability assay

Growth of MDA-MB-231-EGFP/Luc2 following 72 hour exposure to varying concentrations of PX866 and/or AZD6244 was assessed using 3-(4,5-dimethyl-2-thiazol)-2,5-diphynyl-2H-tetrazolium bromide (MTT reagent; Sigma, St. Louis, MO) according to the manufacturer's instructions. Briefly, 4000 cells were plated in triplicate in a 96 well plate and left overnight to adhere. Media was aspirated and varying concentrations of PX866 and/or AZD6244 were diluted in fresh media and added to the wells. Following 72 hours of exposure to the compounds, 20 ul of 5 mg/mL MTT reagent was added to each of the wells and left to incubate for 4 hours at 37^{o}C for cells to develop the formazan crystal product. Subsequently, the MTT-containing media was aspirated and 150 ul of DMSO (Alfa Aesar, Ward Hill, MA) was added to solubilize the formazan crystals. Absorbance values of the solubilized formazan solution were determined on a Multiskan Ascent microplate reader (Thermo Labsystems, Helsinki, Finland), using a background wavelength of 620 nm and a detection wavelength of 550 nm.

2.4 Cell cycle analysis

Analysis of cell cycle was performed using a flow cytometry-based protocol with propidium iodide (PI) stain. Briefly, 2.0 x 10^{6} MDA-MB-231 cells were plated in a 100 mm plate. Once cells had adhered, the media was replaced with media containing no fetal bovine serum for 24 hours, in order to synchronize the cells prior to the addition of any drugs. It should be noted that this is a relative synchronization, as the MDA-MB-231 cells do not have a complete cell cycle arrest and continue dividing, albeit at a much slower rate. PX866, AZD6244 or combinations of these compounds were added to fresh media containing 10% fetal bovine

serum at a concentration of 2.5 μm. Following a 24 hour exposure to the different compounds, cells were harvested with 0.25% Trypsin-EDTA (Invitrogen, Burlington, ON) for 5 minutes at 37^{o}C, washed first with media containing serum to stop the activity of Trypsin, followed by 2 washes in Dulbecco's Phosphate Buffered Saline (PBS) (Sigma, St Louis, MO) and re-suspended at a concentration of 1.0 x 10^6 cells/mL in ice cold PBS. 1 mL of this cell suspension was added to 9mL of cold 70% EtOH for fixation, and left at -20^{o}C for at least a week before analysis. After a week cells were spun down and washed at least twice with cold PBS, followed by re-suspension in 500 μl of PI/Triton X-100 staining solution, containing RNAase (supplied by the University of Calgary Flow Cytometry Facility), and incubated at 37^{o}C for 15 minutes. Cells were then subjected to flow cytometry, and analyzed using ModFit LT software to assess levels of PI and cell cycle phase.

2.5 Annexin V-FITC/propidium iodide apoptosis assay

A BD Pharmingen (San Diego, CA) FITC Annexin V Apoptosis Detection Kit I was used for *in vitro* apoptosis experiments. MDA-MB-231 cells untransfected with EGFP-Luc2 were cultured up using standard protocol, and 10^5 cells were re-plated in a 6-well plate. The cells were left for 24 hours to adhere, and then media was aspirated and replaced with fresh media, containing either 10% FBS (denoted as 'Full Serum'), or 0.1% FBS (denoted as 'Low Serum') and incubated for an additional 24 hours. Following this, PX866, AZD6244, or a combination of the two compounds, were diluted in the same 10% FBS or 0.1% FBS conditions at a concentration of 2.5 μm and left for 48 hours. Identical experimental procedures were used with ABT-263 (Bcl-2 inhibitor). Non-adherent cells were collected from the media, and adherent cells were gently harvested from the plate using 1x Versene (Life Technologies,Grand Island, NY).

Both non-adherent and adherent cells were combined together from the same wells in order to include all cell populations. Cells were then washed twice with PBS, and once with 1x Binding Buffer, and then resuspended at a concentration of 10^6 cells/ml.100 ul of these suspensions were used for a total of 10^5 cells, and these were first stained with 5µl of Annexin V-FITC in the dark for 15 minutes. Propidium iodide (PI) was then added to the cell suspension directly before acquisition. At least 20,000 cells were acquired with the ATTUNE Focus Cytometer, in 3 independent experiments and analyzed for Annexin V-FITC and PI positive cell staining.

2.6 Luminex cytokine secretion assay

MDA-MB-231-EGFP/Luc2 cells were cultured as previously described to near confluency. The cells were then harvested with 0.25% Trypsin-EDTA, as previously described and 200,000 cells were re-plated in a 12-well plate and left overnight to adhere, which led to near confluency of plates. PX866 and/or AZD6244 were then added to the plates diluted in fresh media at a concentration of 2.5 µm for 48 hours. The supernatant was then collected after the cells and debris had been spun down at 1200 rpm for 5 minutes. The media supernatants were then frozen at -80^{o}C, until the time of analysis. Samples were taken to Eve Technologies Corporation (Calgary, AB) for Luminex analysis to be run on a human 64-plex Cytokine/Chemokine Routine Discovery Assay.

2.7 Preparation of protein lysates and western blots

Plated cells were either treated with drugs in 10% or 0% FBS conditions, depending on the experiment, as indicated in the figures. Cells in 0% FBS were initially plated in 10% FBS and allowed to adhere, followed by a replacement with media containing 0% FBS for 24 hours before

treatment with drugs. Drugs or DMSO (vehicle control) concentrations were diluted in DMEM media. For experiments with IGF-1 stimulation, diluted PX866, AZD6244, or the combination was added to the cells in fresh media for 3 hours, followed by the addition of IGF-1 directly into the media at a concentration of 100 ng/mL. For experiments with EGF stimulation, compounds were added to the cells, and EGF was added at a concentration of 20 ng/mL 30 minutes later and cell lysates collected 2 hours later. Ice cold RIPA lysis buffer containing protease and phosphatase inhibitors (Roche, IN, USA) were used to lyse cells directly on the plate and scraped off with a cell scraper. Following 30 minutes in RIPA buffer solution, lysates were centrifuged at 13,000 rpm for 15 minutes and protein was collected from supernatants. Protein levels were determined using a colorimetric assay with Bio-Rad Protein Dye Reagent Concentrate (CA, USA), using varying concentrations of bovine serum albumin (Bio-Rad, NY, USA) as standards to determine protein levels in the experimental samples. A wavelength of 620 nm was used to determine absorbances with a Multiskan Ascent plate reader (Labsystems). In all *in vitro* experiments, protein extracts were loaded at 30 μg per lane, electrophoresed, transferred to polyvinylidene difluoride membranes (Millipore, MA, USA) with a semi-dry transfer apparatus (Bio-Rad). Membranes were then blocked with 5% skim milk in 1X TBS 0.1% Tween-20, and probed with specific antibodies in 1% skim milk in 1X TBS 0.1% Tween-20 at 4^{o}C overnight on a shaker. The following day membranes were exposed to the corresponding secondary antibodies and detected using Immobilon Chemiluminescent HRP Substrate (Millipore, MA, USA). All primary and secondary antibodies were purchased from Cell Signaling Technology (Boston, MA, USA).

2.8 Mice

All mice were housed in the specific pathogen-free biohazard containment unit at the University of Calgary Animal Resources Centre in compliance with the Canadian Council for Animal Care guidelines and ethics approval from the Animal Care Committee. All mice were allowed to acclimatize to the biohazard unit environment for at least 4 days.

Nude-beige (NIH-III) mice (4-5 weeks old) were purchased from Charles River Laboratories (St. Constant, QC). C57BL/6 mice (4 weeks old) were purchased from Jackson Laboratories (Bar Harbor, Maine).

2.9 Experimental bone metastasis model

Initially, MDA-MB-231-EGFPLuc2 cells were cultured *in vitro* to near confluency, and then harvested and suspended in sterile PBS at a concentration of 2×10^6 cells/mL. In order to generate metastases, 5-6 week old NIH-III mice were anaesthetized by intraperitoneal (i.p.) injection of ketamine/xylene (200mg/kg), followed by an intracardiac (IC) injection of 2×10^5 MDA-MB-231-EGFP/Luc2 cells suspended in 100 ul of PBS into the left ventricle with a 26 gauge needle. Successful entry into the left ventricle was visible by a rapid influx of oxygenated blood into the hub of the needle, and the cell suspension was then injected over a span of 30-40 seconds in order to generate appropriate systemic distribution of the MDA-MB-231-EGFP/Luc2 cells into the arterial circulation. Successful IC injection was assessed by immediate bioluminescence imaging (Xenogen/Caliper Life Sciences, IVIS Lumina, MA). Mice were then placed on a heating pad and allowed to recover. The progression of metastases was monitored with bioluminescence imaging bi-weekly (days 7, 10, 14, 17, 21), and mice were sacrificed on day 21 following the IC injection.

2.10 Drug administration

There were a total of three *in vivo* studies done, in which the drug compounds were administered to mice, all with different treatment regimens, as described below.

2.10.1 7-Day treatment of established bone metastases with PX866 and/or AZD6244

Mice with BLI evidence of knee metastases by day 14 following IC injection were randomly assigned into experimental treatment groups and were administered a volume of 5ml/kg of the various compounds in 50nM of vehicle ((2-Hydroxypropyl)-β-cyclodextrin) (Sigma, St. Louis, MO), by means of oral gavage. This was to ensure similar dosing of the compounds in mice based on their weight. PX866 was administered at a concentration of 3 mg/kg and AZD6244 at a concentration of 25 mg/kg. The simultaneous combinatorial administration of the compounds was given at the same concentrations described above. The treatment regimen with PX866 and/or AZD6244 began on day 14, daily, until the end of the experimental end date, day 21, for a total of 7 days of administration. A control group was administered 5ml/kg of vehicle only.

2.10.2 3-Day treatment of late-stage metastases with AZD6244

Following a successful IC injection, bioluminescence of knee metastases was monitored, and once the total photon fluxes (photons/s) reached an average of 10^7, which was taken as an indication of a late-stage tumor, a 3-day drug treatment regimen was commenced. Mice were randomly assigned into experimental treatment groups and were administered AZD6244 (25mg/kg) in vehicle, or vehicle only as a control group, for 3 days.

2.10.3 14-Day treatment of normal mice with PX866 and/or AZD6244

Normal C57BL/6 mice without knee metastases were administered 5 ml/kg of either PX866 (3 mg/kg), AZD6244 (25 mg/kg), or a combination of both compounds at the same concentrations (Combo group), daily for 14 days. Again, there was also a control group administered only vehicle (2-Hydroxypropyl)-β-cyclodextrin (50 mM) (Sigma, St. Louis, MO). For this study n=6 mice for all treatment groups.

2.11 Harvesting mouse tissues

Upon sacrifice, the legs (femur and tibia), were harvested and initially fixed in 4% paraformaldehyde (PFA) (Acros Organics, New Jersey, USA) for 24 hours, followed by scanning by μCT. The harvested legs were then put into fresh 4% PFA for a period of 7 days for appropriate fixation, followed by 14 days of decalcification in 14% EDTA (Avantor, Phillipsburg, NJ). Once the bone tissue was sufficiently decalcified, the legs were sectioned at 6-8μm for immunohistochemistry and histology.

2.12 Bioluminescence imaging

Mice received *D*-luciferin (Gold Bio Techhnology, St. Louis, MO) at a dose of 150 mg/kg i.p. injection, and anaesthetized with 2% isofluorane. After 10 minutes, mice were placed in the light-tight imaging chamber and maintained on 1.5% isofluorane. A Xenogen/Caliper IVIS Lumina system (Caliper Life Sciences) was then used for image acquisition. This instrument has a highly sensitive cooled charge coupled device (CCD) camera. Parameters used for imaging are as follows: f/stop 1, bin 4, field of view 12.5cm and exposure times ranged from 20s to 5 min, depending on the strength of the bioluminescent signal. These parameters were kept consistent

throughout the experimental treatment groups. Mice were imaged in the ventral position, and signal intensity was quantified with the Living Image 3.0 software, as total photon flux (photons/s) in a uniform region of interest (ROI) placed over the knee region of the legs. For *ex vivo* imaging, organs were dissected out, placed in a 24-well plate containing PBS and *D*-luciferin and imaged for 1 minute to detect the presence or absence of soft-tissue metastases.

2.12.1 7-Day treatment study bioluminescence imaging

If mice generated metastases in both legs by day 14, the leg with the largest bioluminescence signal was followed for the remainder of the experiment and used for data analysis in order to reduce variability between treatment groups. Numbers of legs included in the analysis were n=8 for the 'PX866,' n=6 for the 'AZD6244,' n=12 for the 'combo,' and n=16 for the 'vehicle' group.

2.12.2 3-Day treatment study bioluminescence imaging (late-stage knee metastases)

If mice generated metastases in both knees, the largest BLI signal was followed for the remainder of the experiment. The largest BLI signal was used to assess when the 3-day treatment regimen began (10^7 photons/s BLI) and used for all data analysis in order to reduce variability between treatment groups and individual mice. Numbers of legs included in the analysis were n=5 for 'AZD6244,' and n=6 for the 'vehicle' group.

2.13 μCT

Bone loss as a result of colonized MDA-MB-231-EGFP/Luc2 cells was assessed by μCT. At 21 days post-intra-cardiac injection, mice were sacrificed and tissues harvested. Legs were

dissected, cleared of the majority of soft tissue and placed in 4% paraformaldehyde for 24 hours, and then placed in fresh fixative.

2.13.1 Mouse tumor studies

For scanning, a maximum of 6 legs were placed in a cylinder sample holder for the μCT instrument (VivaCT 40, Scanco Medical, Brüttisellen, Switzerland.) and the whole leg was scanned. Serial tomographic slices were acquired with 10 μm high resolution at 70kVp, 114 μA and 250 ms integration time. 3D reconstructed images and analysis was done separately on a 2.5 mm region of the distal femoral growth plate, and the proximal tibial growth plate.

2.13.2 Normal mouse study

On days 0, 7, and 14 of treatment, a consistent measurement of the distal femur growth plate and the proximal tibia growth plate of mice legs were scanned *in vivo* using isofluorane anesthesia. Serial tomographic slices were acquired with 15 μm resolution, at 55kVp, 145 μA and 200ms integration time.

2.14 Immunohistochemistry

All slides used for histological examination were baked at 60^{o}C for 15 minutes to loosen the paraffin wax, followed by chemical deparaffinization with two changes of xylene (VWR, West Chester, PA). This was followed by subsequent changes of decreasing concentrations of ethanol (100%, 95%, 70%), and final rehydration in distilled water. Following staining of the slides as described below, an exact reverse process of dehydration was done (with exception to the TUNEL stain – explained below), and completed with mounting and cover slipping.

2.14.1 Tri-chrome stain

A tri-chrome stain was done by Leona Barclay for histological examination of tumor and normal mouse studies. Briefly, hydrated sections were placed in hematoxylin gill No. 2 (Sigma, St. Louis, MO) for 20 minutes, followed by a wash in water for 5 minutes. Then, slides were placed into fast-green stain for 5 minutes and 1 minute in 1% acetic acid and a quick rinse with water. Finally, slides were placed in Saf-O stain for 2 minutes.

2.14.2 TRAP stain

TRAP staining protocol was done as manufacturer's directions from the Acid Phosphatase Leukocyte kit for TRAP staining (Sigma, St. Louis, MO). Briefly, hydrated sections were placed in incubation buffer (45mL dH_2O, 0.5mL Napthol, 2mL Acetate solution, 1mL Tartrate), for 25 minutes in a 37^{o}C water bath. Slides were then placed in a colour solution (1:1 GBC fast garnet and Nitrite solution) for approximately 2-5 minutes, watching for a maroon-brown colour reaction to occur. A counterstain was then done with hematoxylin gill No.2 for 2 minutes, followed by quick rinses in PBS and dH_2O.

2.14.3 TUNEL stain

For TUNEL staining, an ApopTag Plus Peroxidase In Situ Apoptosis Detection Kit (Millipore, Temecula, CA) was used, as per the manufacturer's protocol. Briefly, an initial pre-treatment was done directly on the slides with 20 μg/mL proteinase K (Invitrogen, Grand Island, NY) for 15 minutes and washed in dH_2O for 2 minutes. Equlibration buffer was then added to slides for up to 1 minute and then tapped off. Working strength TdT enzyme was then added to the slides and incubated at 37^{o}C for 1 hour. A stop/wash buffer was added to slides for 1 minute

at room temperature, followed by 3 changes in PBS for 1 minute each. Room temperature anti-digoxignenin conjugate was applied and placed in a humidifier chamber for 30 minutes, followed by 3 changes of PBS for 1 minute each. Peroxidase substrate was then applied directly to slides for colour development for approximately 5 minutes, watching for reaction to take place. Counterstain with 0.5% methyl green was done for 10 minutes at room temperature in a coplin jar. Slides were then washed in dH_2O 3 times for 1 minute each, followed by 3 changes of 100% N-Butanol for 1 minute each, and a final 3 changes of Xylene at 2 minutes each.

2.15 Statistical analysis

All data were plotted as mean +/- standard error of the mean (SEM) and statistical analysis was performed using one-way or two-way ANOVA, depending on the nature of the data, with Bonferonni post-tests to determine statistical significance, in Graphpad Prism 4.03 software.

Chapter Three: **The effect of PI3K and/or MEK inhibition using small-molecule inhibitors on MDA-MB-231 bone metastases**

3.1 Confirmation of PI3K and MEK inhibition with PX866 and AZD6244 *in vitro*

In order to ensure that PX866, and AZD6244 would be effective at inhibiting PI3K, and MEK, respectively, in bone-colonized MDA-MB-231 cells *in vivo*, these compounds were first examined *in vitro*. It should be noted that PX866 and AZD6244 were purchased from two different sources, and were confirmed for similar effects of pathway inhibition *in vitro.*

MDA-MB-231 cells have a low basal level of PI3K activity and p-AKT. Therefore, the cells were stimulated with IGF-1, resulting in an induction of p-AKT. In the presence of PX866, IGF-1-stimulated PI3K activity and AKT phosphorylation was blocked. Similarly, the high endogenous level of Ras pathway activity and downstream p-ERK was inhibited with AZD6244 exposure. The simultaneous inhibition of both pathways resulted in further inhibition of common convergent downstream components, such as p-S6 and p-mTOR. Interestingly, increased concentration of PX866 resulted in additional inhibition of p-S6, whereas increased concentration of AZD6244 demonstrated elevated levels of p-S6. Additionally, the presence of the AZD6244 MEK inhibitor, followed by IGF-1 stimulation, demonstrated a slight enhancement of AKT phosphorylation (**Figure 3-1)**. Crosstalk between these pathways has been established in an EGF-dependent manner [79], however it is possible that other signaling modalities can induce such compensatory pathway communication, such as with IGF-1 (or other factors), as seen here. IGF's are produced by osteoblast cells and are also the most abundant growth factors within the bone matrix. Furthermore, increased IGFR signaling in MDA-MB-231 cells demonstrated enhanced metastatic bone disease [111]. Therefore, this axis could be an

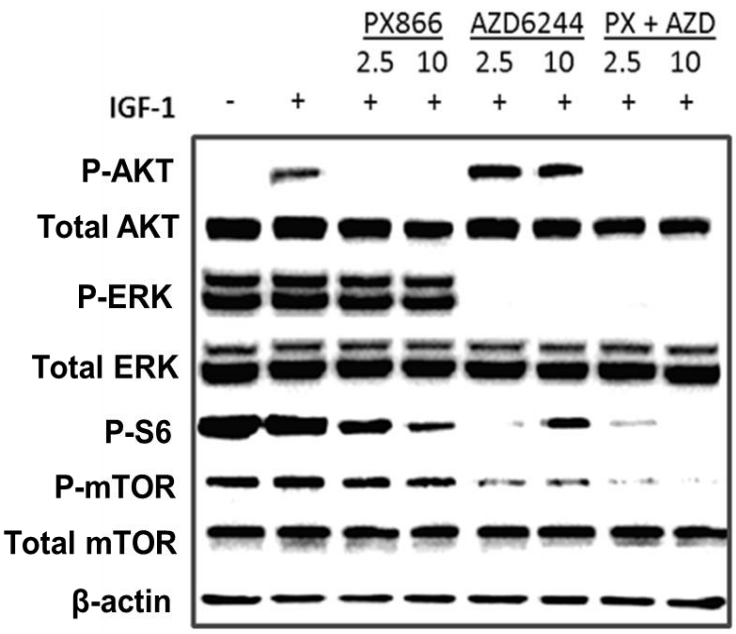

Figure 3-1. Confirmation of PI3K and MEK inhibition with PX866 and AZD6244.

Following stimulation with IGF-1 a strong induction of p-AKT occurs in cultured MDA-MB-231 cells. In the presence of the PI3K inhibitor PX866, IGF-1 stimulated p-AKT is blocked. Furthermore, Ras pathway activity and downstream ERK phosphorylation were effectively inhibited by AZD6244. The simultaneous inhibition of both pathways resulted in the further inhibition of downstream components, as reflected by decreased S6 and mTOR phosphorylation. However, an increased concentration of AZD6244 led to elevated levels of p-S6. Furthermore, the presence of the AZD6244 MEK inhibitor, followed by IGF-1 stimulation, demonstrated enhanced AKT phosphorylation. Blot shown is representative of three independent experiments.

important form of cellular signaling within the bone microenvironment, with simultaneous PI3K and MEK inhibition demonstrating maximal downstream pathway inhibition.

3.1.1 Examination of PI3K and Ras signaling pathway crosstalk in vitro

A strong induction of p-AKT occurred following MEK inhibition and stimulation with EGF, as compared to EGF stimulation alone **(Figure 3-2A)**, indicating that pathway crosstalk and feedback loops exist between these pathways. Although this has been demonstrated before, it was important to verify that the MDA-MB-231 cells used in this study exhibit crosstalk between PI3K and Ras components. This may be experimentally and clinically relevant, as a high proportion of breast cancer patients exhibit overexpression of the EGFR-Ras-MAPK cascade [60], and the MDA-MB-231 cells harbor similar features. Additionally, in serum-containing media conditions, there was an increase in p-AKT following MEK inhibition **(Figure 3-2B)**, in the absence of EGF stimulation. This indicates that PI3K and Ras signaling crosstalk may not be completely reliant on the presence of potent extracellular ligand-receptor activation, and media-containing serum may be sufficient for this to occur. This implies that inhibition of constitutively activated oncogenic signaling pathways that do not require upstream receptor activation, may also lead to crosstalk, enhanced survival and therapeutic resistance. Collectively, it is evident that crosstalk between PI3K and Ras is possible in MDA-MB-231 cells and can be examined in an appropriate *in vivo* model of breast cancer bone metastasis.

Simultaneous exposure to PX866 and AZD6244 was able to effectively eliminate the observed feedback loop, as demonstrated by loss of p-AKT and P-ERK. Downstream components were also further reduced, such as P-S6 and P-mTOR levels, which are important regulators of protein translation and cell growth. These results suggest that the simultaneous

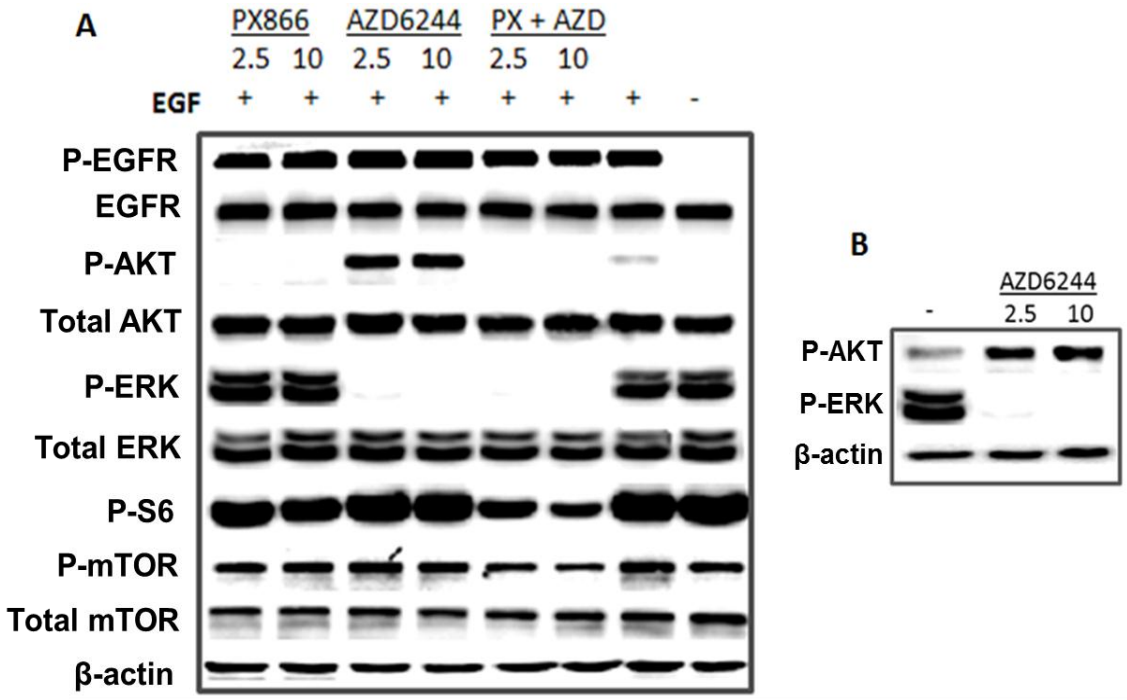

Figure 3-2. PI3K and Ras signaling pathway crosstalk in MDA-MB-231 cells.

Following stimulation with EGF in non-serum containing media conditions, a strong induction of p-Akt was evident following inhibition of MEK with AZD6244, as compared to EGF stimulation alone. Simultaneous inhibition of both pathways with PX866 and AZD6244 was able to completely ablate p-AKT and p-ERK induction, and also reduce downstream convergent components such as p-S6 and p-mTOR. (B) An increase of p-AKT levels occurred following MEK inhibition in serum-containing media conditions, without addition of EGF receptor stimulation. This demonstrates that pathway crosstalk and feedback loops exist between these pathways, which may be significant *in vivo*. Blots shown are representative of three independent experiments.

inhibition of these pathways may provide maximal dampening of signaling pathway activation and eliminate crosstalk and feedback loops that might otherwise lead to resistance with administration of either compound alone.

3.2 The effect of PX866 and/or AZD6244 on MDA-MB-231 cells *in vitro*

In order to assess and interpret potential consequences of PX866 and/or AZD6244 *in vivo,* several *in vitro* experiments were used to determine the effects on cell viability, cell cycle, and cell death of cultured MDA-MB-231 cells.

3.2.1 Cell viability

The 3-(4,5-dimethyl-2-thiazol)-2,5-diphynyl-2H-terazolium bromide (MTT) assay is a colorimetric method for quantifying viable cells. It allows detection of functioning mitochondria that are able to convert MTT into formazin crystals, which can be dissolved and quantified using a spectrophotometer. Thus, the MTT assay is able to quantifiably measure viable cells that harbor functioning mitochondria. However, a caveat of this assay is that it cannot provide a mechanism for changes in cell viability due to certain treatment conditions, such as cytostasis or cytotoxicity. The MTT result is an assumed effect on cell proliferation, however to confirm this cell counts would also be necessary. As a substitute, flow cytometry based cell cycle analysis and apoptosis/necrosis assays were performed, following any effect observed.

The MTT assay was first used to determine whether the compounds had any effect on reducing MDA-MB-231 cell viability following 72 hour exposure. PI3K inhibition had no significant effect on cell viability at all concentrations examined, whereas MEK inhibition demonstrated a much more robust reduction of viable cells in a dose dependent manner **(Figure**

3-3). Exposure to both compounds resulted in a similar pattern to MEK inhibition alone, with a slight further reduction. This latter reduction in cell viability was most likely due to a further decrease in downstream signaling effectors that are responsible for growth, translation, cell cycle progression and survival.

3.2.2 Cell cycle analysis

We next investigated if the effects of pathway inhibition on MDA-MB-231 cell viability were due to a cytostatic mechanism that is by inducing cell cycle arrest and therefore reducing the proportion of actively proliferating cells. Using a flow cytometry-based cell cycle analysis, a quantifiable measure of DNA content is obtained following exposure to propidium iodide (PI), which has a strong affinity for DNA. Therefore, the relative ratios of cells in different phases of the cell cycle can be determined.

We found that PI3K inhibition resulted in a similar cell cycle profile to that of cells without treatment. In contrast, MEK inhibition induced a significant G1 cell cycle arrest, and the combination of PI3K and MEK inhibition resulted in nearly 100% of the cells being arrested in G1 **(Figure 3-4)**. This type of cell cycle arrest has been attributed to the PI3K and ERK1/2 MAP kinases cooperative role in sustaining proliferative signals through cyclin-depdendent kinases, cyclin D1 as well as cellular machinery involved in cell growth such as mTOR, eIF4E and S6 [112].

3.3 Cell apoptosis and necrosis

Although it was demonstrated that MEK inhibition lead to G1 cell cycle arrest, it was possible that sustained impediment of transition through cell cycle checkpoints would eventually

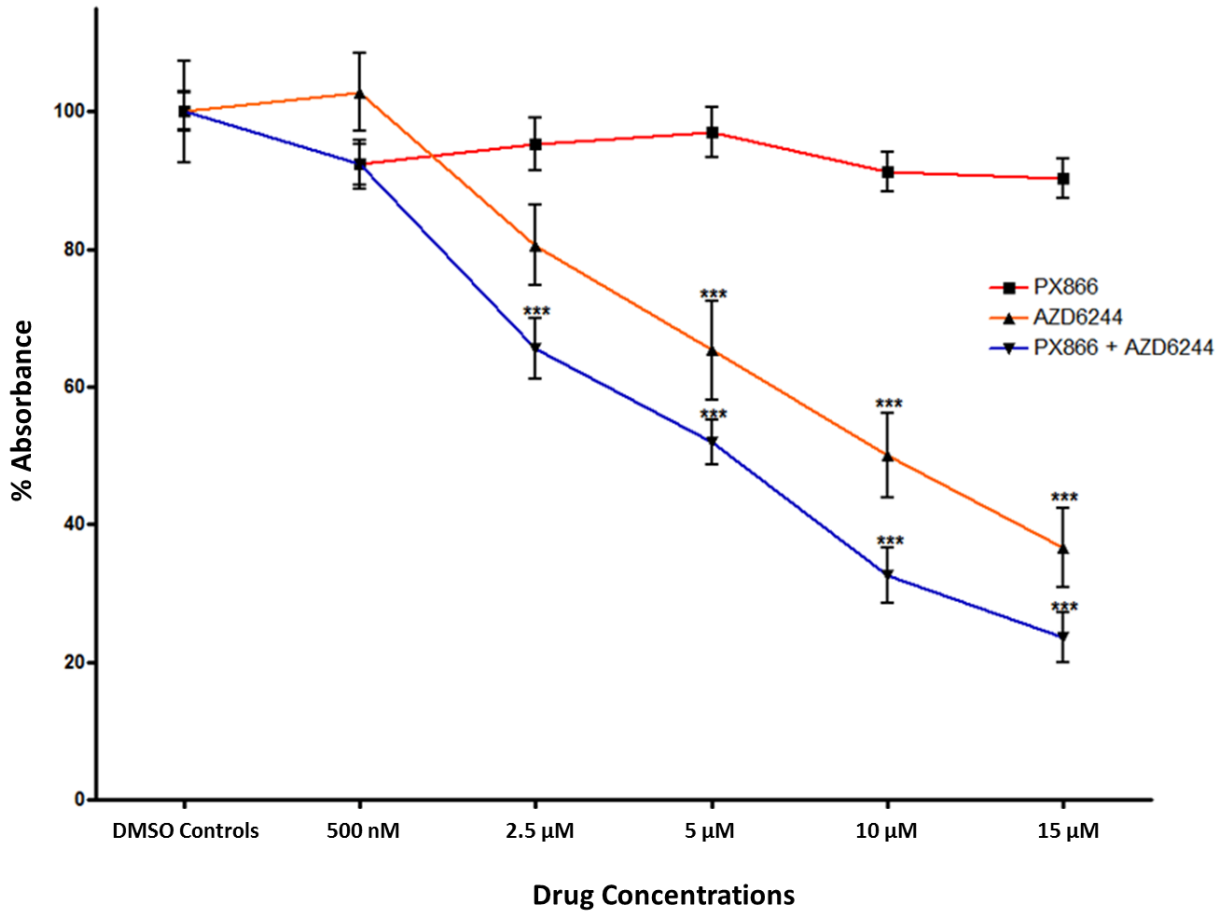

Figure 3-3. Cell viability following PI3K and/or MEK inhibition.

Following a 72 hour exposure to PX866, AZD6244 or the combination of both compounds cell viability was quantified by means of an MTT assay. PI3K inhibition with PX866 resulted in no appreciable reduction in cell viability at all concentrations tested. In contrast MEK inhibition with AZD6244 resulted in a much more robust decrease in viable cells, with the combination of both compounds resulting in a slight further reduction, in a dose dependent manner Data represents three independent experiments, each in triplicates, and is plotted as the mean ± SEM. Asterisks indicate statistical significance (* $p<0.05$; ** $p<0.01$; *** $p<0.001$).

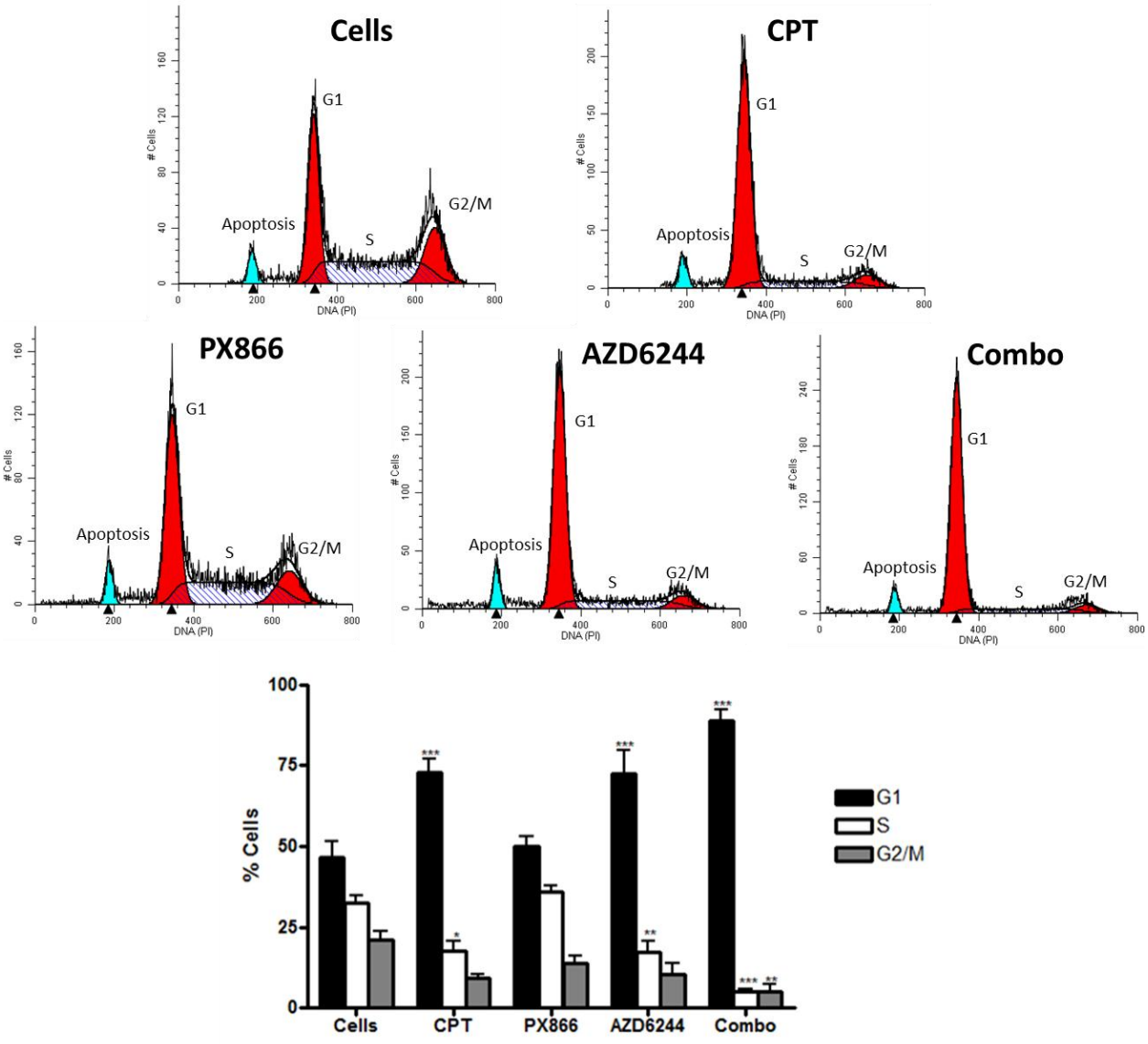

Figure 3-4. Cell cycle analysis following PI3K and/or MEK inhibition.

Using a flow cytometry-based analysis, propidium iodide (PI) was used to determine the level of genetic material, and therefore the phase of the cell cycle. Camptothecin, used as a positive control, demonstrated a modest induction of G1 cell cycle arrest. PI3K inhibition resulted in a similar cell cycle profile to that of cells without treatment. MEK inhibition induced a significant G1 cell cycle arrest, and the combination of PI3K and MEK inhibition resulted in nearly 100% of the cells arrested in G1 phase. Representative cell cycle analysis plots are also included, demonstrating the relative PI peaks in each treatment group. Data represents three independent experiments and is plotted as the mean ± SEM. Asterisks indicate statistical significance (* $p<0.05$; ** $p<0.01$; *** $p<0.001$).

lead to cell apoptosis or necrosis. Thus, the observed reduction in cell viability could also have been due to a combination of cell cycle arrest and apoptosis induction. An Annexin V-FITC PI apoptosis assay was therefore carried out following exposure to each of the compounds alone, as well as in combination. Annexin-V has a strong binding affinity to exposed outer membrane phosphatidylserine, which can signal the start of apoptosis, and also serves as a trigger for phagocytic recognition of an early apoptotic cell [113]. PI, as previously mentioned, has a strong binding affinity for DNA, and therefore, if the outer cell membrane is compromised, as occurs in late apoptotic or necrotic cells, PI will penetrate and bind to nuclear DNA. Therefore, Annexin-V+/PI- is an indication of early apoptosis, whereas Annexin-V+/PI+, or PI+ is an indication of late apoptotic/necrotic cells [114].

It was determined that basal levels of apoptosis and/or necrosis in MDA-MB-231 cells without any treatment (DMSO control) was on average 8.8%, including all positive staining for Annexin-V-FITC and PI together. PX866 PI3K inhibition resulted in an average of 7.9%, AZD6244 MEK inhibition an average of 10.9%, and the simultaneous inhibition an average of 11.05% positive staining for apoptosis and/or necrosis **(Figure 3-5)**. The individual levels of Annexin-V+/PI- (early apoptosis), Annexin-V+/PI+ or PI+ (late apoptosis/necrosis), were similar across all treatment groups, as well as the control population with no treatment. Camptothecin, a topoisomerase I inhibitor, was used as a positive control, and demonstrated significant induction of total cell apoptosis and/or necrosis with an average of approximately 30%, with the majority of these cells staining positive for both Annexin-V and PI **(Figure 3-5)**. Therefore, taken together these results suggest that PI3K inhibition has little to no effect on MDA-MB-231 cells, whereas MEK inhibition results in significant cytostasis, but not cytotoxicity. Surprisingly, the combination of both compounds did not result in any dramatic additive or synergistic effect

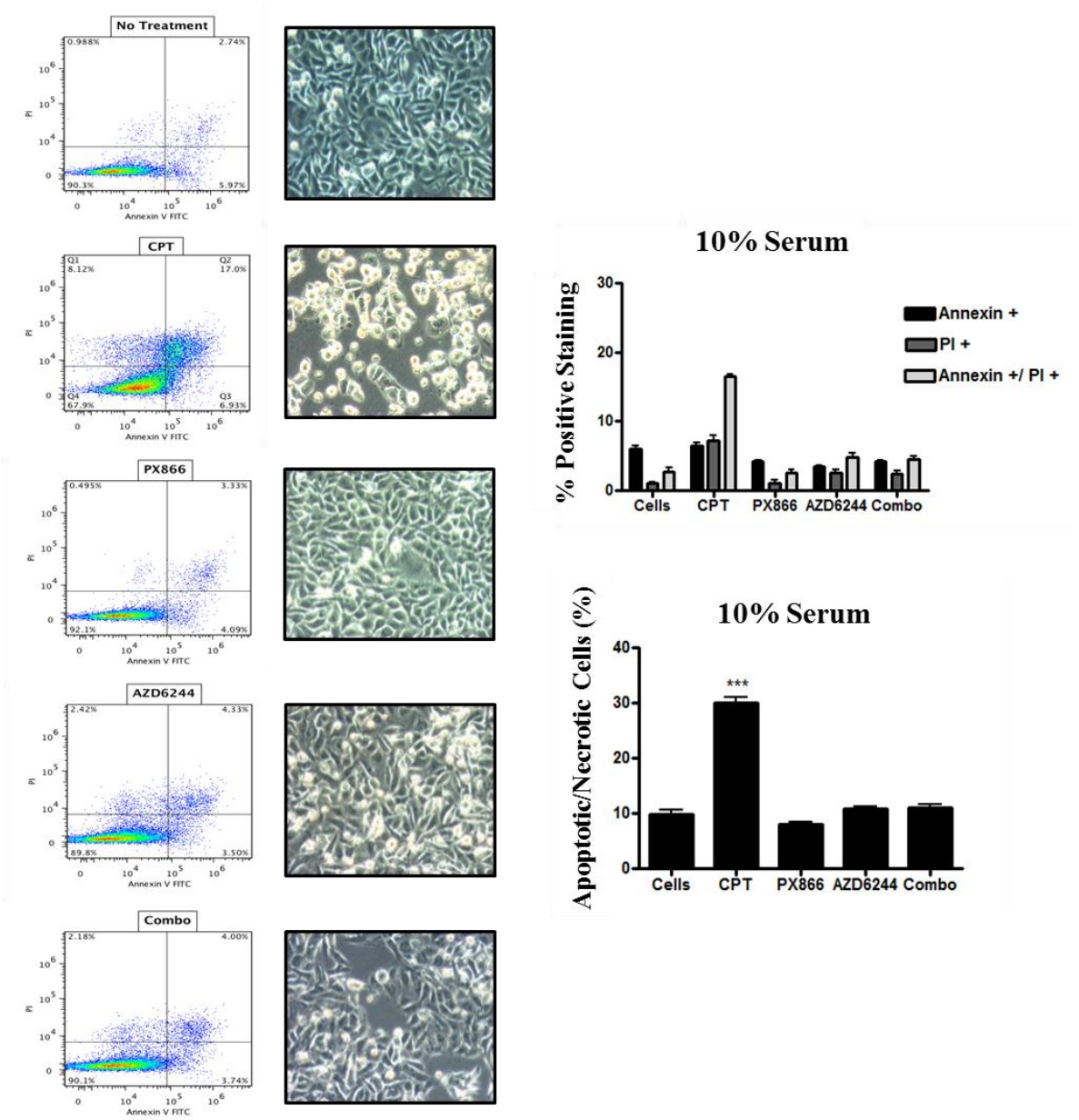

Figure 3-5. Apoptosis/necrosis analysis following PI3K and/or MEK inhibition.

A flow cytometry-based analysis was carried out to determine levels of apoptosis and/or necrosis following exposure to PI3K and/or MEK inhibition. Camptothecin was used as a positive control and resulted in significant positive staining of about 30% of cells, with the majority of these cells staining for both Annexin V-FITC and PI. Exposure to PX866 or AZD6244 alone and in combination did not result in any significant levels of apoptosis and/or necrosis. The individual levels of Annexin-V+/PI- (early apoptosis), Annexin-V+/PI+ or PI+ (late apoptosis/necrosis), were similar across all treatment groups, as well as the untreated control population. Data represents three independent experiments and is plotted as the mean ± SEM. Asterisks indicate statistical significance (* $p<0.05$; ** $p<0.01$; *** $p<0.001$).

on inducing apoptosis, however, demonstrated a slightly more potent effect on G1 cell cycle arrest. This implies that in serum-containing media conditions, other mechanisms are responsible for the survival of MDA-MB-231 cells following exposure to PI3K and MEK inhibition.

3.4 MDA-MB-231 cytokine and chemokine cell secretion *in vitro*

Bone-colonized breast cancer cells undoubtedly produce and secrete extracellular growth factors and cytokines in the bone microenvironment. As such environmental cues are thought to be important in the 'vicious cycle' and ultimately perpetuate the outgrowth of bone metastases leading to local bone loss, it was important to determine if these PI3K and MEK inhibitors had any potential effect on reducing cytokine and growth factor secretion *in vitro.* This was determined with a Luminex assay of cell culture supernatants.

3.4.1 PI3K and/or MEK inhibition effects on MDA-MB-231 cytokine secretion in vitro

PI3K inhibition, after a 48 hour exposure to PX866, did not demonstrate any significant attenuation of cytokine or growth factor secretion, with the exception of TGF-α, and therefore this inhibitor could theoretically result in a reduction of EGFR autocrine signaling. In contrast, MEK inhibition, after a 48 hour exposure to AZD6244, significantly reduced the secretion of a number of factors, including G-CSF, GM-CSF, MCP-1, PDGF, IL-8 and TGF-α **(Figure 3-6)**. Importantly, these factors have been implicated in the recruitment of monocyte/macrophage precursor cells, and the activation, proliferation and differentiation of osteoclasts either directly, at the level of the monocytic precursors, or indirectly, via regulation of osteoblast-derived RANKL. Interestingly, G-CSF is used to treat chemotherapy-induced neutropenia, however, there is strong evidence that it is associated with increased osteoclast numbers and decreased

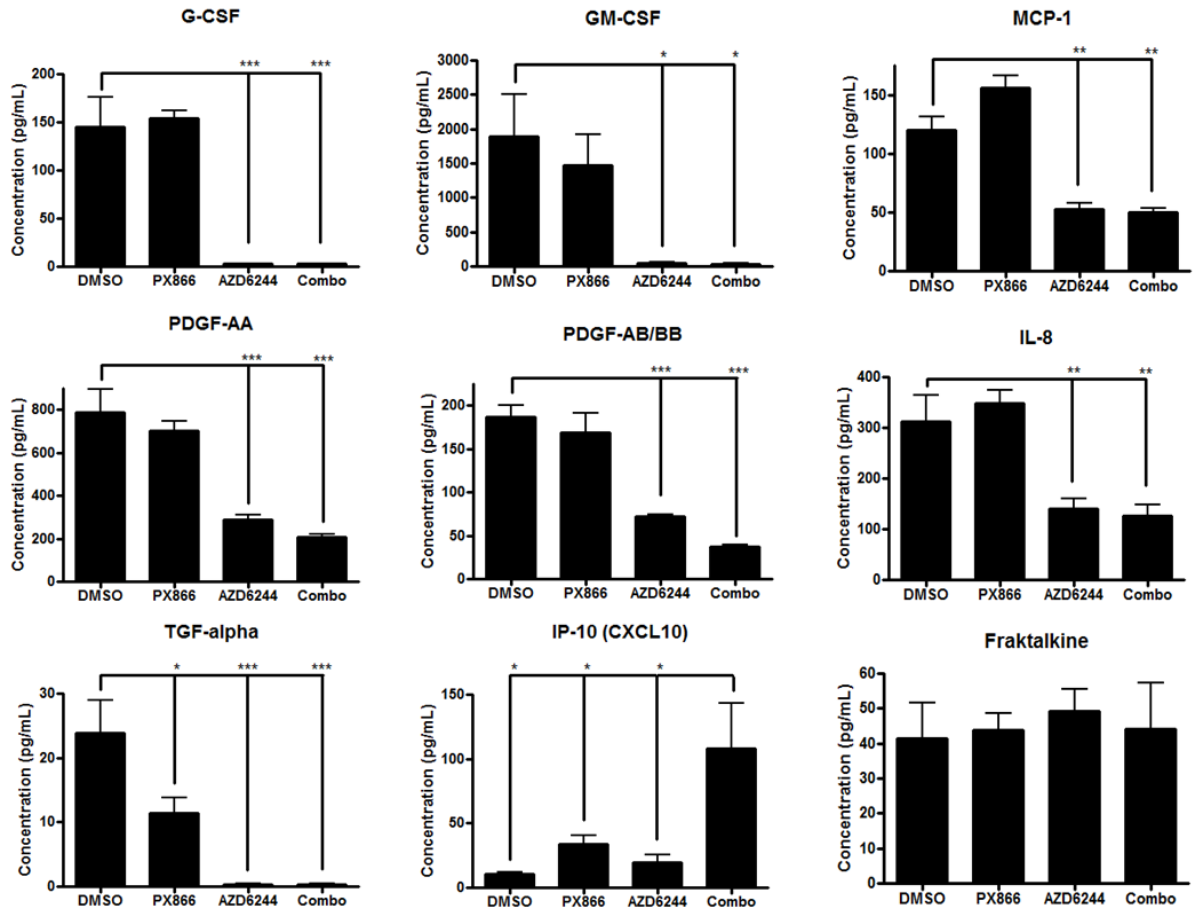

Figure 3-6. Luminex analysis following PI3K and/or MEK inhibition.

PX866 exposure did not demonstrate any significant attenuation of cytokine or growth factor levels in MDA-MB-231 supernatants, with the exception of TGF-α. In contrast, AZD6244 significantly reduced the secretion of a variety of factors, such as G-CSF, GM-CSF, MCP-1, PDGF, IL-8 and TGF-α, all of which have been implicated in autocrine and paracrine loops within the 'vicious cycle of bone metastasis.' Data represents three independent experiments and is plotted as the mean ± SEM. Asterisks indicate statistical significance (* $p<0.05$; ** $p<0.01$; *** $p<0.001$).

bone mineral density [115], indicating that this treatment may exacerbate metastatic osteolysis. GM-CSF expression has been implicated in enhanced osteoclastogenesis caused by MDA-MB-231 cells, as well as by human breast cancers [51]. MCP-1 has many functions, such as monocyte and macrophage recruitment, angiogenesis, and the promotion of tumor growth [116]. IL-8 can play a dual role, as cancer cell secretion generates an autocrine-loop that can self-promote cancer growth, in addition to its role as a potent direct inducer of osteoclastogenesis [117, 118]. IL-8 has also been detected at high levels in the serum of breast cancer patients, and has been associated with breast cancer bone metastasis [119]. TGF-α has been similarly implicated in tumor-promotion in an autocrine fashion through stimulation of cancer cell EGFR, and is also associated with increased bone turnover [120]. This signaling axis could also provide one explanation for high Ras-MAPK activity associated with breast cancer bone metastasis.

MDA-MB-231 cells that were simultaneously exposed to PX866 and AZD6244 resulted in a similar cytokine secretion profile to that of AZD6244 MEK inhibition alone. However, the combination resulted in enhanced secretion of the chemokine IP-10. Although this factor has not generated much interest in the context of bone metastasis, it is regarded as a potent factor in the recruitment, proliferation and differentiation of osteoclast precursors, as well as in chemotaxis and adhesion of multinucleated osteoclasts to the bone interface [53]. Therefore, it is possible that the combined administration of PI3K and MEK inhibitors may actually enhance osteoclastogenesis, thus functioning to exacerbate bone destruction, via the enhanced recruitment of osteoclast precursors to the tumor-bone microenvironment.

3.5 The effect of PX866 and AZD6244 on established bone metastasis

As previously mentioned, the intracardiac injection of MDA-MB-231 cells into the left

ventricle of nude NIH-III mice frequently results in distant metastasis, and serves as a model of osteolytic breast cancer metastases. Upon successful injection and systemic distribution of MDA-MB-231-EGFP/Luc2 cells, mice were imaged for knee bioluminescence on days 7, 10, 14, 17 and 21 post IC injection, and mice with established bone metastases were started on day 14 with daily treatment of PX866 and/or AZD6244. μCT bone parameters and qualitative images of bone integrity were also obtained upon sacrifice on day 21 and correlated with results of BLI.

3.5.1 Treatment efficacy as assessed by tumor bioluminescence

Daily administration of PX866 at a concentration of 3mg/kg did not result in a significant reduction of tumor bioluminescence over the 7-day treatment period. At day 21 there was a slight reduction of knee photon emission rates, however there was no evidence that the growth kinetics of bone-colonized MDA-MB-231-EGFP/Luc2 cells was significantly attenuated. In contrast, MEK inhibition resulted in a much more robust attenuation of knee photon emission throughout the treatment period **(Figure 3-7)**, showing approximately 1 log difference as compared to vehicle-treated controls at day 21 **(Figure 3-8)**. The combination of PX866 and AZD6244 resulted in reductions in bioluminescence, similar to those seen with AZD6244 administration. There was no initial indication of tumor regression, as indicated by losses of bioluminescence. Instead, photon fluxes plateaued throughout the treatment period, suggesting growth inhibition without major cell death. Similar to the results of the *in vitro* experiments, the combination of both compounds did not result in any additive or synergistic effects reduction of knee tumor bioluminescence **(Figure 3-7/3-8)**. The data suggests that combination therapy using PI3K and MEK inhibitors may not be as effective as hypothesized.

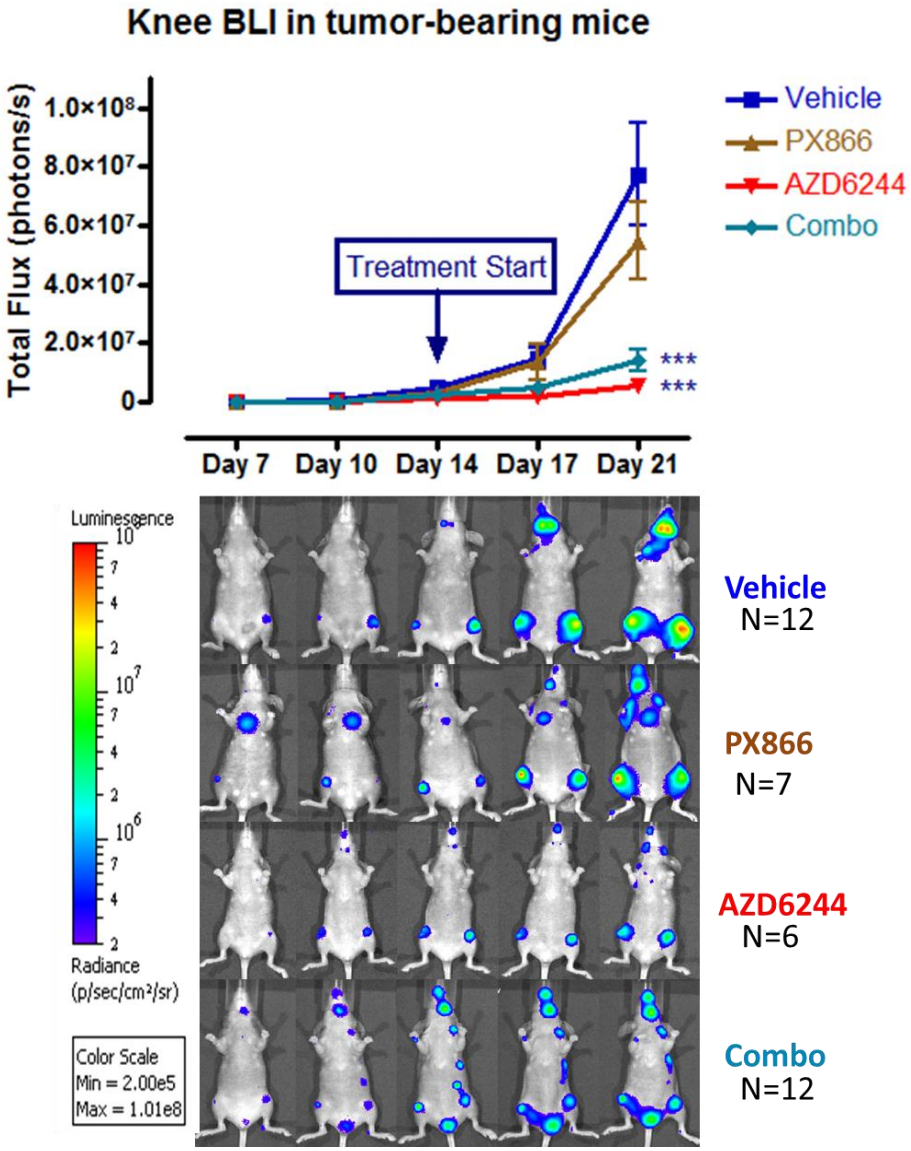

Figure 3-7. The effect of PX866/AZD6244 on MDA-MB-231-EGFP/Luc2 bone metastasis.

Daily administration of PX866 at a concentration of 3mg/kg for 7 days did not result in a significant reduction of tumor bioluminescence. In contrast, MEK inhibition resulted in a much more significant attenuation of knee tumor bioluminescence throughout the treatment period. The combination of both compounds did not result in any additive reduction in tumor bioluminescence, demonstrating similar growth kinetics to MEK inhibition alone. 'Vehicle' control group n=12, 'PX866' n=7, 'AZD6244' n=6, 'Combo' n=12. Data plotted as mean ± SEM. Asterisks indicate statistical significance (* $p<0.05$; ** $p<0.01$; *** $p<0.001$), relative to vehicle-treated control mice.

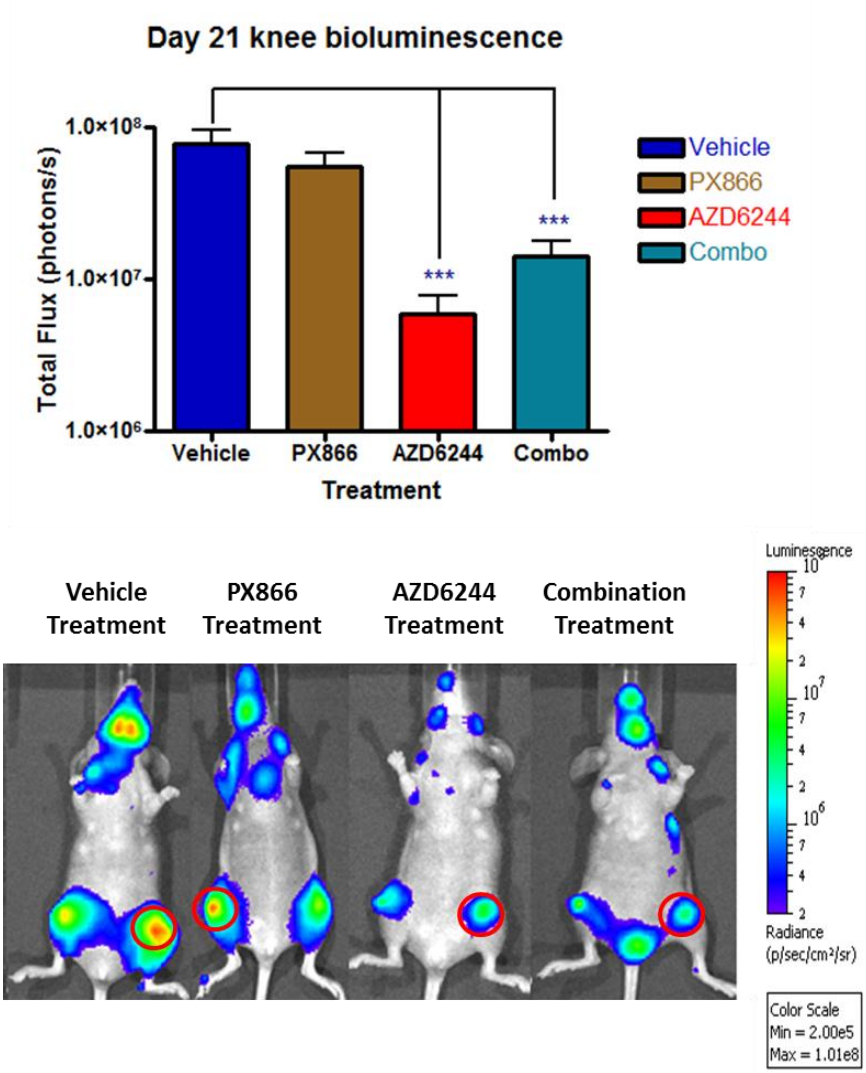

Figure 3-8. Knee tumor bioluminescence on day 21 post-IC with PX866 and/or AZD6244.

Following 7 days of treatment, mice treated with AZD6244 resulted in an approximate 10-fold reduction of tumor bioluminescence by day 21. PX866 did not have any significant effect on reducing tumor BLI. 'Vehicle' control group n=12, 'PX866' n=7, 'AZD6244' n=6, 'Combo' n=12. Data plotted as mean ± SEM. Asterisks indicate statistical significance (* $p<0.05$; ** $p<0.01$; *** $p<0.001$), relative to vehicle-treated control mice.

3.5.2 Micro-computed tomography assessment of bone integrity

μCT technology in combination with *in vivo* bioluminescence imaging has been described before [121], and has proven to be a reliable technique in the assessment of tumor-induced osteolysis. This study utilized a similar approach in order to determine the efficacy of the previously described small-molecule inhibitors. On the experimental end date (day 21), the legs of mice with established bone metastases were scanned by μCT, enabling an analysis of the following bone parameters: bone mineral density (BMD), connectivity density (ConnD), trabecular number (TbN), bone surface (BS), and trabecular separation (TbSp).

BMD is a measure of hydroxyapatite, which is the inorganic mineral component of the bone matrix, such as calcium. BMD is considered to be a reliable and accurate measure of mineralized bone, and is associated with overall strength and mechanical properties [122]. ConnD is a measure of the microarchitectural connections made by the trabeculae bone in a given area [123]. It should be noted that increased connectivity density may not be an overall indicator of increased bone, and could indicate enhanced bone loss. For example, bone that is constantly being resorbed will likely demonstrate increased perforations, resulting in increased trabecular connections. However, there is an obvious threshold to this trend, where trabecular interconnectivity will eventually decrease once perforations transition into larger cavities. Regardless, comparison to normal controls without bone metastasis is necessary to ensure proper interpretation of bone analysis. TbN, as the name implies, is the average number of trabeculae per millimeter. BS is a measure of the surface area of bone. Lastly, TbSp utilizes a sphere-filling model within the spaces of bone that is a measure of the separation between adjacent trabeculae. This parameter has been designed to be a sensitive method to evaluate the integrity of the bone microarchitecture [124]. All of these parameters have been widely utilized as a reliable

approximation of cortical and trabecular architecture in the setting of pathological conditions in bone [125], and is used in this study to determine the subsequent effect of PI3K and MEK inhibition in osteolytic breast cancer metastasis.

Administration of PX866 and AZD6244 compounds individually resulted in an attenuation of tumor-induced bone osteolysis, demonstrating consistent preservation of bone integrity as assessed by all bone parameters, BMD, ConnD, TbN, BS, and TbSp **(Figure 3-9)**. Either of these compounds used as a single-agent in mice with established bone metastases reliably demonstrated bone more similar to that of normal mice, as indicated by bone mineral density (BMD), which has been consistently used as an accurate parameter in the assessment of bone architecture [126]. When compared with tumor-BLI, it is interesting that mice administered PX866 displayed similar knee metastasis bioluminescence as vehicle-treated mice, and yet relative preservation of bone, determined by μCT. This is suggestive that PI3K inhibition, while showing no effect on colonized MDA-MB-231- EGFP/Luc2 cells, may be targeting the stromal cell population, such as osteoclast differentiation, survival, or resorptive function. In contrast, AZD6244 resulted in an attenuation of knee metastasis bioluminescence, as well as a reduction in osteolysis. This preservation of bone could be attributed to AZD6244-induced cancer cell growth inhibition, and possibly direct effects on stromal cells, including osteoclasts. Alternatively, it is possible that MEK inhibition resulted in a reduction of MDA-MB-231-EGFP/Luc2 secretion of osteoclastogenic cytokines.

Interestingly, the simultaneous administration of both compounds in mice with established bone metastasis resulted in an exacerbated osteolytic phenotype, with bone parameters demonstrating levels similar to those of vehicle-treated tumor-bearing controls **(Figure 3-9)**.

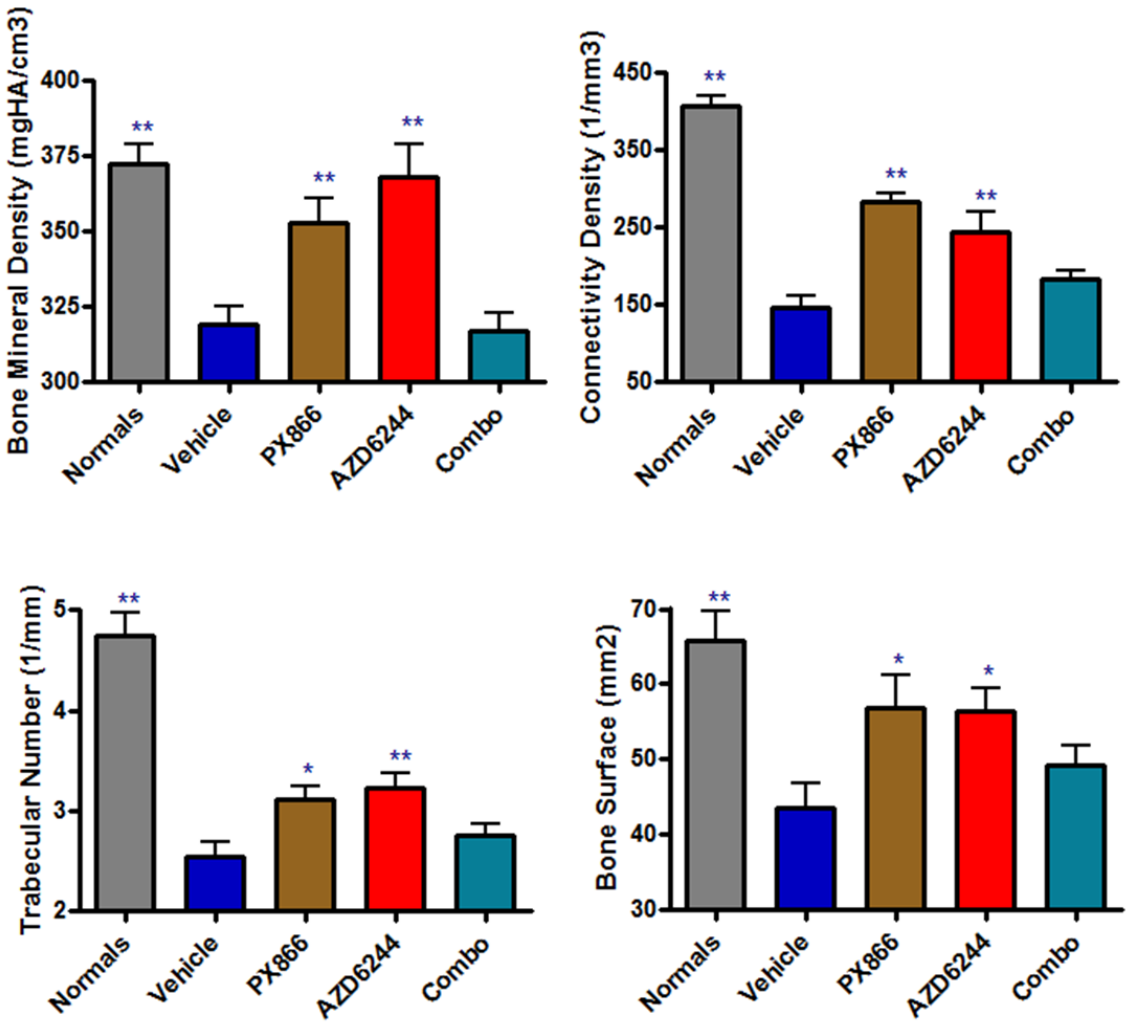

Figure 3-9. µCT bone parameter analysis of mice with established bone metastasis treated with PX866 and/or AZD6244.

Administration of the PX866 and AZD6244 compound alone resulted in an attenuation of tumor-induced bone osteolysis by the experimental end date, day 21. This was demonstrated through a consistent preservation of bone integrity as assessed by all bone parameters, BMD, ConnD, TbN, and BS. Despite a significant reduction in tumor bioluminescence, the combination of both compounds together resulted in an exacerbation of bone loss, displaying similar bone loss to that of tumor-bearing vehicle-treated controls. Tibia and femur data was pooled together following confirmation of similar trends in bone parameter quantification when analyzed separately. 'Vehicle' control group n=24, 'PX866' n=14, 'AZD6244' n=12, 'Combo' n=24. Data plotted as mean ± SEM. Asterisks indicate statistical significance (* $p<0.05$; ** $p<0.01$; *** $p<0.001$), relative to vehicle-treated control mice.

This suggests that combination treatment induces an osteolytic phenotype that is as harmful as no treatment at all. It is possible that the simultaneous PI3K and MEK inhibition has an adverse effect on the maintenance of bone integrity, such as inhibiting bone formation and/or promoting bone resorption by osteoclasts. For example, the combination of PX866 and AZD6244 led to an approximate 10-fold increase in the levels of IP-10 *in vitro*, which is a potent factor in the recruitment of monocytic precursors [53] into the tumor-bone microenvironment, potentially enhancing osteoclast presence.

3.5.2.1 Trabecular separation as a more sensitive parameter of bone microarchitecture

The dense network of trabeculae within the confines of thick cortical bone is an integral structure that provides stability and strength to the skeleton. Weakening or loss of structural integrity in the trabeculae can result in fracture (eg. vertebral compression fractures as seen in osteoporosis). The μCT parameter trabecular separation (TbSp), quantifiably measures the amount of total separation between adjacent trabeculae using a sphere-filling model. Briefly, this model generates spheres in the space between trabeculae until a point of contact occurs with adjacent bone, and it is the size of these spheres that is then quantified. Consistent with other μCT parameters, the PX866 and AZD6244 single-agent administration resulted in reduced separation of trabeculae compared to vehicle-treated controls, suggesting a preservation of microarchitecture. The combination of both compounds displayed an increased separation of trabeculae, similar to that of vehicle-treated controls. This can be visualized through the generation of 3D reconstructed images that display a heat map of the level of trabecular separation **(Figure 3-10)**. A more sensitive approach to quantify and visualize the range of separation is with a histogram distribution plot (**Figure 3-11)**. This method graphically compares

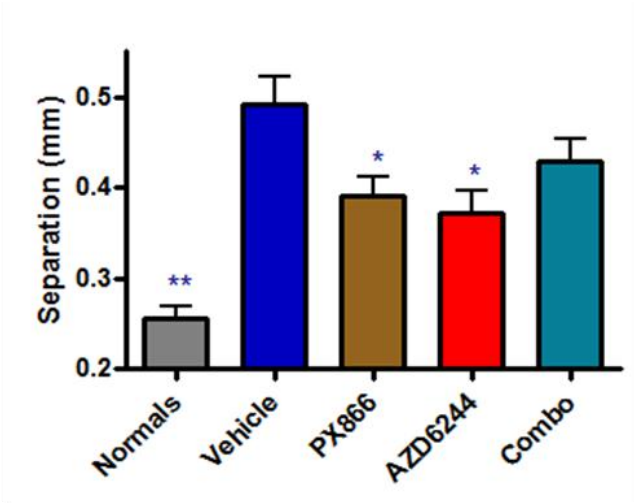

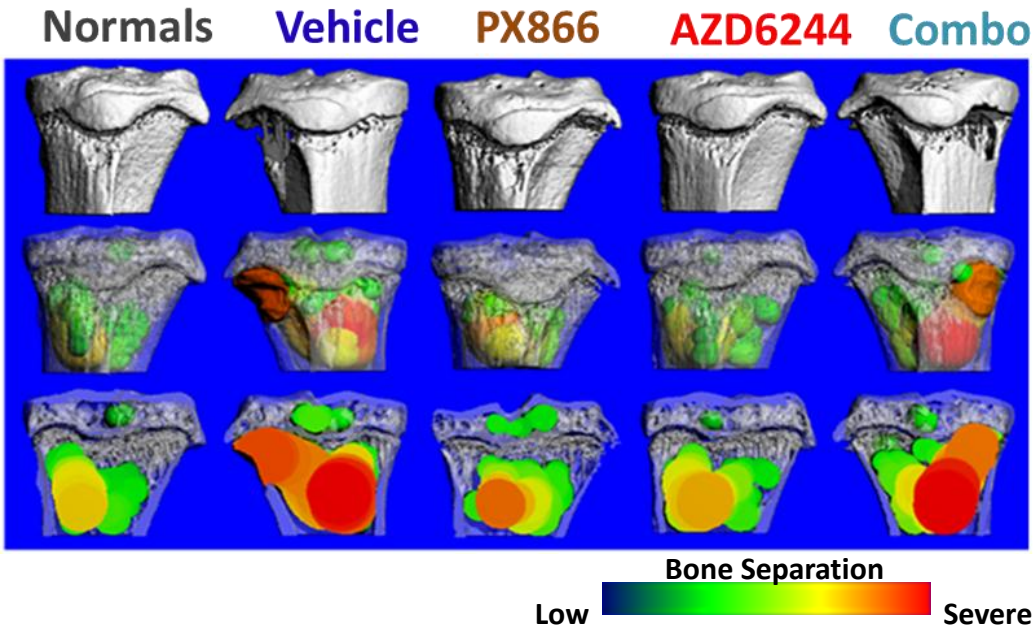

Figure 3-10. Trabecular separation analysis of mice with established bone metastasis treated with PX866 and/or AZD6244.

The trabecular separation parameter quantifiably measures the amount of total separation between adjacent trabeculae using a sphere-filling model, and has proved to be a more sensitive measure of tumor-induced bone loss. Consistent with other bone parameters, PX866 and AZD6244 administration alone effectively resulted in less trabecular bone loss, as assessed qualitatively, and with quantification of separation between trabeculae. Combination treatment led to a worsening of these parameters. Tibia and femur data was pooled together after confirmation of similar trends in bone parameter quantification. 'Vehicle' control group n=12, 'PX866' n=7, 'AZD6244' n=6, 'Combo' n=12. Data plotted as mean ± SEM. Asterisks indicate statistical significance (* $p<0.05$; ** $p<0.01$; *** $p<0.001$), relative to vehicle-treated control mice.

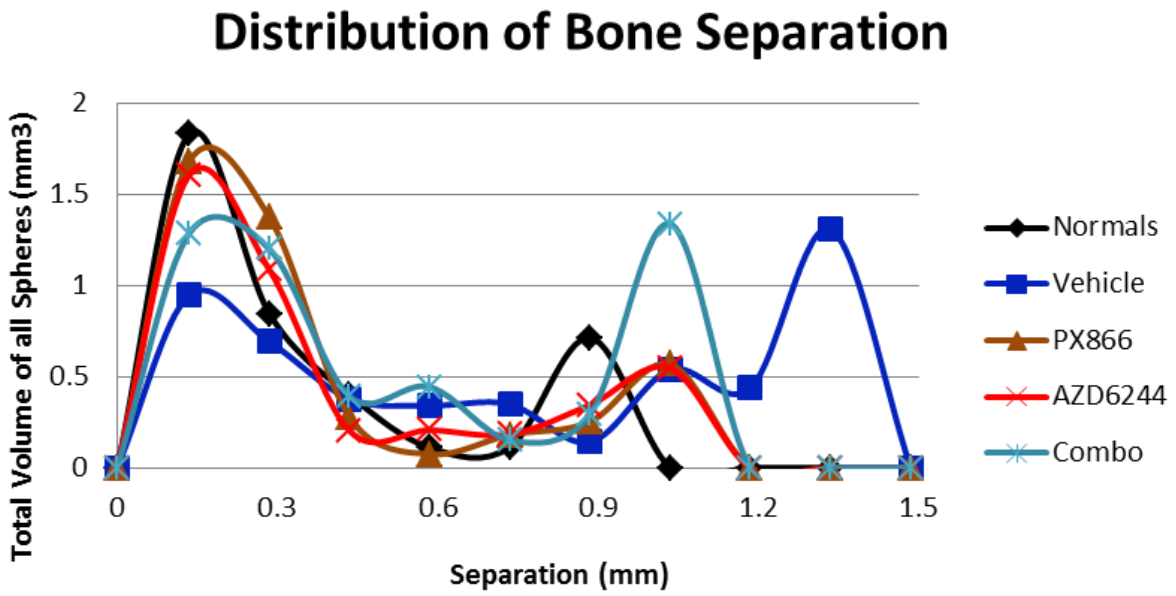

Figure 3-11. Histogram distribution of trabecular separation of mice with established bone metastasis treated with PX866 and/or AZD6244.

Histogram of trabecular separation can be a more sensitive approach to quantify and visualize the range of separation and trabecular bone loss. The total volume of spheres or simply the frequency of different sizes of trabecular separation can be determined, and therefore the distribution of small or large bone loss. Peaks on the left side of the graph display the amount of small, whereas the peaks on the right side demonstrate the frequency of large separations. PX866 or AZD6244 led to a higher frequency of small trabecular separations associated with preservation of bone integrity. Vehicle-treated mice, and mice administered both compounds simultaneously, displayed a loss of small trabecular separations, and an associated increase in large separations, indicative of increased bone loss. Data plotted is from individual mice.

the total volume of spheres generated against the separation. In other words, the frequency of different sizes of trabecular separation can be determined, and hence the distribution of small or large regions of bone loss can be quantified. Essentially, peaks on the left side of the graph display the amount of small trabecular separations, whereas the peaks on the right side of the graph demonstrate the frequency of large separations. This proved to be a more sensitive method to determine the extent of tumor-induced bone loss and treatment effects. For example, administration of either PX866 or AZD6244 resulted in a preservation of a large number of small separations, similar to those seen in normal controls. In contrast, bone lesions in vehicle-treated and combination treatment mice displayed a loss of small separations on the left side of the graph and a corresponding gain of large separations on the right side of the graph, indicating enhanced bone loss.

3.5.3 TRAP staining to quantify osteoclasts in bone metastases

Breast cancer and stromal cells promote osteoclast development and activity within the tumor microenvironment, and this ultimately results in an osteolytic phenotype. Therefore, the prevalence of osteoclast cells in the tumor-bone environment may provide a relative indication of potential resorptive capacity. Although semi-quantitative, an estimate of osteoclast numbers through the use of a distinct stain for tartrate resistant acid phosphatase (TRAP), may reveal evidence of treatment effects on established bone metastases. A caveat of this histological method is TRAP can be expressed by osteoclast cells that are not fully mature, and therefore may not be entirely representative of resorptive capacity. However, TRAP is a critical enzyme responsible for the degradation of bone and collagen matrices, and is therefore considered an important indicator of osteoclast activation and potential resorption [38].

Consistent with the μCT assessment of tumor-induced bone loss and treatment effects, similar levels of osteoclasts were detected in vehicle-treated controls, and in mice treated with the combination of PX866 and AZD6244. However, mice treated with either compound alone showed a reduced presence of osteoclasts as assessed by TRAP staining **(Figure 3-12)**.

3.6 Histology of PX866 and/or AZD6244 treated mice with established bone metastases

Tri-chrome staining allows discrimination between cancer cells, resident bone-marrow cells and mineralized bone. Vehicle-treated control mice frequently demonstrated large tumors that had expanded throughout the medullary cavity of the distal femur and/or proximal tibia, often breaking through the cortical bone. The proliferating MDA-MB-231-EGFP/Luc2 cells appeared visually healthy regardless of size or location of tumors. Similarly, mice administered with PX866 frequently displayed large sized tumors, without any significant indication that PI3K inhibition had affected cancer cell survival or proliferation. In contrast, mice treated with the AZD6244 MEK inhibitor, including mice administered with the combination of both compounds, frequently revealed large sized holes within the center of established bone tumors **(Figure 3-13)**. On the periphery of these holes was a small layer of approximately 10-20 cells that appeared viable and contained mitotic figures. These AZD6244-induced spaces, likely due to cell death, probably occurred early upon treatment, allowing time for dead cells to be cleared. Furthermore, the central locations of the holes raised the possibility that they may have arisen in ischemic areas and that these might be especially sensitive to MEK inhibition.

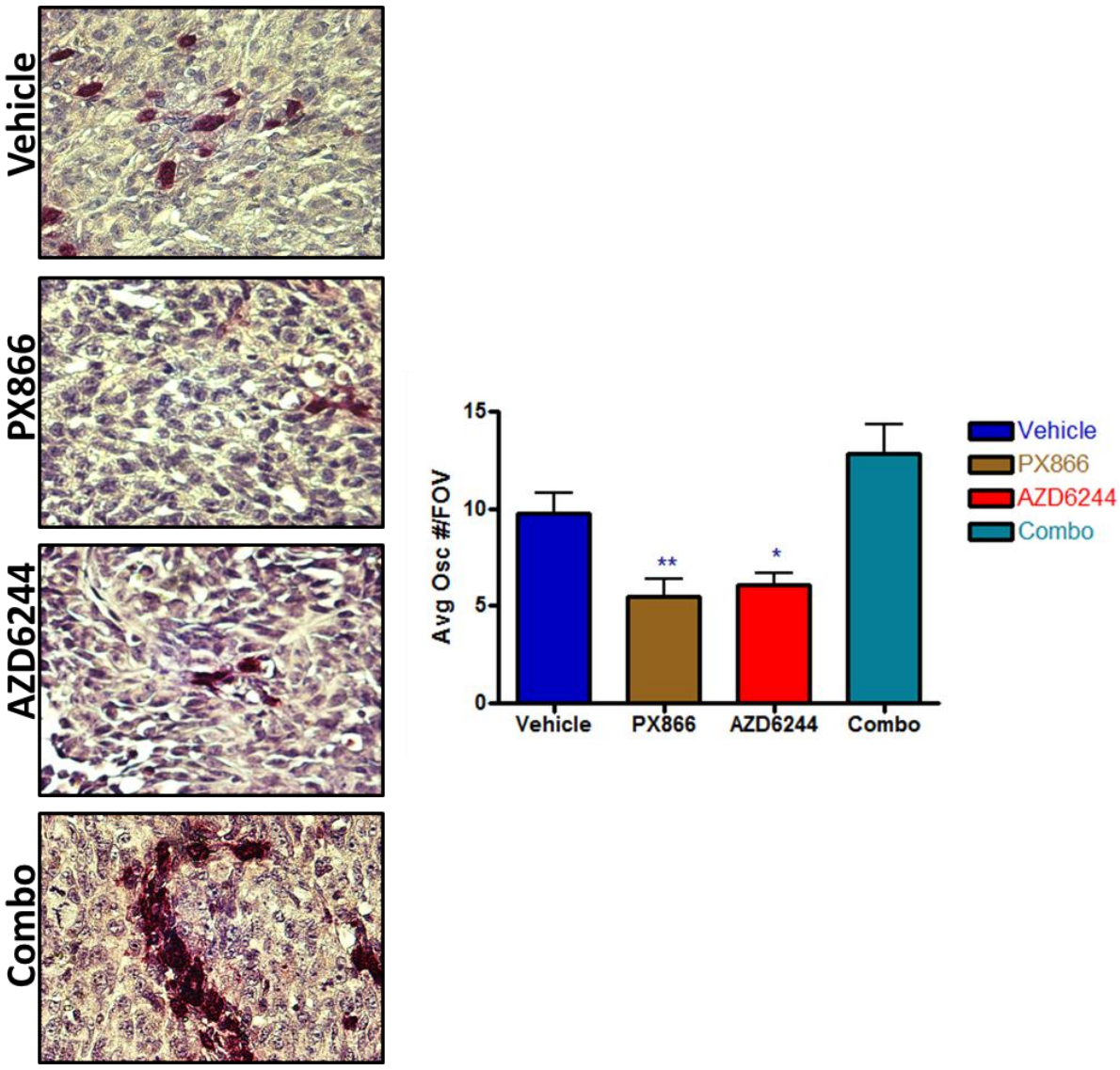

Figure 3-12. TRAP+ osteoclast quantification in bone-colonized MDA-MB-231 cells.

Quantification of TRAP positive cells demonstrated similar levels of osteoclasts in vehicle-treated controls, and mice treated with the combination of PX866 and AZD6244. Mice treated with either compound alone showed reduced numbers of osteoclasts. TRAP positive cells were counted in 4 random fields of view at a magnification of 40X.. Number of sections, n=4 for all groups, and n=16 for total quantified field of view for each treatment group. Data plotted as mean ± SEM. Asterisks indicate statistical significance (* $p<0.05$; ** $p<0.01$; *** $p<0.001$).

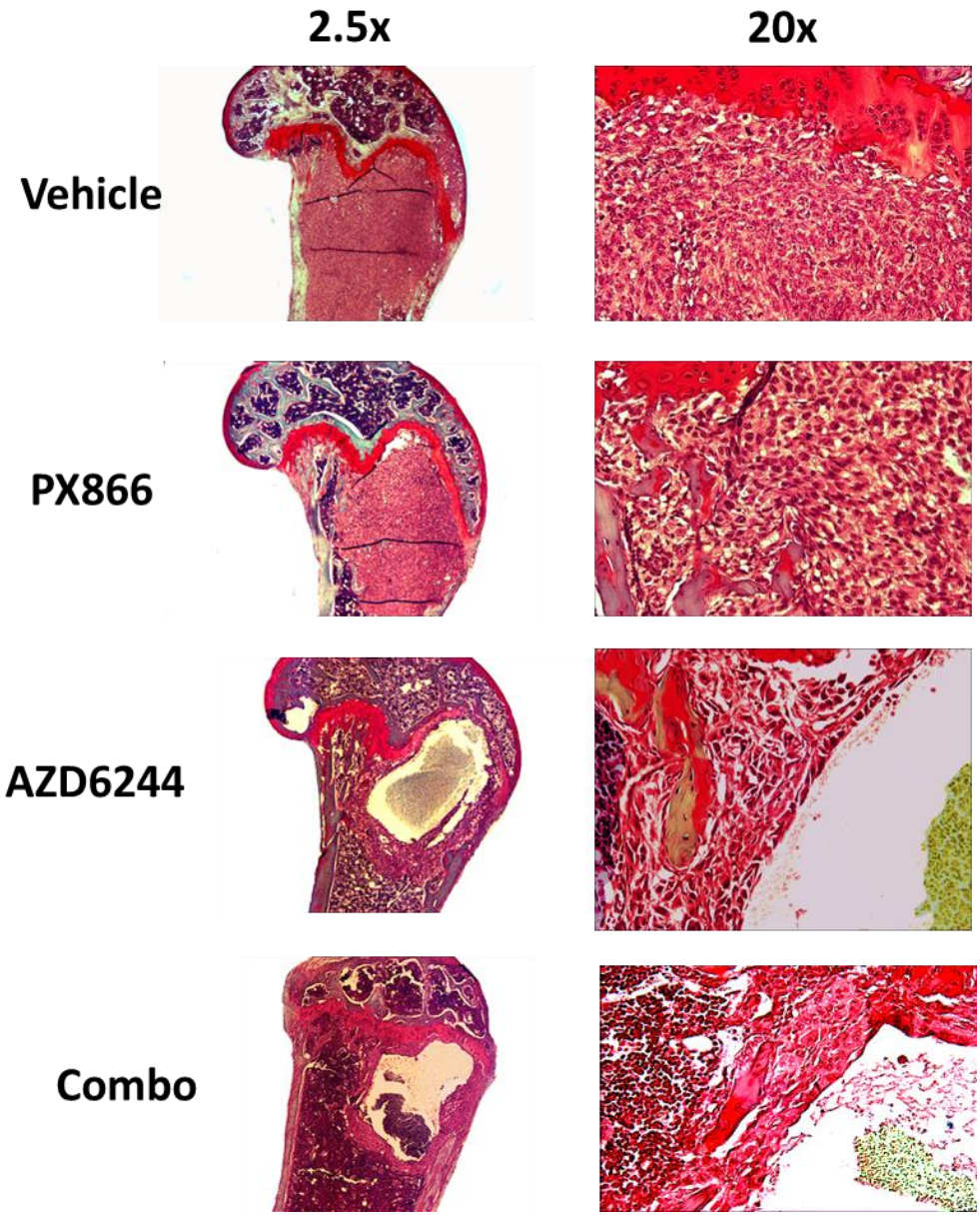

Figure 3-13. Histology of drug treated MDA-MB-231-EGFP/Luc2 knee metastases.

Vehicle-treated controls and mice treated with PX866 displayed large tumors without cavities. Mice treated with the AZD6244 MEK inhibitor, or mice administered with the combination of both compounds, frequently revealed large cavities within the centers of established tumors. Sectioning and tri-chrome stained done by Leona Barclay.

3.7 Sensitivity of nutrient-deprived MDA-MB-231 cells to MEK inhibition

Due to the presence and location of large holes seen in mice with established bone metastases following a 7-day treatment with AZD6244, it was hypothesized that areas of low nutrient perfusion might sensitize MDA-MB-231 cells to MEK inhibition.

3.7.1 Cultured MDA-MB-231 cell sensitivity in low serum conditions to MEK inhibition

As was previously demonstrated, PX866, AZD6244 or the simultaneous exposure to both agents was unable to induce any significant cytotoxic effect in cultured MDA-MB-231 cells. However, the observation that mice with established bone metastases treated with AZD6244 developed large central cavities in the bone metastases led us to test the idea that deprivation of nutrients and/or oxygen might sensitize the cells to AZD6244. To evaluate this, an Annexin V-FITC/PI assay was performed with MDA-MB-231 cells grown in 0.1% FBS media conditions and exposed to the drugs for 48 hours. Interestingly, as compared to cultured MDA-MB-231 cells in 10% FBS media, in 0.1% FBS the cells became dramatically sensitive to MEK inhibition **(Figure 3-14).** Similar to previous experiments done in 10% FBS, camptothecin was used as a positive control, as it is known to induce apoptosis in MDA-MB-231 cells. As was expected, camptothecin demonstrated a potent effect, generating approximately 35% apoptosis and/or necrosis, as assessed by positive staining for Annexin V FITC and PI. PX866 did not produce any significant increase in cell death, and resulted in similar staining to control cells. These observations were comparable to assay results in 10% FBS. This indicated that MDA-MB-231 cells are relatively resistant to nutrient deprivation, with PI3K inhibition providing no increase in sensitivity. In contrast, MDA-MB-231 cells exposed to AZD6244 exhibited approximately 25% apoptosis and/ or necrosis, and simultaneous PI3K and MEK inhibition demonstrated no

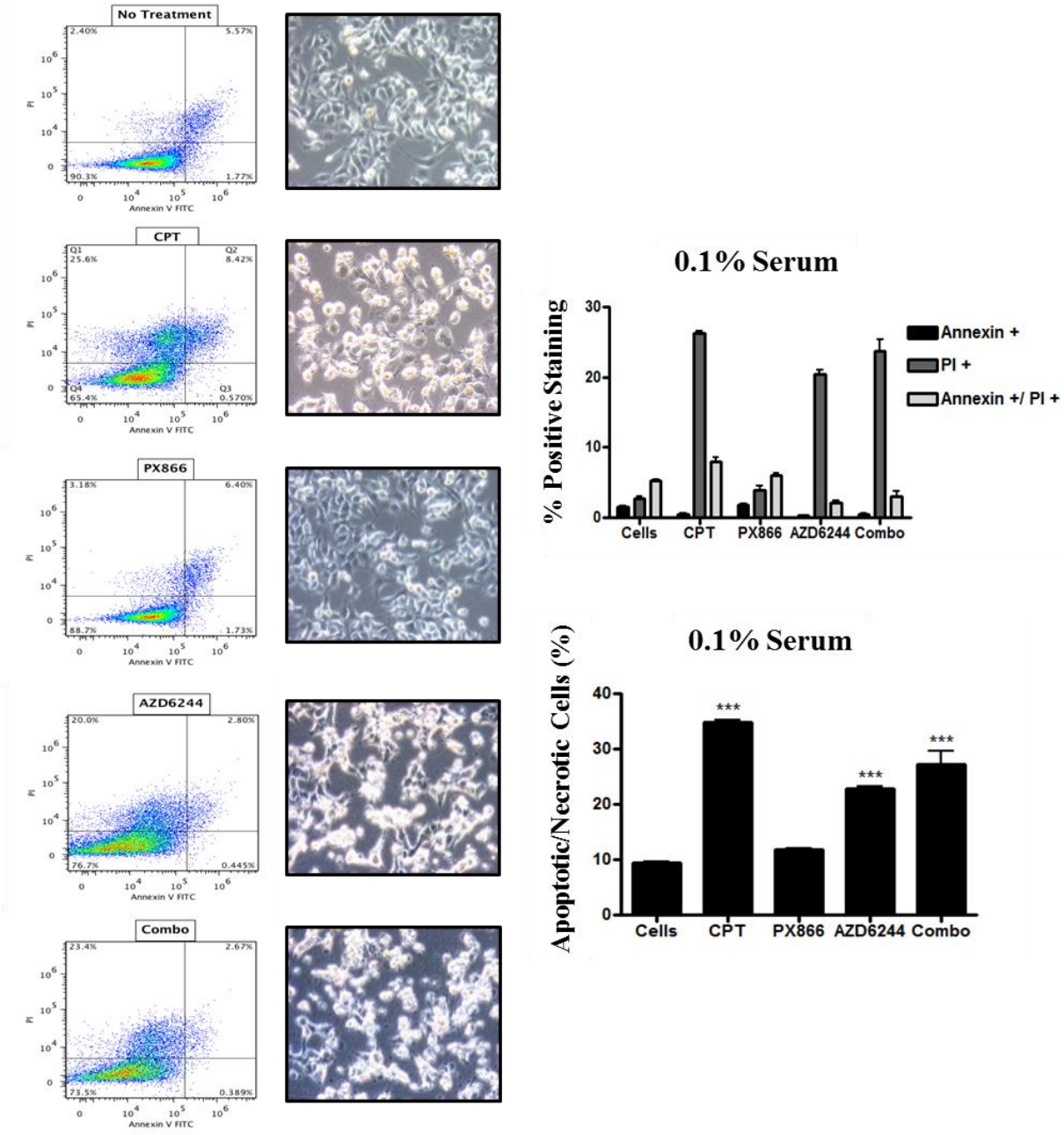

Figure 3-14. MDA-MB-231 sensitivity to MEK inhibition under low serum conditions.

MEK inhibition, but not PI3K inhibition, resulted in increased MDA-MB-231 cell death, cultured in media containing 0.1% FBS. Similar to other experiments, the combination of both compounds did not result in any significant additive apoptosis and/or necrosis. Camptothecin was used as a positive control and resulted in similar apoptosis/necrosis to that in 10% FBS conditions. Data represents three independent experiments and is plotted as the mean ± SEM. Asterisks indicate statistical significance (* $p<0.05$; ** $p<0.01$; *** $p<0.001$).

significant additive effect. This showed that the Ras-MAPK pathway was important in delivering survival signals when exposed to nutrient deprivation, and that blockade of this pathway resulted in increased MDA-MB-231 cell death.

A qualitative analysis can be visualized from images taken of the cultured cells following a 48 hour exposure to the two drugs **(Figure 3-14).** Cells without treatment in 0.1% FBS develop an altered morphology, demonstrating a more spindle-shaped and fibroblastic character that has been associated with an increased migratory capacity of cancer cells, compared to cells in nutrient-rich conditions [127]. The latter may serve as a survival mechanism enabling tumor cells to escape regions of nutrient and/or oxygen deprivation. PX866 treated cells demonstrated a similar appearance to vehicle-control MDA-MB-231 cells, whereas camptothecin or AZD6244 induced obvious cellular death, a finding that correlated with Annexin V FITC/PI quantification.

In order to confirm results from the Annexin V FITC/PI assay and to ensure an apoptotic mechanism of cell death following exposure to AZD6244, a western blot for cleaved caspase-3 levels was performed **(Figure 3-15)**. Caspase-3 is a frequently activated protease that is cleaved and activated upon induction of programmed cell death [128]. Therefore, measuring protein levels of cleaved caspase-3 is a reliable and frequently used assay to determine levels of apoptosis in a cell population. Results obtained were consistent with 10% and 0.1% FBS conditions using the flow cytometry based analysis. In 10% FBS, camptothecin was the only compound to demonstrate significant levels of cleaved caspase-3. In contrast, in 0.1% FBS, a dramatic increase of cleaved caspase-3 levels was evident following exposure to AZD6244 **(Figure 3-15)**. This demonstrated that, in the absence of adequate serum factors, MDA-MB-231 cells become sensitive to MEK inhibition, resulting in significant levels of cellular apoptosis.

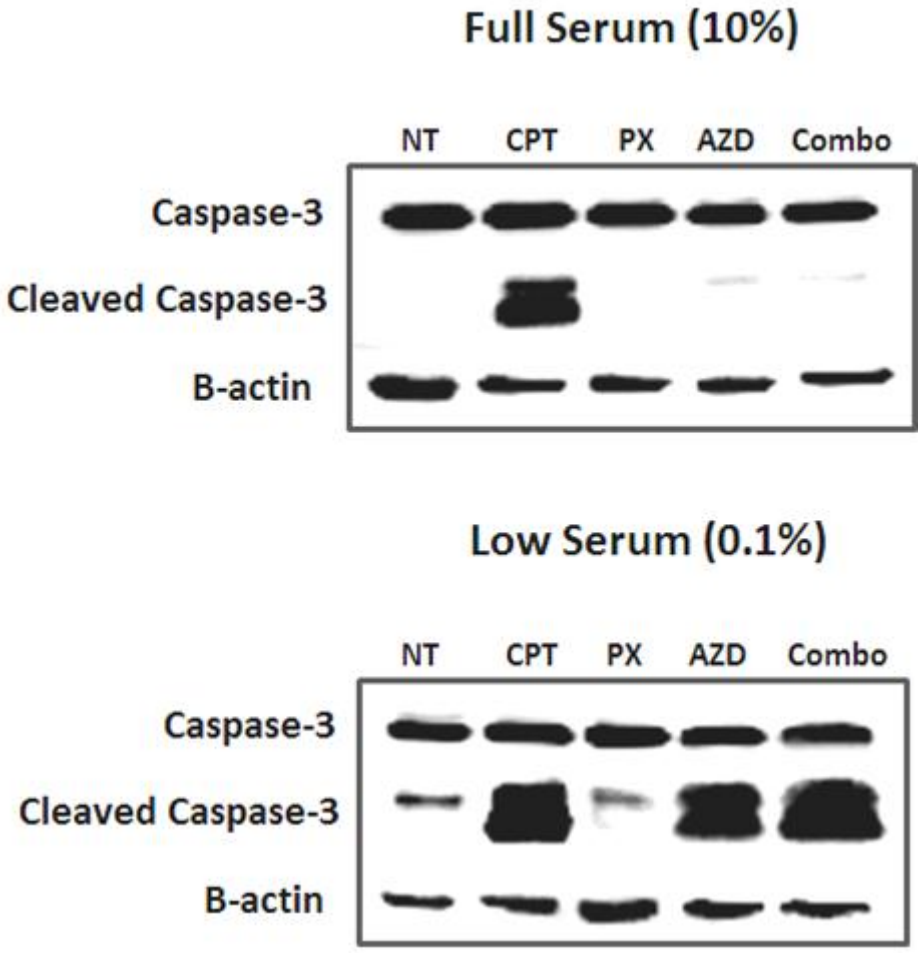

Figure 3-15.Caspase-3 cleavage to assess MDA-MB-231 sensitivity to AZD6244 during serum deprivation.

To assess MDA-MB-231 cell sensitivity as a function of FBS levels in low serum conditions, western blotting for cleaved caspase-3 was performed. Camptothecin was used as a positive control. There was a slight elevation of cleaved caspase-3 protein in control cells with no treatment and PX866 exposed cells in low serum versus full serum conditions, most likely due to minimal apoptosis induced by the stress of serum deprivation. MDA-MB-231 cells exposed to AZD6244 under low serum conditions, resulted in a dramatic increase of cleaved caspase-3 protein levels, relative to full serum conditions. Blot shown is representative of three independent experiments.

3.7.2 Short treatment regimen of AZD6244 MEK inhibition on late-stage bone metastases

A short 3 day treatment regimen with AZD6244 on late stage knee metastases was performed in an attempt to reveal whether large tumors, likely having regions starved for nutrients, would be sensitive to MEK inhibition *in vivo.* BLI of mice with large knee metastases following AZD6244 administration for 3 days demonstrated an inhibition of tumor growth as reflected by photon flux determinations **(Figure 3-16)**. Following day 2 of treatment with AZD6244 there was a consistent drop of BLI in all mice, followed by an increase in photon flux on the last experimental date, however, there was still a significant overall reduction of tumor BLI, as compared to vehicle-treated control mice. These results showed that even short treatment with MEK inhibitors can have a striking effect on the growth and/or survival of MDA-MB-231-EGFP/Luc2 bone metastases.

In order to visualize the *in vivo* consequences of AZD6244 treatment, a histological examination was performed. The tri-chrome stain was carried out to distinguish between mineralized bone, resident bone marrow cells, and colonized MDA-MB-231-EGFP/Luc2 cells. In contrast to controls, AZD6244 treatment led to the development of regions of cell death within the knee metastases **(Figure 3-17)**. Furthermore, TUNEL staining revealed a significant amount of positively staining cells within the affected areas. The involved regions were likely consistent with previous histological examination of mice treated with AZD6244 in the 7 day treatment regimen that demonstrated central zones that were cleared of MDA-MB-231 cells **(Figure 3-13)**. Hallmarks of the apoptotic process include the fragmentation of DNA, chromatin condensation and the formation of rounded apoptotic bodies, followed by rapid clearance of dead cells by macrophage phagocytosis [129]. The latter feature would be predicted to be the cause of the large cavities seen within bone metastases in the 7 day treatment group.

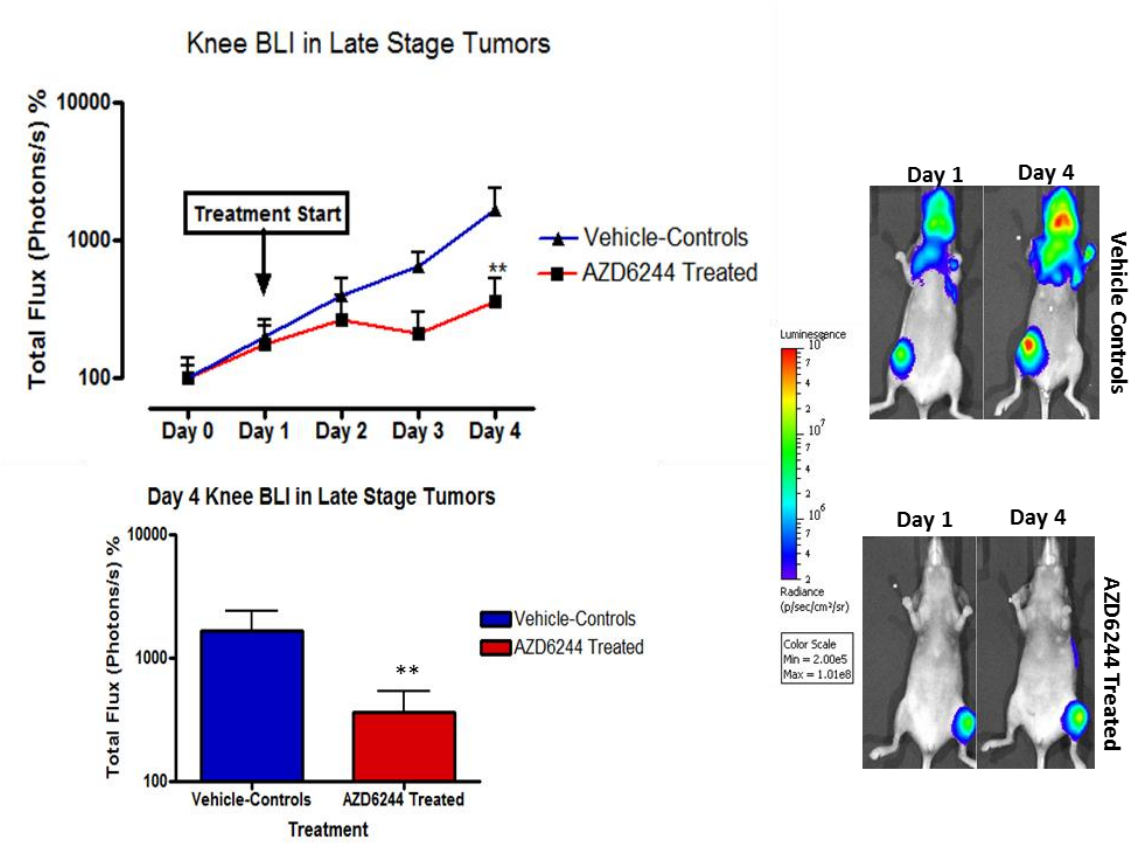

Figure 3-16. Short treatment regimen of MDA-MB-231 knee metastases with AZD6244.

A 3 day treatment with AZD6244 was performed on mice with late stage tumors. At the experimental end date (day 4), vehicle-treated controls displayed over 1 log increase in tumor bioluminescence, as compared to AZD6244 treated mice. For 'Vehicle-Treated' group n=6, and 'AZD6244' n=5. Data plotted as mean ± SEM. Asterisks indicate statistical significance (*$p<0.05$; ** $p<0.01$; *** $p<0.001$).

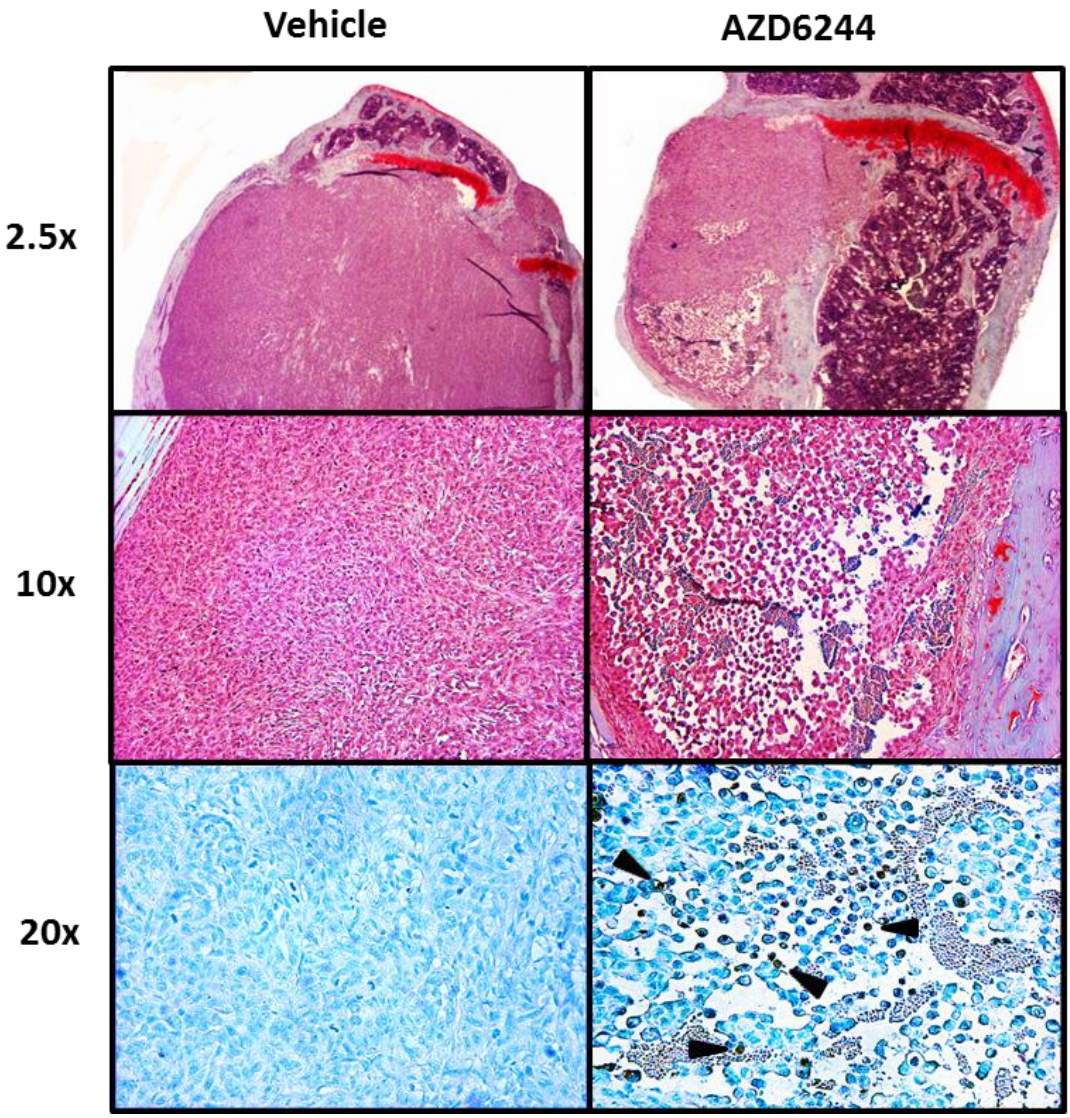

Figure 3-17. Histology of bone metastases after a 3 day treatment with AZD6244.

Representative regions of an MDA-MB-231-EGFP/Luc2 knee metastasis demonstrate a large region of cell death at the lower pole of the tumor (upper right image), following treatment with AZD6244. TUNEL staining (bottom left and right images) demonstrates the presence of TUNEL-positive cells in the region of cell death in mice treated with AZD6244 (right lower image). Sectioning and tri-chrome stain (top four boxes) done by Leona Barclay.

3.8 Discussion

3.8.1 Potential mechanism of action of PX866 and AZD6244 on bone metastases

It is complicated and difficult to decipher specific *in vivo* effects of systemically administered signaling pathway inhibitors, primarily due to potential pleiotropic effects on all cells in the body. However, appropriate analysis is possible through the application of a combination of *in vitro* and *in vivo* methods of experimentation. This study aimed to specifically evaluate the effects of PX866 and AZD6244, PI3K and MEK inhibitors, respectively, on breast cancer bone metastases and their effects on bone integrity. Using the evidence obtained, a mechanism of action can be proposed (**Figure 3-18)**, taking into consideration the players in the 'vicious cycle,' including the bone-colonized MDA-MB-231-EGFP/Luc2 cells, as well as osteoblasts and osteoclasts.

Although PX866 resulted in no significant effects *in vitro* or on tumor bioluminescence *in vivo*, it was able to attenuate the extent of bone destruction, likely by inhibiting hyper-active osteoclast activity. It was previously demonstrated that PI3K activity is important in osteoclast cytoskeletal processes, such as chemotaxis, attachment to the bone surface, and formation of the actin ring responsible for resorption [130, 131]. In fact, the osteoclast αvβ3 integrin is a major upstream activator of the PI3K pathway. Furthermore, inhibition of PI3K has been demonstrated to inhibit osteoclast bone resorption [132]. Alternatively, as reported by others, PI3K inhibition can inhibit the differentiation of pre-osteoclast cells into mature TRAP-positive resorptive osteoclasts *in vivo,* likely due to inhibition CSF-1R signaling [133].

We found that AZD6244 was able to effectively reduce tumor bioluminescence, and also resulted in an attenuation of bone loss. Consistent with our *in vitro* data, AZD6244 was able to cause growth inhibition of MDA-MB-231 cells in full serum culture conditions, and to trigger

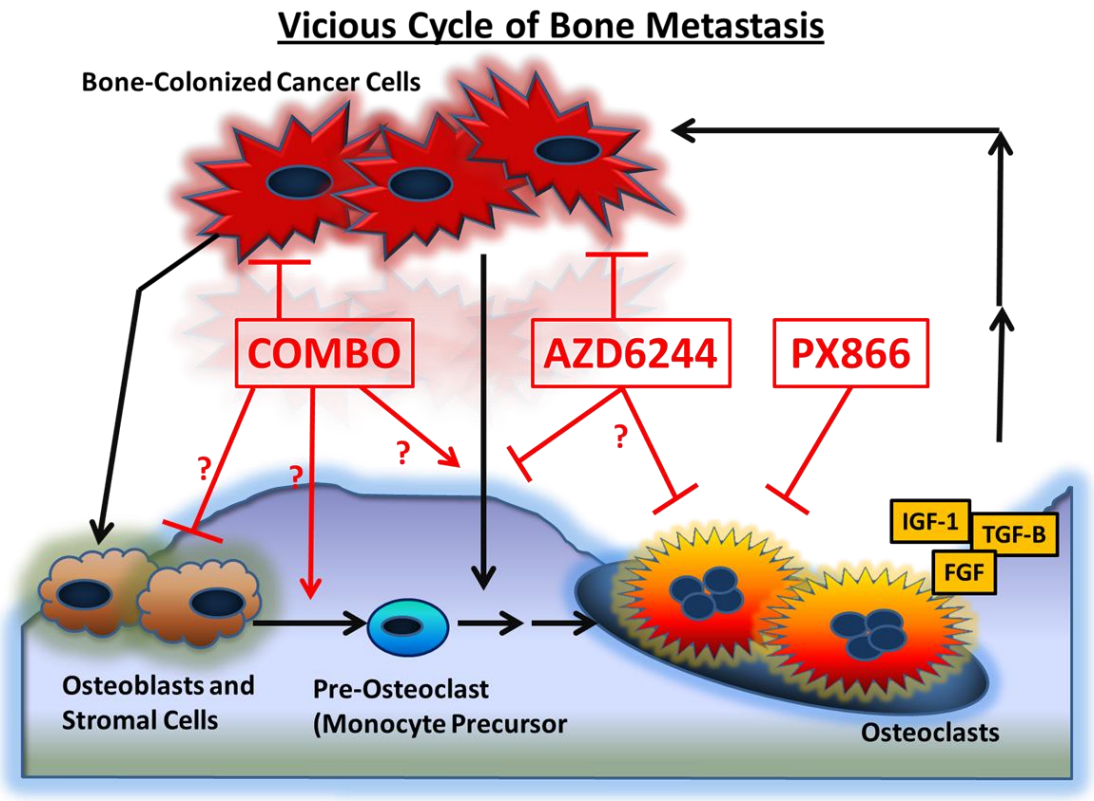

Figure 3-18. Potential mechanism of action of PX866 and AZD6244 on bone metastases.

PX866 administration was unable to affect MDA-MB-231 cells *in vitro*, and was ineffective at reducing tumor bioluminescence *in vivo*, however, resulted in an attenuation of tumor-induced bone osteolysis. Therefore, PI3K inhibition may ultimately target osteoclast cell resorptive function or differentiation, either directly, or indirectly through decreased osteoblast expression of RANKL. In contrast, AZD6244 inhibited growth of MDA-MB-231 cells *in vitro*, and demonstrated a reduction of cancer cell growth *in vivo*, with a corresponding preservation of bone integrity. Alternatively, AZD6244-induced reduction of MDA-MB-231 cytokine secretion of osteoclastogenic factors could indirectly affect osteoclasts. As well, it is possible that MEK inhibition directly targets osteoclast cells in the bone microenvironment. The combination of both compounds resulted in a similar negative effect on tumor growth as seen with AZD6244 administration alone, but displayed enhanced bone destruction. Therefore, multiple mechanisms are possible that would favor osteoclast activity, such as inhibition of osteoblast-mediated bone deposition, or induction of osteoclastogenic factors from these cells, or from bone-colonized MDA-MB-231 cells.

cell apoptosis under low serum conditions. Therefore, the reduction in tumor bioluminescence *in vivo* was likely a consequence of both of these processes. It is possible that the AZD6244-mediated reduction of tumor mass abrogated osteoclast-induced bone destruction. Alternatively, the possibility exists that MEK inhibition might directly target osteoclasts. Previous studies have determined that the MEK-ERK signaling axis is integral in the survival, differentiation, maintenance of cell polarity and function of the ruffled border of osteoclasts [109, 134]. Additionally, AZD6244 effectively reduced MDA-MB-231 cytokine and growth factor secretion *in vitro* **(Figure 3-6)**, thereby potentially reducing osteoclast recruitment, differentiation, and resorptive function. Reduced expression of factors in the bone microenvironment, such as G-CSF, GM-CSF, MCP-1, TGF-α and IL-8, all of which have demonstrated to promote osteoclastogenesis [135], might plausibly be involved in the AZD6244-associated preservation of bone we observed.

Interestingly, the combination of both compounds resulted in reduced tumor bioluminescence, however, this treatment displayed an exacerbation of bone damage. The AZD6244 component was the most likely cause of reduced tumor bioluminescence (levels were similar to those of AZD6244 administration alone). The addition of PX866 conferred no additional therapeutic benefit as assessed by tumor bioluminescence. However, it was possible that the combination treatment was able to further tip the balance towards osteoclast bone resorption, leading to enhanced destruction. This would be achievable through multiple mechanisms, such as the inhibition of mature, bone depositing osteoblasts or through the induction of osteoblast-derived factors, such as the osteoclast activator RANKL. Furthermore, and consistent with *in vitro* luminex cytokine secretion data, the simultaneous inhibition of PI3K and MEK might actually induce cancer cell secretion of potent osteoclastogenic factors, such as

IP-10. Interestingly, IP-10 has not received much attention in the context of osteolytic metastases. However, in a genome-wide study of circulating monocytes, IP-10 was demonstrated to be amongst the most potent recruiters of monocytic osteoclast precursors into the bone microenvironment [53]. Furthermore, it has been demonstrated that human breast cancer patients, and breast cancer cell lines (primarily the basal subtype) frequently overexpress IP-10 [136].

It is possible that an assault on two key signaling pathways, such as that occurs with PX866 and AZD6244 combination treatment, results in an upregulation and/or dependency on other signaling modalities, such as those downstream of NFκB. Interestingly, it is known that pathway convergences between PI3K, MEK, and NFκB exist [69], further complicating potential avenues for pathway crosstalk and cancer cell resistance to therapeutic intervention.

Numerous studies have demonstrated the importance of both PI3K and MEK-ERK signaling, including crosstalk between them [73, 110], in osteoclast survival, differentiation and function, however, this has only been investigated in the *in vitro* setting. Therefore, such approaches are unable to account for stromal-cell interaction and important extracellular cues derived from cytokines and growth factors in the microenvironment.

This study demonstrates that investigation of potential therapies must take the appropriate microenvironments into consideration, in order to ensure the inclusion of multiple cell types and their interactive effects. Collectively, the results suggest crosstalk between the PI3K and the Ras-MAPK pathways is not a critical mechanism in continued MDA-MB-231 survival *in vitro* and *in vivo.* Also implicated is that MEK inhibition alone may be a valuable option for the treatment of osteolytic breast cancer metastases, either alone, or most likely in conjunction with other agents, such as alternative signaling pathway inhibitors or chemotherapeutic drugs.

3.8.2 MDA-MB-231 sensitivity to MEK inhibition following nutrient-deprivation

It is apparent that cancer cells have developed sophisticated mechanisms to perpetuate proliferative expansion and survival, even in the face of normally toxic stimuli. For example, it has been demonstrated that conventional chemotherapeutic compounds, such as doxorubicin or docetaxel can activate the Ras-MAPK pathway, leading to drug resistance [74]. Furthermore, the finding that signal transduction pathways contain numerous points of regulation, leading to positive and negative feedback loops, only complicates matters. Cell signaling propagation and regulation are extremely complex processes that must be carefully evaluated when considering novel potential therapeutic interventions in patients with any type of cancer. For example, as demonstrated before, as well as in this study, the PI3K and Ras signal transduction pathways harbor multi-level crosstalk mechanisms, and generate similar downstream effects. This leads to the notion that inhibition of one pathway alone may not be sufficient for cancer therapy. However, tumor cell dependency on the Ras and PI3K pathways may not be as critical as previously thought and may vary depending on the specific cancer type examined. Indeed, both our *in vitro* and *in vivo* investigations demonstrated that simultaneous inhibition of both pathways did not lead to any significant additive effects on MDA-MB-231 cells. However, this is unquestionably cell type and location specific, in terms of the corresponding microenvironment. For example, signals that arise within the microenvironment, such as in the bone are important regulators of signal pathway propagation, and therefore crosstalk could be more evident depending on the nature of the available extracellular cues. Similarly, different types of cancers or cancer subtypes could act differently, primarily based on their inherent transcriptional and mutational profiles. For example, a study demonstrated that basal-like breast cancer cells that harbor wild-type p53 tumor suppressor, and that are exposed to simultaneous PI3K and MEK

inhibition, underwent additive apoptosis, whereas in the context of mutant p53, additive cell cycle arrest occurred [79]. Consistent with this finding, the MDA-MB-231 cells used in this study harbor mutant p53 and similar results of enhanced cytostatsis without any significant apoptosis were found following simultaneous PI3K and MEK inhibition.

Our finding that serum deprivation can sensitize MDA-MB-231 cells to MEK inhibition has important therapeutic implications. The Ras-MAPK pathway is highly deregulated in many cancers and it seems to provide an important signaling mechanism to resist times of stress, such as in nutrient deprivation [137]. Therefore, if it were possible to starve tumors of nutrients *in vivo*, it might be possible to render them sensitive to MEK inhibition. Furthermore, it has been demonstrated that mutant p53 in MDA-MB-231 cells is stabilized by phospholipase D (PLD), and is required for survival during a stress response [137]. Interestingly, it was also shown that either inhibition of PLD activity or MEK resulted in the de-stabilization of mutant p53, and this led to significant apoptosis following serum deprivation [137]. It is now collectively agreed that mutant p53 can exert an oncogenic dominant negative or gain of function property, in contrast to the tumor suppressive activity of wild-type p53 [138]. This can occur through mutant p53-mediated inhibition of wild type p53 (dominant negative), or alternatively, direct binding and transcription of diverse proto-oncogenes (gain of function). For example, genome-wide approaches have determined that mutant p53, but not wild-type p53, regulates the transcription of EGFR and c-myc [139], molecules that are important in tumorigenesis. In fact, this may account for the overexpression of EGFR seen in the MDA-MB-231 cells, as well as in breast cancer patients. Indeed, a large portion of aggressive breast cancers associated with a triple-negative profile, harbor p53 mutations [139]. Furthermore, a positive feedback loop has been demonstrated, in which the product of PLD activity, phosphatidic acid (PA), results in increased

Ras-MAPK signaling, and conversely, EGFR signaling through the Ras-MAPK pathway is able to activate PLD [140]. Therefore, it is evident that a connection between mutant p53, PLD and the Ras-MAPK pathway has developed to suppress default apoptotic programs, such as during nutrient-deprived stress conditions. Further delineation of signaling transduction pathway connections and their regulation will surely generate avenues for potential therapeutic intervention in diverse cancers that harbor common mutations.

3.9 Future directions

3.9.1 Establishing more effective therapeutic avenues for breast cancer metastasis

Although it is significant to understand that the Ras-MAPK pathway is able to generate survival signals during nutrient deprivation, the ultimate goal for cancer therapy is specific and effective targeting of all cancer cells. Therefore, induction of tumor cell death of cancer cells, regardless of the presence or absence of nutrients or oxygen represents an effective therapeutic intervention. Roles for signal transduction pathways in promoting potent anti-apoptotic mechanisms have been under intense investigation in order to determine susceptibilities that can be taken advantage of for cancer therapy. The Ras-MAPK pathway is one such signaling axis that is now known to induce multiple pro-tumorigenic effects, such as proliferative and anti-apoptotic signals. For example, in the nucleus, ERK-mediated phosphorylation of c-myc and ELK-1 leads to sustained expression of genes controlling cell cycle progression. Similarly, ERK-induced phosphorylation of Bcl-2 family members has been implicated in mediating the strong anti-apoptotic phenotype of cancer cells [141]. Bcl-2 family members consist of anti-apoptotic proteins, such as Bcl-2, Bcl-xL and Mcl-1, and pro-apoptotic members such as Bim, Bax and Bak. Anti-apoptotic Bcl-2 is frequently elevated in breast cancer, and is now used as a diagnostic

and prognostic evaluation since it has been highly implicated in resistance to chemotherapeutic agents [142]. It is known that ERK-induced phosphorylation of the pro-apoptotic factor Bim induces its proteasomal degradation, thereby impeding any potential induction of apoptosis [141]. Therefore, it was postulated that inhibition of MEK would inhibit this phosphorylation, freeing Bim to promote mitochondrial-dependent cell death. However, despite strong theoretical evidence, there have been disappointing results with MEK inhibitors in the clinic [90]. Recently, an explanation for the failure of MEK inhibitor-induced apoptosis may have been uncovered, at least in part; elevated levels of Bcl-2 were shown to be able to sequester and neutralize MEK inhibition-increased Bim, thus inhibiting the latter's pro-apoptotic function [141]. Therefore, simultaneous inhibition of the MEK-ERK axis, as well as Bcl-2 may be able to effectively promote Bim-induced cancer cell apoptosis. In fact, this type of treatment has been demonstrated to transition MEK inhibitor cytostatic effect into a cytotoxic effect with long-term tumor regression in B-Raf mutant cell lines *in vitro* and *in vivo* [143].

It was of interest to briefly investigate whether this type of combinatorial treatment was also able to sensitize MDA-MB-231 cells, irrespective of growth factor presence within serum-containing media. Interestingly, we found that the combination of Bcl-2 and MEK inhibition resulted in a strong induction of apoptosis, with approximately 40% of the cells staining Annexin+/PI – or Annexin+/PI+. Use of the Bcl-2 inhibitor, ABT-263, alone also induced appreciable levels of apoptotic cells, at approximately 25%, however the most dramatic effect was seen when this agent was used in conjunction with AZD6244 **(Figure 3-19)**. This data is suggestive that cancers with elevated levels of Bcl-2 and demonstrate evidence of Ras-MAPK pathway activation may be sensitive to simultaneous Bcl-2 and MEK inhibition and represents

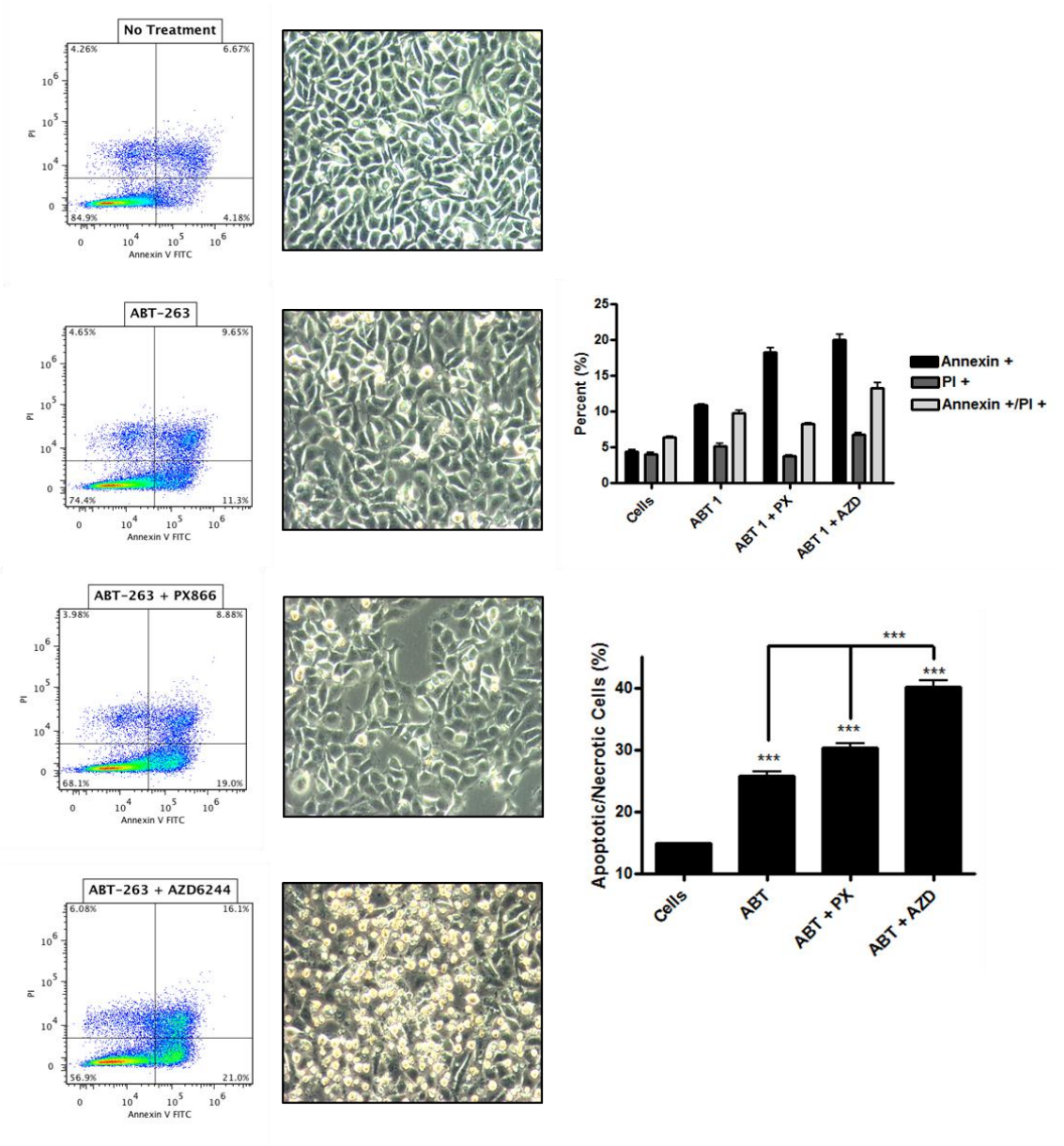

Figure 3-19. Bcl-2 and MEK inhibition as a potential therapeutic intervention.

The high frequency of increased Bcl-2 expression and hyperactivation of Ras-MAPK signaling in breast cancer makes simultaneous inhibition of these proteins an attractive strategy for therapeutic intervention. ABT-263-mediated Bcl-2 inhibition alone, as well as in combination with PX866 PI3K inhibition resulted in a significant induction of apoptosis. However, ABT-263 in conjunction with the AZD6244 MEK inhibitor demonstrated the most dramatic induction of apoptosis (approximately 40% of all cells). All groups were exposed to the corresponding compounds for 48 hours (1μm for ABT-263 and 2.5μm for PX866 or AZD6244). Data represents three independent experiments and is plotted as the mean ± SEM. Asterisks indicate statistical significance (* $p<0.05$; ** $p<0.01$; *** $p<0.001$).

an approach that should be investigated further in the context of primary and metastatic breast cancer.

It has recently been demonstrated that signaling pathway inhibition results in adaptive resistance in matrix-attached cancer cells, through the upregulation of Bcl-2. This study revealed that only subsets of matrix-attached cells were resistant to pathway inhibition, and that additional targeting of Bcl-2 was able to completely sensitize all cells to undergo apoptosis [144]. It is known that a direct link exists between p53 and Bcl-2 family members. Wild-type cytoplasmic p53 is able to activate pro-apoptotic proteins that are able to antagonize the anti-apoptotic effects of Bcl-2, such as sequestration of Bim [145]. However, the presence of mutant p53, such as in the MDA-MB-231 cells, would result in an impaired modulation of pro-apoptotic proteins, leading to enhanced anti-apoptotic function. Interestingly, wild-type p53 has demonstrated to reduce Bcl-2 function, thereby leading to induction of apoptosis in the face of toxic stimuli. Conversely, mutant p53 has the capacity to increase anti-apoptotic Bcl-2 levels and function in a transcription-dependent and independent manner [146], leading to cancer cell survival under cytotoxic conditions. As was previously mentioned, MEK inhibition during nutrient deprivation causes destabilization of mutant p53. Therefore, it is possible that reduced mutant p53 activity in this scenario results in a down-regulation of Bcl-2 or other anti-apoptotic family members, thereby sensitizing MDA-MB-231 cells to MEK inhibition, as we observed *in vivo*.

It is evident that a connection with p53 exists in many different settings, and is seemingly responsible for pro-survival effects, even in nutrient-deprived environments. The p53 transcription factor modulates many cellular processes, and the fact that it is considered to be the most frequently mutated in all cancer types, lends importance into further investigation of its role in metastatic breast cancer, as well as in the generation of creative ways to target or reverse its

pro-tumorigenic effects. Signal propagation and crosstalk between different pathways is a complicated and challenging process to decipher, however, further delineation of these mechanisms, along with personalized genetic screening will surely prove beneficial in the treatment of many different types of cancer.

Chapter Four: **The effect of PI3K and/or MEK inhibition using small-molecule inhibitors in normal bone development**

4.1 Introduction

4.1.1 Endochondral versus intramembranous ossification

Prior to an analytical evaluation of the effects of small-molecule signaling pathway inhibition in normally developing mice, a brief overview of bone development and maintenance is required. As described in more detail below, longitudinal bone growth occurs through dynamic sequential events that are tightly regulated, in a process termed endochondral ossification [49, 147]. In contrast, outward growth and thickening of cortical bone occurs through distinct mechanisms, through a process termed intramembranous ossification [148].

Endochondral ossification of long bones in a developing organism occurs at the growth plate, primarily containing cartilage, or more specifically, chondrocytes **(Figure 4-1)**. Chondrocytes in the growth plate undergo a sequential modification of cellular states, including proliferation, hypertrophy, and eventually cell death. These latter events result in the release of membrane-bound matrix vesicles, containing proteins, such as annexins, and phosphatases, which are thought to provide necessary signals and sites for mineralisation by osteoblasts. Osteoclasts are also present, and are responsible for the removal of cartilage matrix, thereby providing a suitable framework for differentiating osteoblasts and bone deposition. Therefore, a concerted process involving chondrocytes, osteoblasts and osteoclasts is required for proper longitudinal bone growth and trabeculogenesis. In humans, during puberty, the ossification front begins to invade the growth plate, eventually resulting in a fusion of the bones (metaphysis and epiphysis) [149, 150]. However, in mice this fusion event never occurs, and essentially, continued growth occurs throughout lifetime, albeit progressively decelerates in adulthood.

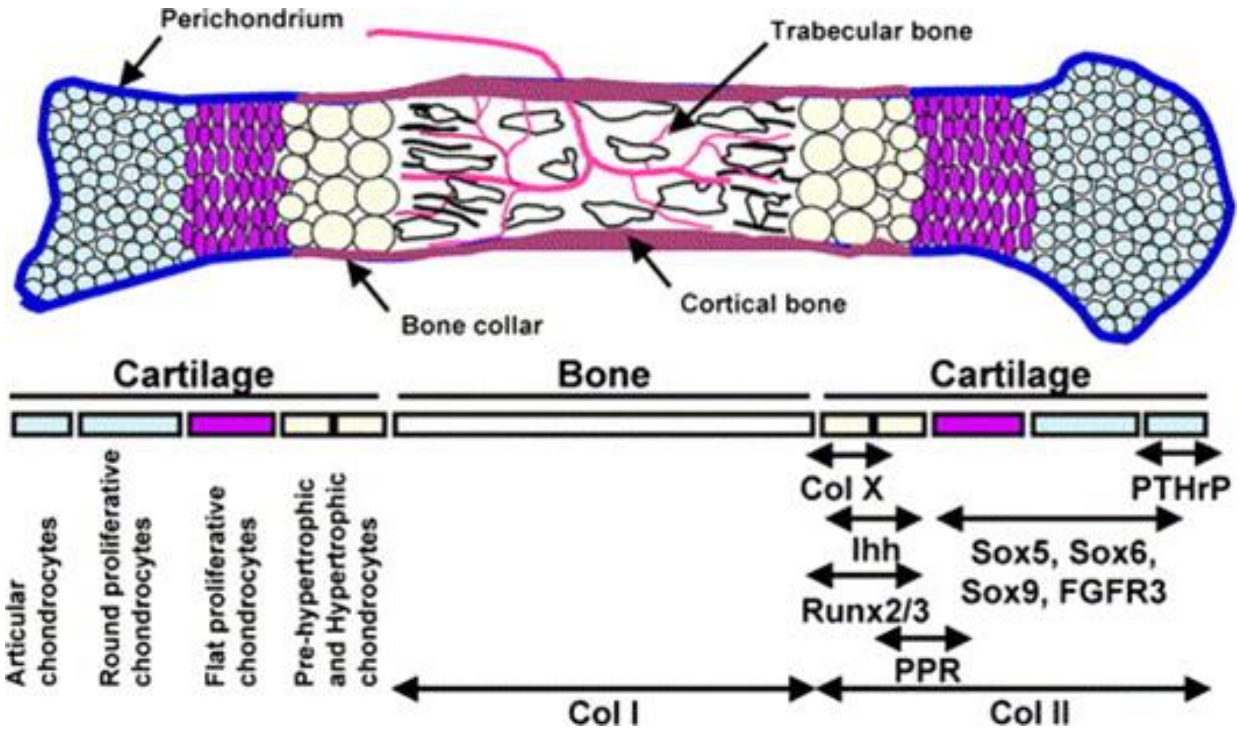

Figure 4-1. Endochondral and intramembranous ossification.

Endochondral ossification results in the longitudinal growth of bones through the concerted efforts of various cell types, including chondrocytes, osteoblasts and osteoclasts. Chondrocytes show an orderly progression through several states, including proliferation, hypertrophy, and death. The latter stage is a signal for osteoblast deposition of bone matrix at the ossification front, leading to matrix mineralisation and growth. Osteoclasts are responsible for cleanup and remodelling of matrix, and aid in generating an appropriate foundation for osteoblast bone deposition. In contrast, intramembranous ossification is responsible for the outward growth of cortical bone in the absence of a cartilage template. Reprinted from Biochemical and Biophysical Research Communications, 328(3), Provot, S., Schipani, E., "Molecular mechanisms of endochondral bone development," 658-665, 2005, with permission from Elsevier.

Intramembranous ossification accounts for the thickening of cortical bone (**Figure 4-1)**. This process occurs in the absence of chondrocytes, and results from the recruitment of mesenchymal stem cells from the periosteum and their subsequent differentiation into mature osteoblasts, capable of bone deposition [148]. Osteoclasts are also involved in bone remodelling in the context of responding to applied stresses to the bone as an organism grow.

4.1.2 Effects of PI3K and MEK inhibition on normal bone development

As described previously, the PX866 and AZD6244 studies on tumor-induced bone remodelling suggested that these agents might be affecting osteoclast and/or osteoblast activity. There is evidence that both the Ras and PI3K pathway are important in osteoclast and osteoblast development and function. For example, it was demonstrated in culture systems with mouse bone marrow cells, inhibition of MEK or PI3K resulted in inhibition of osteoclast differentiation [109]. The authors of this study postulated that this was, at least in part, due to a blockade of RANKL downstream signaling activation. Another investigation also demonstrated that inactivation of ERK1/2 significantly reduced osteoblast RANKL expression, resulting in a delay of osteoclast formation *in vivo* [151]. Similarly, two independent studies demonstrated that Akt1 can induce the expression of RANKL, and stimulate the differentiation and survival of osteoclasts, resulting in enhanced bone resorption *in vitro* and *in vivo* [152, 153]. Loss of Akt1 *in vivo* demonstrated osteoblast differentiation, and an inhibition of coupled-osteoclastogenesis, resulting in a net bone acquisition [153]. Interestingly, crosstalk between the Ras and PI3K pathways has been implicated in supporting osteoclast, differentiation, survival and function [73, 110, 154]. Therefore, there is potential for simultaneous inhibition of the Ras and PI3K pathways to result in an additive reduction in osteoclast activity *in vivo,* similar to osteopetrosis.

4.2 Results

4.2.1 μCT assessment of PX866 and/or AZD6244 administration in normal mice

Vehicle-treated control mice demonstrated a normal pattern of bone growth, consistent with μCT bone parameter analysis. Parameters included BV/TV (bone volume fraction), BMD (bone mineral density), CtTh (cortical thickness), TbTh (trabecular thickness), ConnD (connectivity density), TbN (trabecular number), TbSp (trabecular separation), and BS/BV (bone surface/bone volume). Interestingly, the major effects on bone growth in mice administered PX866, AZD6244, or the combination of both compounds, were primarily a consequence of PI3K inhibition. Thus, AZD6244 did not result in any significant quantitative effects on all bone parameters analyzed. In contrast, PX866 or the combination of both agents resulted in a similar dramatic impairment of endochondral ossification (**Figure 4-2)**. This showed that this process is heavily reliant on PI3K signal transduction, but not the Ras-MAPK pathway. However, as can be visualized in the images that show trabecular thickness, AZD6244 led to a distinct elevation of bone growth under the growth plate, at the ossification front (**Figure 4-3)**. It is possible that the length of treatment with AZD6244 was insufficient to generate a significant quantitative measure (by μCT) of increased trabecular thickness. Additionally, this parameter is a measure of the average trabecular thickness, and is therefore not sensitive to the spatial location of enhanced mineralisation specifically at the ossification front of the growth plate. The qualitative analysis is suggestive that MEK inhibition potentially targeted resorptive osteoclast cells directly, or alternatively enhanced osteoblast differentiation and subsequent bone deposition at the growth plate. Regardless of the mechanism, the results suggest that MEK inhibition may be able to tip the balance back towards osteoblasts.

In contrast to the results obtained with AZD6244, PX866 (See Figure 4-2 for details on

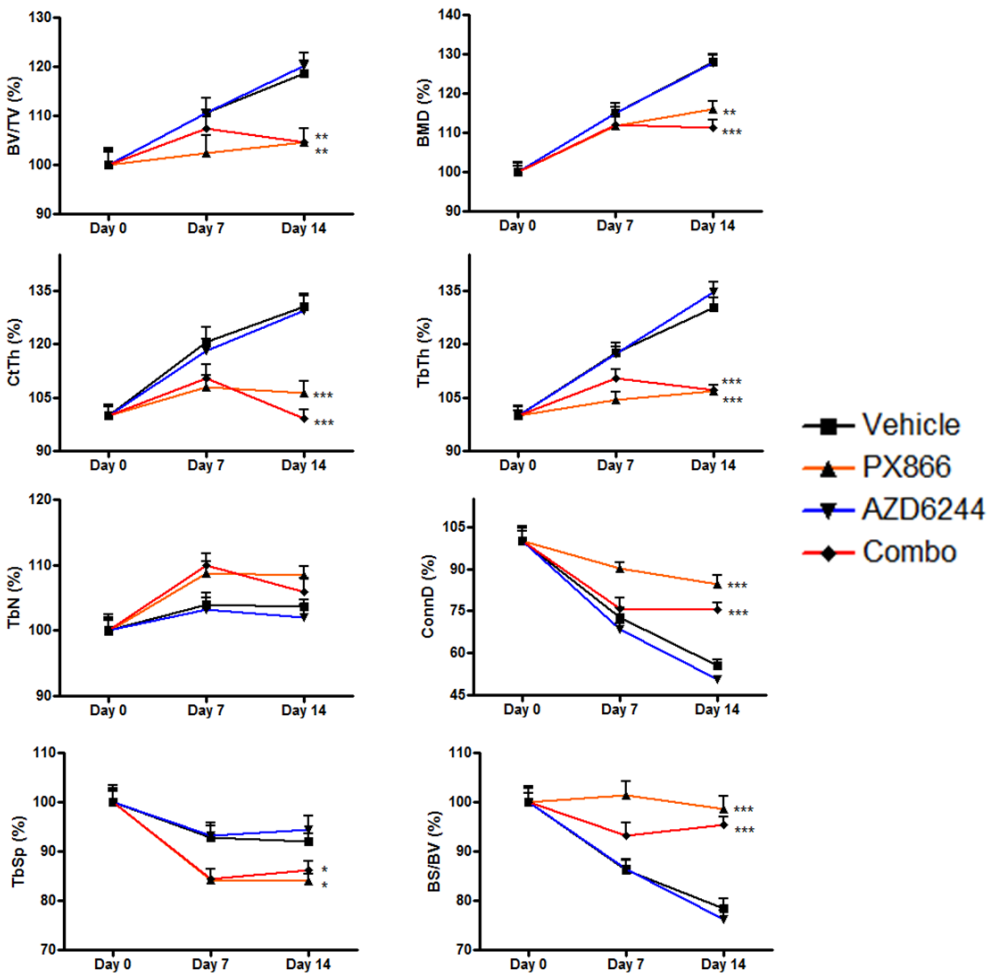

Figure 4-2. Bone quantification of normal mice treated with PX866 and/or AZD6244.

Mice were treated daily with PX866, AZD6244, the combination of both, or vehicle only, at 4-5 weeks of age for 14 days and scanned with microCT on days 0, 7 and 14 to assess the level of bone growth, development and maintenance. Vehicle-treated mice were undergoing obvious considerable growth during this time, implying greater osteoblast presence, and appreciable bone deposition. All bone parameters analyzed, with exception to trabecular number, demonstrated similar and consistent results, in which AZD6244 had no significant effect on bone growth, whereas mice treated with PX866 displayed impaired bone growth. Abbreviations: BV/TV – Bone Volume/Total Volume, BMD – bone mineral density, CtTh – cortical thickness, TbTh – trabecular thickness, TbN – trabecular number, ConnD – connectivity density, TbSp – trabecular separation, BS/BV – bone surface/bone volume. For all treatment groups n=6. Data plotted as mean ± SEM. Asterisks indicate statistical significance (* $p<0.05$; ** $p<0.01$; *** $p<0.001$).

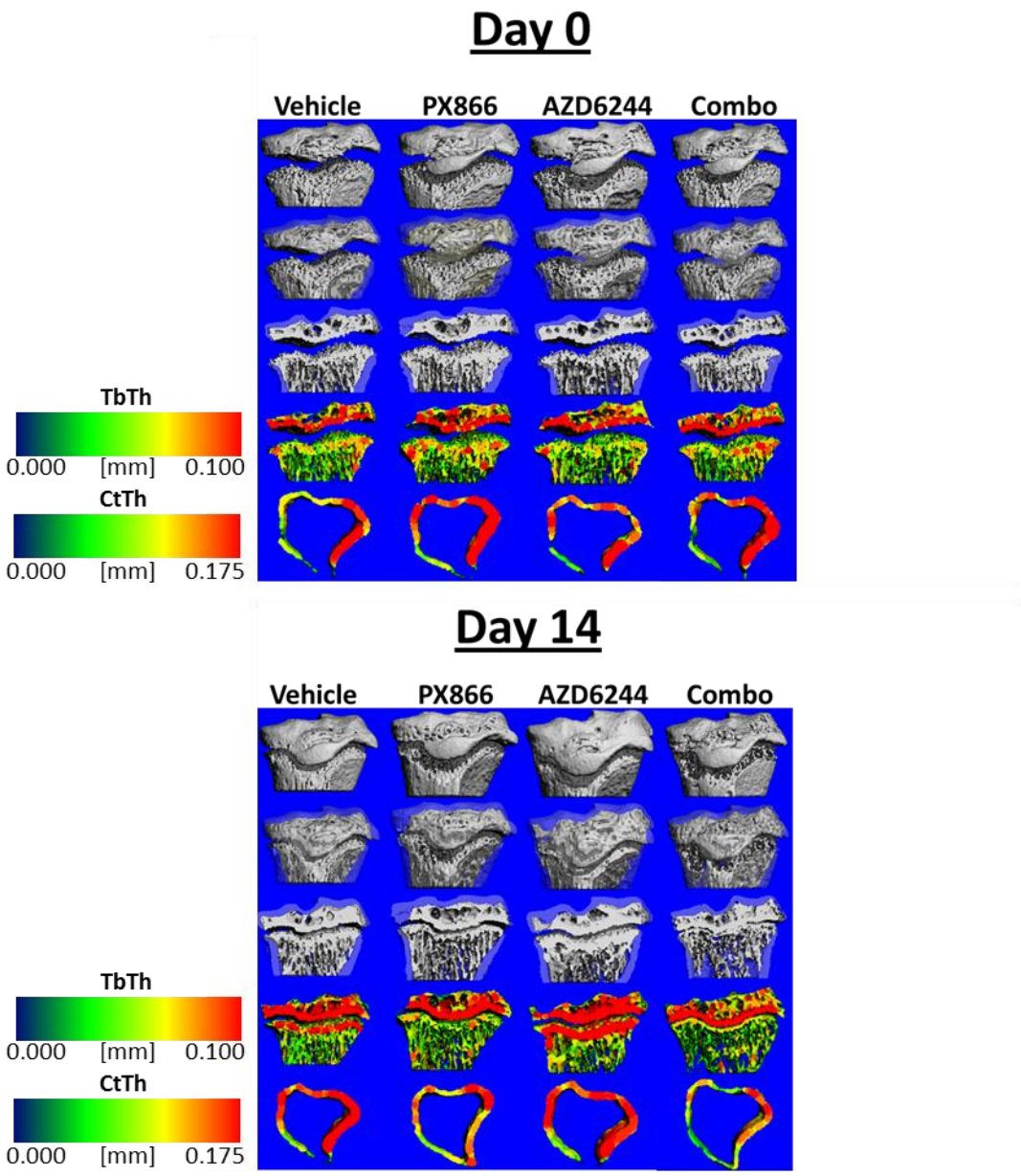

Figure 4-3. µCT bone images of normal mice treated with PX866 and/or AZD6244.

Following 14 days of treatment, mice treated with PX866 resulted in the near complete loss of the cartilage growth plate containing chondrocytes, resulting in an impairment of endochondral ossification and bone mineralisation at the ossification front. In contrast, mice treated with the AZD6244 alone resulted in enhanced endochondral ossification process, and increased the level of bone deposition at the growth plate, Although the mechanism is unknown, it is evident that PI3K inhibition holds the potential to disrupt bone growth, whereas MEK inhibition may actually enhance bone growth.

dosing) resulted in a dramatic impairment of endochondral ossification. Similar results were seen with the combination of PX866 and AZD6244, suggesting that PI3K inhibition alone was responsible for the impairment of bone growth. Trabecular thickness images of PX866-treated animals demonstrated a thinning, and most strikingly, a virtual disappearance of the cartilage growth plate (**Figure 4-3)**, suggesting a direct effect on chondrocyte proliferation and/or differentiation. This would obviously impact osteoblast recruitment and bone formation at the growth plate. It is also plausible that PI3K inhibition could have resulted in a direct inhibition of osteoblast function, differentiation or survival, however, the most profound defect caused by PX866 was the ablation of the growth plate.

The bone parameter trabecular separation was more closely examined with a histogram sphere distribution analysis. There were no PX866-induced differences in large separations, thus only the small separations portion of the graph were analyzed. As mentioned in the previous chapter, an inherently small separation between trabeculae is necessary for the maintenance of proper bone integrity. In the context of bone disease that favors bone-resorbing osteoclasts, such as osteolytic metastases, a loss of the small separations is generally associated with the gain of large separation, generating areas of weakness and predisposition to fracture. However, during normal bone development, some small trabecular separations become filled-in as new bone is laid down. As demonstrated by the histogram distribution, vehicle-treated controls and AZD6244 treated mice demonstrated similar levels of small trabecular separation loss throughout the 14 day period, whereas the PX866 (and combo) treated mice displayed a static level of small trabecular separation between days 7 and 14 of the treatment period (**Figure 4-4)**. Consistent with other bone parameters, the histogram distribution of trabecular separation indicates that PI3K inhibition, but not MEK inhibition, results in impairment of normal bone growth.

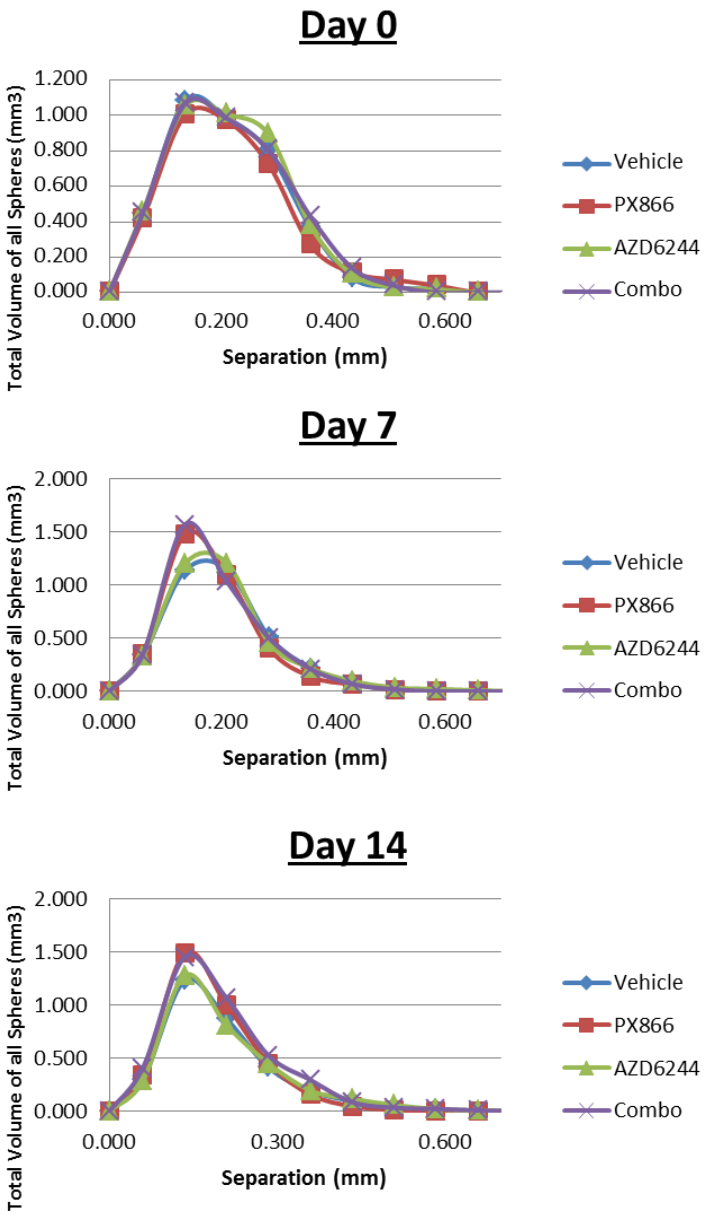

Figure 4-4. Histogram distribution of trabecular separation of normal mice treated with PX866 and/or AZD6244.

Vehicle-treated controls and AZD6244 treated mice demonstrated similar losses of small trabecular separations throughout the 14 day period. In contrast, PX866-treated (and combination) mice displayed a constant level of small trabecular separation at day 7 and 14 of the treatment period, indicating an impaired capacity for new bone deposition. For all treatment groups n=6.

4.2.2 Histological examination of PX866 and/or AZD6244 administration in normal mice

Histological examination of mice in this investigation was consistent with results obtained with μCT **(Figure 4-5)**. Vehicle-treated control mice demonstrated normal endochondral ossification, with intact chondrocyte stages of differentiation. These include resting cells (chondrocyte progenitors), stacks of proliferating chondrocytes, followed by pre- and late-stage hypertrophy. The latter stimulate angiogenesis and recruitment of marrow derived osteoclasts, and also osteoblasts that will imitate the process of ossification beneath the growth plate. Mice treated with PX866 demonstrated significantly less bone deposition at the growth plate, most likely due to a negative influence on any one or more of these processes. Mice treated with both PX866 and AZD6244 demonstrated a further effect on chondrocyte development, with an obvious reduction in the width of the epiphyseal growth plate and decreased bone formation. It has been demonstrated previously that PI3K inhibition can affect endochondral ossification through a reduction in the proliferative, and particularly the hypertrophic zone of chondrocytes both *in vitro* and *ex vivo* [155]. Therefore, the observed endochondral ossification impairment seen here *in vivo* was most likely due to PX866. However, as crosstalk between PI3K and Ras occurs, it is possible for the combination of both compounds to produce an additive impairment of the endochondral ossification process. In contrast, mice treated with AZD6244 alone appeared to have an enhanced level of chondrocyte development with an apparent increase of the proliferative and hypertrophic zone of chondrocytes. It has been demonstrated in embryonic limb tissue that pharmacological MEK inhibition can enhance chondrocyte differentiation and the accumulation of cartilage matrix [156]. Therefore, it is likely that AZD6244 is causing a qualitative increase of bone deposition at the ossification front, as assessed by μCT, suggesting an overall enhancement of endochondral ossification.

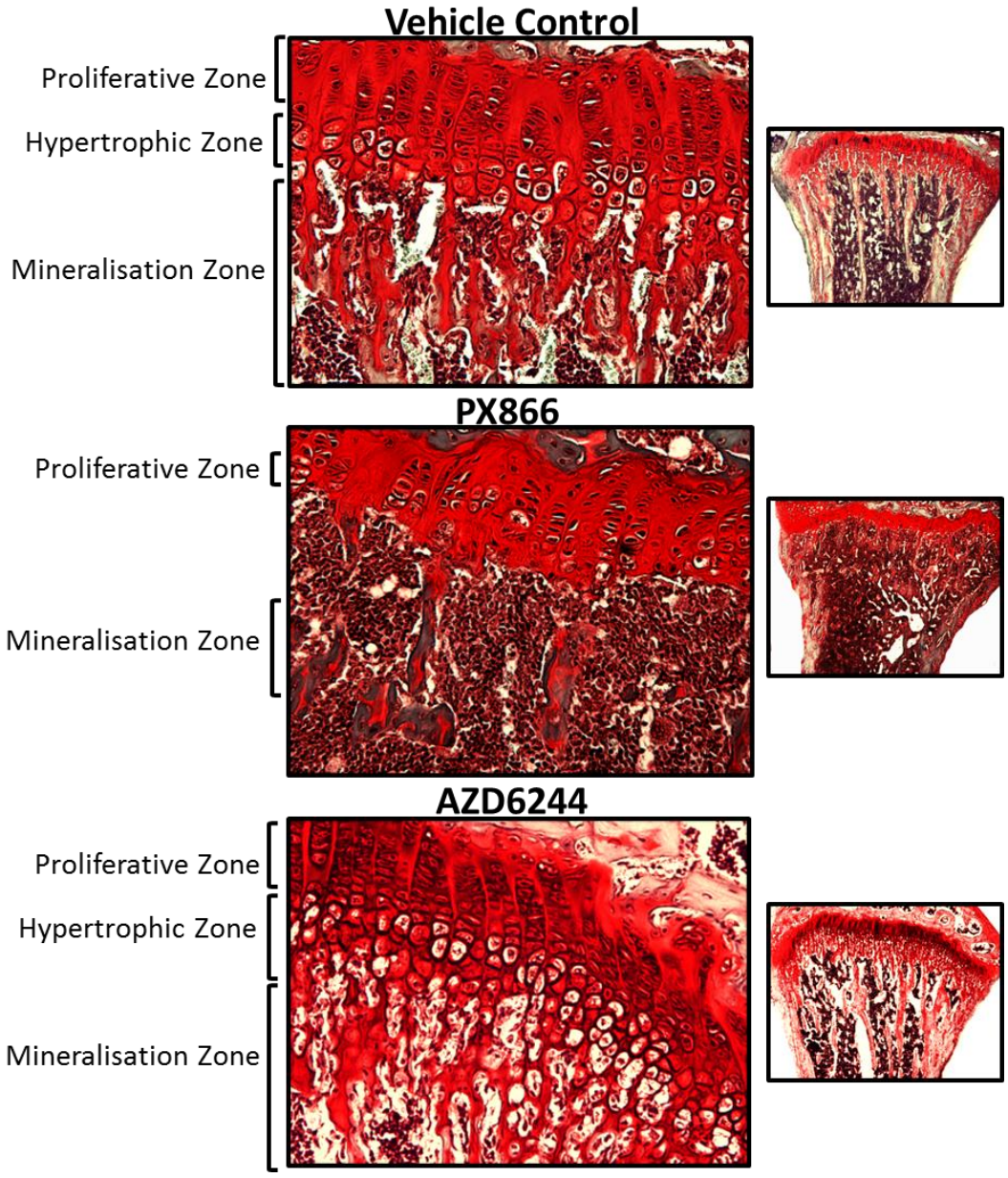

Figure 4-5. Histological examination of growth plates from normal mice treated with PX866 or AZD6244.

Vehicle-treated control mice demonstrated normal endochondral ossification. Mice treated with PX866 demonstrated an inhibition of endochondral ossification, likely due to an impairment of chondrocyte differentiation, visualized by a reduction in the proliferation zone and near disappearance of the hypertrophic zone. Mice treated with both PX866 and AZD6244 showed a similar appearance to PX866 treatment alone, and therefore was not shown. In contrast, mice treated with AZD6244 alone appeared to harbor larger zones of chondrocyte proliferation and hypertrophy, potentially enhancing endochondral ossification. Sectioning and tri-chrome stained done by Leona Barclay.

4.3 Discussion

Differential effects of pathway inhibition are likely to exist within diverse environmental contexts, such as in the presence of bone metastases, or during normal bone growth and maintenance. It is difficult to make direct comparisons in each situation; however, an evaluation of PI3K and Ras-MAPK signal pathway inhibition in mice without tumors is an important and useful determinant. The subsequent direct effects on resident bone cells may aid in predictive effects of pathway inhibitor administration in the context of different bone diseases, such as rheumatoid arthritis, or osteolytic metastases.

We demonstrated that PI3K inhibition resulted in a severe impairment of endochondral ossification, an important process required for normal bone growth. Extrapolating from mice to humans, it raises the possibility that PI3K inhibitors given to children and adolescents might stunt long bone growth. This would depend on the dose and duration of treatment obviously. However, in adult humans whose growth plates have fused, PI3K inhibition may have no such negative effect and may be more effective as a therapeutic agent under certain pathological conditions, such as those involving excess osteoclast activity. For example, joint destruction that occurs in rheumatoid arthritis is thought to arise due to the direct effect of osteoclasts [157]. In an arthritis mouse model, PI3K inhibition effectively resulted in reduced bone destruction, and inhibition of osteoclast numbers and activity [61]. PI3K inhibition may be able to effectively impair osteoclast function in this setting through disruption of RANKL and CSF-1 induced osteoclastogenesis [71, 158]. Alternatively, loss of PI3K activity may directly inhibit osteoclast function, via disruption of the ruffled border and attachment to the bone matrix, or inhibition of osteoclast survival and differentiation [130]. In contrast, normal bone remodelling and growth is heavily reliant on osteoblast function at the ossification front, and PI3K inhibition may result in

the inhibition of both chondrocytes and osteoblasts. It is also possible that chondrocytes, osteoblasts and osteoclasts all rely on PI3K signaling, for diverse purposes at different times, such as differentiation, migration, survival and function. Interestingly, it has been shown that increased PI3K activity, through PTEN deletion in chondrocytes and osteoblasts, resulted in an enhancement of growth plate matrix production and accelerated hypertrophic differentiation [159]. This demonstrates the consequences of disproportionately high PI3K activity, resulting in abnormal skeletogenesis. Since we found that PX866 was able to inhibit proliferation, and/or induce apoptosis of chondrocytes, it might prove useful in the treatment of chondrosarcoma.

In contrast, we found that MEK inhibition demonstrated no significant quantitative effect on growth over a 2-week treatment period with AZD6244. However, histological analysis displayed an appreciable increase in bone deposition at the ossification front beneath the growth plates. Representative μCT cross-sections of tibial bones, including heat map trabecular thickness, show that MEK inhibition may be enhancing the endochondral ossification process, although the precise mechanism remains nebulous. It is possible that MEK inhibition resulted in an increased proliferative and/or transit of chondrocytes into the hypertrophic state thus enhancing osteoblast recruitment and bone matrix deposition at the growth plate. The reverse effect was demonstrated by others using constitutively-active MEK in chondrocytes that resulted in dwarfism that was associated with an inhibition of hypertrophic chondrocyte differentiation [160]. In addition, it is possible that MEK inhibition either increased the differentiation and numbers of osteoblasts, or reduced the number of osteoclast cells. Indeed, it has been demonstrated that inactivation of MEK reduced osteoblast expression of RANKL [151], one of the critical factors supporting osteoclastogenesis. Qualitative examination of histological sections suggested that AZD6244 was able to enhance the proliferative and hypertrophic zones of

chondrocytes, perhaps accounting for the increased endochondral ossification observed. Regardless of the exact mechanism, we found qualitative evidence that MEK inhibition was able to increase the level of bone mineralisation during normal bone development. This suggests that MEK inhibition may be useful as a therapeutic intervention in bone diseases characterized by pathological osteoclast activity, such as osteolytic metastases, inflammatory arthritis, and Paget's disease.

It should also be noted that inherent genetic differences between the strains of mice used in the tumor and normal mouse studies may generate distinct results. Therefore, direct comparison between these studies may not be entirely appropriate. For example, nude NIH-III mice possess a vestigial thymus incapable of producing mature T-cells [161], and theoretically could demonstrate differential effects upon PI3K and MEK inhibition. However, the C57/Bl6 mouse strain is immunocompotent, and is likely to represent a more accurate mechanism of normal human bone development.

4.4 Future directions

Although not a central consideration for this study, a brief investigation on PI3K and Ras pathway inhibitor administration in normal healthy mice was an important preliminary step in understanding the pleiotropic effects that agents employed for the treatment of pathological conditions might show. Without sufficient understanding of systemically administered signaling pathway inhibitors, the potential exists for either exacerbating disease phenotypes, or for side effects on normal tissues. Indeed, much more investigation is necessary to fully comprehend both the early and late effects of pathway inhibitors.

This brief examination into PI3K and MEK inhibition in young normal C57Bl/6 mice revealed that PI3K inhibition was harmful to the endochondral ossification process, and hence, to the growth of long bones. The dramatic results obtained in this study merit further investigation into the molecular and cellular mechanisms by which PX866 and AZD6244 alter endochondral ossification. For example, using the Cre-Lox recombination method, it is possible to generate mice that have a deletion of PI3K, MEK or ERK in specific cell types including osteoblasts, osteoclasts, or chondrocytes. This would allow for a more specific delineation and understanding of the effects seen when systemically administering small-molecule signaling pathway inhibitors. If PI3K were toxic to human growth plates, it could still be a useful therapeutic option in bone diseases that are prevalent in adults, such as rheumatoid arthritis, or osteolytic metastases. Furthermore, for the latter, MEK inhibition may prove to be a more beneficial treatment, as this can reduce tumor burden, attenuate tumor-induced bone resorption, while at the same time enhancing bone deposition.

It would also be valuable to examine the potential efficacy of PI3K pathway inhibition in the treatment of chondrosarcoma or osteosarcoma. Chondrosarcoma is a type of cancer that is generated from transformed chondrocyte precursors [162], whereas osteosarcoma arises from mesenchymal cells with preferential osteoblastic differentiation. Indeed, both cell types arise from common osteo-chondro progenitor cells [151], and therefore harbour similar characteristics that may prove to be both susceptible to similar PI3K pathway inhibition treatment. Based on the dramatic effects of PI3K inhibition that we observed, PX866 (possibly in conjunction with AZD6244) might be a worthwhile therapeutic strategy to pursue for these debilitating bone tumors.

Chapter Five: **Discussion**

5.1 Implications, translational relevance and future directions

There are a variety of significant implications that this study reveals, and generates innovative questions for the development of appropriate and effective treatment modalities for osteolytic metastasis arising from breast cancer progression. Throughout the history of cancer research, it is consistently revealed that cancer cells evolve and develop sophisticated mechanisms to perpetuate growth, and survival, despite significant advances in the generation of potent and creative therapeutic agents. For example, the rapid expansion of approaches for identifying commonly mutated and ectopically activated signaling pathways has led to the rapid production of signaling pathway inhibitors for the treatment of particular cancers. Indeed, genetic screening and further understanding of cancer cell molecular mechanisms will be the necessary approach in order to determine the most effective and appropriate therapeutic agents to use.

The PI3K and Ras signal transduction pathways are considered to be among the most commonly mutated and aberrantly activated in all cancer types, particularly in aggressive forms of breast cancer [60, 67]. Therefore, a variety of small-molecule inhibitors have been developed, in hopes of targeting cancer cell exploitation of these pathways, as an effective therapeutic intervention. Furthermore, the mutual dependency of these pathways through complicated signaling crosstalk networks has revealed resistance patterns when either pathway is targeted alone. This has led to the notion that simultaneous inhibition of these pathways will be necessary for effective treatment [69, 79, 103]. However, this study suggests that cancer cell dependency on both pathways may not be as critical as previously thought [163], at least as a universal

certainty, and is likely predictive with specific mutations or cancer cell types; again, meriting the necessity for personalized genetic screening, prior to treatment.

Both *in vitro* and *in vivo* components of this study demonstrated that simultaneous inhibition of both PI3K and MEK did not lead to any significant additive effects on MDA-MB-231 cells (perhaps with exception to the induction of *in vitro* cell cycle arrest). However, these observations may be a cell type specific event, and therefore further examination is necessary using a broad range of different human breast cancer cell lines, as well as with samples taken directly from breast cancer patients. This will allow for a more comprehensive examination of effects, following treatment with PI3K and MEK inhibitors, categorized based on the transcriptional profile of breast cancer subtypes. For example, as previously mentioned in section 3.8.2, a study demonstrated that basal-like breast cancer cell lines that harbor the wild-type p53 tumor suppressor, exposed to simultaneous PI3K and MEK inhibition, resulted in additive apoptosis, whereas those that harbored mutant p53 demonstrated additive cell cycle arrest [79]. The latter finding is similar to results observed in this study. This is suggestive that genetic screening for p53 status in breast cancer patients can be a potential determinant of therapeutic effectiveness when treated with PI3K and MEK inhibitors.

The additional finding in this study that MDA-MB-231 cells in low serum conditions can result in dramatic sensitivity to MEK inhibition leads to further important implications. It is well known that the Ras-MAPK pathway is highly deregulated in many cancers and can be exploited to perpetuate cancer cell survival when confronted with toxic stimuli, such as nutrient deprivation [137]. For example, Ras-MAPK signaling was shown to be critical for the stabilization of mutant p53 during times of nutrient-deprived stress, which led to enhanced cancer cell survival [137]. Therefore, if it is possible to mimic a state of nutrient deprivation,

such as inhibiting cancer cell mechanisms for energy production, it may be conceivable to make the cells susceptible to MEK inhibition. For example, agents that target the highly exploited glycolytic process [164], may demonstrate a heightened sensitivity to MEK inhibitors. Again, this may be cell type specific, and therefore examination in multiple cell lines and samples is important.

Strong evidence now suggests that mutant p53 can exert an oncogenic gain of function, in contrast to the tumor suppressive activity of wild-type p53 [165]. Further investigation should be directed towards mutant p53 in breast cancer, as there is a high incidence among triple-negative breast cancer patients [139]. There are a variety of processes that can be examined to determine if mutant p53 elimination in MDA-MB-231 cells may induce a variety of anti-cancer effects, such as reduced migration, invasion, survival, colonization, growth, and in the context of specific breast cancer metastasis, impede tumor-induced osteolysis. RNA interference (RNAi) [166], or the more recently developed zinc finger nuclease (ZFN) method [167] are capable of providing potent and effective down-regulation of specific genes, such as mutant p53 in MDA-MB-231 cells *in vitro.* Interestingly, a group recently used zinc-finger nucleases to induce the repair of mutant p53 and restore wild-type tumor-suppressive functioning [168]. Therefore, similar techniques in MDA-MB-231 cells, that only harbor mutant p53, could be used to assess whether reconstitution of wild-type p53 tumor-suppressive capacity is able to produce anti-cancer effects. Upon confirmation of mutant p53 knockdown or re-introduction of wild-type p53, MDA-MB-231 breast cancer cells could be examined *in vitro* for enhanced sensitivity to chemotherapeutic or PI3K and MEK inhibitors (alone and in combination). This could determine if the presence of mutant p53 is responsible for the inherent resistance observed following exposure to such agents [79]. Additionally, MDA-MB-231-EGFP/Luc2 cells, devoid or repaired of mutant p53 could

similarly be intracardiac injected into NIH-III mice. This could determine if mutant p53 is a critical factor in cancer cell survival in the blood stream, and responsible for the invasive behavior of the MDA-MB-231 cells into the bone microenvironment. Furthermore, if the cancer cells successfully colonized the bone, the growth rate and expansion of the MDA-MB-231-EGFP/Luc2 cells could be monitored with bioluminescence imaging, permitting an investigation into *in vivo* growth kinetics and survival. PI3K and/or MEK inhibitors could also be employed in this setting to determine if bone-colonized MDA-MB-231-EGFP/Luc2 cells are susceptible to this type of treatment, in the absence of mutant p53.

It would also be of interest to introduce other p53 family members, such as p73, which have been documented to produce similar tumor-suppressive functions as wild-type p53 [169]. Gene introduction, under the control of constitutively active promoters, could allow determination if the implementation of p73 tumor-suppressive functions are capable of sensitizing aggressive triple-negative breast cancer cells that have developed mutations in p53. Exposure to chemotherapeutic agents, or PI3K and MEK inhibitors *in vitro* and *in vivo* would be useful to investigate if enhanced sensitivity can be acquired in the presence of normally functioning tumor-suppressive capacity. In a translational sense, knockdown of mutant p53 is currently unrealistic as a treatment modality, however, there have been reports of compounds that are able to increase levels of p53 family members, such as p73 [169, 170]. This could prove to be a potential therapeutic avenue, possibly in combination with chemotherapeutic agents or PI3K/MEK inhibitors. The p53 transcription factor modulates many cellular processes, and the fact that it is considered to be one of the most frequently mutated in all cancer types provides a strong rationale for further investigation of its role in metastatic breast cancer, as well as generating creative ways to target or reverse its pro-tumorigenic effects.

As was mentioned in section 3.9.1, it is possible that the presence of mutant p53 in MDA-MB-231 cells may be a potential explanation for the high levels of the anti-apoptotic protein Bcl-2 [142, 146], which has been implicated in the resistance to various compounds, including PI3K and MEK inhibitors [141]. Therefore, gene knockdown of mutant p53, or re-introduction of wild-type p53 or family members, such as p73, could decipher the regulatory connections with Bcl-2 or other anti-apoptotic machinery. This could potentially provide a possible mechanism of action for the dramatic sensitivity of MDA-MB-231 cells exposed to MEK inhibition in low serum conditions. More specifically, it has been observed that MEK inhibition, under nutrient deprived conditions, destabilizes mutant p53 [137], and mutant p53 can positively regulate Bcl-2 levels [146]. Therefore, this would suggest that low (0.1%) serum conditions may generate an inherent sensitivity to AZD6244, based on the de-regulation of anti-apoptotic Bcl-2. This type of investigation would also provide an explanation for the dramatic sensitivity of cultured MDA-MB-231 cells in full (10%) serum, exposed to simultaneous Bcl-2 (ABT-263) and MEK inhibition, observed in this study. As p53 is inherently difficult to target, Bcl-2 and MEK inhibition could prove to be a more effect mode of treatment, and should be more closely examined *in vivo*. Further delineation of signaling transduction pathway connections and their regulation will surely generate avenues for potential therapeutic intervention in many cancers that harbor diverse transcriptional profiles.

Employing techniques for *in vitro* knockdown of PI3K or MEK in MDA-MB-231 cells, such as with RNAi or ZFN approaches, would permit a closer examination of these pathways in the context of metastatic progression. Following successful pathway termination, an intracardiac injection could reveal the significance of PI3K and Ras-MAPK signaling in MDA-MB-231, or other breast cancer cells, in invasion, extravasation, and colonization in the bone

microenvironment. Furthermore, if cancer cells successfully colonized the bone, tumor-induced effects on resident bone cells could more specifically be monitored. For example, the systemically administered PX866 and AZD6244 agents generate pleiotropic effects that are difficult to specifically monitor. In contrast, removal of specific signaling pathway components in MDA-MB-231 cells, prior to the generation of established bone metastasis, could be an effective means to identify explicit molecular mechanisms *in vivo.*

This study also revealed the potential for certain treatment regimens to be more detrimental rather than beneficial, resulting in exacerbation of disease phenotypes. The simultaneous inhibition of PI3K and MEK in mice with established bone metastasis resulted in no additive tumor reduction, relative to MEK inhibition alone, but exacerbated the tumor-induced bone destruction. In fact, mice treated with both PX866 and AZD6244, demonstrated similar, and at times more severe bone loss, when compared to vehicle-treated control mice harboring much greater tumor presence. This exacerbated phenotype was not observed in healthy mice (Chapter Four) administered both compounds concomitantly, suggesting that the presence of MDA-MB-231 cells in the bone-microenvironment, along with simultaneous signaling pathway inhibition, accelerated the pathological condition. As *in vitro* cytokine secretion data suggests, this could possibly be due to enhanced MDA-MB-231 cytokine secretion of osteoclast-promoting factors, such as IP-10, which is a potent recruiter of osteoclast monocyte precursor cells into the bone microenvironment [53]. TRAP quantification of osteoclasts also suggests that combinatorial treatment resulted in increased osteoclast numbers in the tumor-bone microenvironment and could be a potential explanation for the enhancement of bone destruction. Numerous studies have demonstrated additive beneficial effects of PI3K and MEK inhibition in targeting MDA-MB-231 cells, as well as others cell lines, *in vitro* and *in vivo* [79, 80]. However,

these investigations used subcutaneous models of breast cancer, and therefore did not consider the primary or metastatic microenvironment. Therefore, the data here suggests that caution should be taken when employing PI3K and MEK inhibitors for the treatment of osteolytic metastases, as no apparent benefit was observed, and may potentially result in an exacerbation of tumor-induced bone destruction.

Because this study attempted to utilize a model of breast cancer metastasis that incorporates the tumor-bone microenvironment, a brief examination of PX866 and AZD6244 effects on normal bone development, in the absence of an established tumor, was a logical next step. Although initially unexpected, PX866 induced a potent impairment of endochondral ossification. This was initially unanticipated, because in the presence of established bone metastasis, PX866 demonstrated an attenuation of tumor-induced osteolysis. This is suggestive that PI3K inhibition is able to directly or indirectly reduce osteoclast numbers or resorptive function, in the context of osteolytic metastases. However, in normally developing mice, PX866 is likely targeting chondrocyte differentiation in the growth plate that is critical for endochondral ossification, as assessed by μCT and histological examination. PI3K signaling is important in many different cell types for various functions, such as migration, invasion, growth and survival. In this sense, it is likely that employing PX866 under diverse physiological conditions, such as in developing mice, as opposed to more mature mice with established bone metastasis, will result in diverse outcomes. Therefore, in the context of certain pathological conditions, such as those that favor osteoclast activity, PI3K inhibition could be useful as a potential treatment. However, this study also reveals that caution should be taken when administering PI3K inhibitors, particularly to children and adolescents that are undergoing times of intense growth and development. Furthermore, this data also suggests that PX866 administration may be a valuable treatment for

other forms of cancer, such as osteosarcoma or chondrosarcoma, cancers that are confined to osteo-chondro progenitor lineage [151]. Further examination of PI3K inhibition should be investigated *in vitro*, as well as in accurate models of these cancers.

In contrast to the detrimental effects of PI3K inhibition in developing mice, MEK inhibition didn't have a significant effect on endochondral ossification. However, μCT generated images demonstrated an increase in bone growth at the growth plate. Furthermore, histological examination of mice treated with AZD6244 showed enlarged zones of chondrocyte proliferation and hypertrophy, as well as mineralisation. Although the mechanism is unknown, this is suggestive that MEK inhibition can accelerate and enhance endochondral ossification.

Simultaneous PX866 and AZD6244 administration demonstrated an impairment of chondrocyte differentiation and endochondral ossification, similar to PX866 alone, suggesting this process is highly reliant on the PI3K signaling pathway.

Although quite laborious, a mechanism of action of systemically administered PI3K or MEK inhibitors in developing mice, could be investigated by generating mice with an inducible Crelox recombinase method [171]. This would produce cell-specific knockdown of PI3K or MEK in chondrocytes, osteoblasts or osteoclasts, at any point of time, upon administration of an inducible factor. This aspect could be studied in the context of normally developing mice or mice with established bone metastases. The latter situation could be useful in determining signaling pathways involved in the osteolytic process, within specific resident bone cells. For example, the presence of MDA-MB-231-EGFP/Luc2 cells in the bone microenvironment would attempt to stimulate resident bone cells through cytokine and growth factor secretion; however, disabling PI3K and/or MEK specifically in chondrocytes, osteoblasts or osteoclasts could potentially determine critical signaling pathway involvement in tumor-induced osteolysis.

Although it is difficult to decipher the mechanism of action of systemically administered agents, such as small molecule pathway inhibitors, relevant information can be acquired that is useful for determining effective therapeutic avenues. In our study, AZD6244 achieved the highest effectiveness as a therapeutic agent, resulting in reduced tumor bioluminescence (with enhanced sensitivity to nutrient deprived cells), an attenuation of tumor-induced osteolysis, and an enhancement of endochondral ossification in normally developing mice. This is suggestive that AZD6244, perhaps in conjunction with an additional therapeutic agent, should be considered a potentially valuable option for the treatment of pathological bone diseases that favor osteoclasts, such as osteolytic bone metastasis.

5.2 Concluding remarks

As pre-clinical examination of potential therapeutic agents are investigated, more accurate models portraying human disease need to be utilized in order to appropriately assess efficacy. Although the intracardiac route for generating distant metastasis is not a perfect model, it is an improvement that exemplifies important processes during cancer progression in humans. This model was valuable to examine PI3K and MEK inhibition with PX866 and AZD6244, respectively. Furthermore, the use of μCT technology allowed a closer inspection of direct or indirect effects within the tumor-bone microenvironment.

Collectively, the results in this study suggest diverse effects can occur following systemic administration of small-molecule signaling pathway inhibitors. For example, combinatorial treatment regimens, such as with PX866 and AZD6244, may exacerbate pathological conditions. Furthermore, inhibition of important signaling pathways may have detrimental effects under non-pathological conditions, such as that seen with PX866 on proper bone development. Therefore, a

key element of our study indicates that consideration of the microenvironment is essential in determining safety and efficacy of therapeutic agents. Although closer examination of specific molecular interactions is necessary using gene manipulation techniques, realistic pre-clinical therapeutic effectiveness is ultimately achieved through the systemic administration of such agents, similar to the treatment of human diseases.

Further delineation of signaling pathway regulation and crosstalk, along with personalized genetic screening will be crucial in determining the most appropriate treatment modality for cancer patients. The data here is suggestive that MEK inhibition may prove to be a valuable addition to the frontline of treatment for osteolytic breast cancer metastasis, likely achieving maximal benefit in conjunction with other agents. However, it is evident that much more scientific exploration is necessary in order to determine the most tolerable, safe and effective approach for therapeutic intervention.

References

1. Jemal, A., et al., *Global cancer statistics.* CA Cancer J Clin, 2011. **61**(2): p. 69-90.
2. Bocker, W., *[WHO classification of breast tumors and tumors of the female genital organs: pathology and genetics].* Verh Dtsch Ges Pathol, 2002. **86**: p. 116-9.
3. Lavasani, M.A. and F. Moinfar, *Molecular classification of breast carcinomas with particular emphasis on "basal-like" carcinoma: A critical review.* J Biophotonics, 2012. **5**(4): p. 345-66.
4. Blows, F.M., et al., *Subtyping of breast cancer by immunohistochemistry to investigate a relationship between subtype and short and long term survival: a collaborative analysis of data for 10,159 cases from 12 studies.* PLoS Med, 2010. **7**(5): p. e1000279.
5. Molyneux, G., et al., *BRCA1 basal-like breast cancers originate from luminal epithelial progenitors and not from basal stem cells.* Cell Stem Cell, 2010. **7**(3): p. 403-17.
6. Perou, C.M., et al., *Molecular portraits of human breast tumours.* Nature, 2000. **406**(6797): p. 747-52.
7. Sorlie, T., et al., *Repeated observation of breast tumor subtypes in independent gene expression data sets.* Proc Natl Acad Sci U S A, 2003. **100**(14): p. 8418-23.
8. Sorlie, T., et al., *Gene expression patterns of breast carcinomas distinguish tumor subclasses with clinical implications.* Proc Natl Acad Sci U S A, 2001. **98**(19): p. 10869-74.
9. Callagy, G., et al., *Molecular classification of breast carcinomas using tissue microarrays.* Diagn Mol Pathol, 2003. **12**(1): p. 27-34.
10. Nielsen, T.O., et al., *Immunohistochemical and clinical characterization of the basal-like subtype of invasive breast carcinoma.* Clin Cancer Res, 2004. **10**(16): p. 5367-74.
11. Cheang, M.C., et al., *Ki67 index, HER2 status, and prognosis of patients with luminal B breast cancer.* J Natl Cancer Inst, 2009. **101**(10): p. 736-50.
12. Tischkowitz, M., et al., *Use of immunohistochemical markers can refine prognosis in triple negative breast cancer.* BMC Cancer, 2007. **7**: p. 134.
13. Eroles, P., et al., *Molecular biology in breast cancer: Intrinsic subtypes and signaling pathways.* Cancer Treat Rev, 2011.
14. *Tamoxifen for early breast cancer.* Cochrane Database Syst Rev, 2001(1): p. CD000486.
15. De Mattos-Arruda, L. and J. Cortes, *Advances in First-Line Treatment for Patients with HER-2+ Metastatic Breast Cancer.* Oncologist, 2012.
16. Piccart-Gebhart, M.J., et al., *Trastuzumab after adjuvant chemotherapy in HER2-positive breast cancer.* N Engl J Med, 2005. **353**(16): p. 1659-72.
17. Carotenuto, P., et al., *Triple negative breast cancer: from molecular portrait to therapeutic intervention.* Crit Rev Eukaryot Gene Expr, 2010. **20**(1): p. 17-34.
18. Dent, R., et al., *Triple-negative breast cancer: clinical features and patterns of recurrence.* Clin Cancer Res, 2007. **13**(15 Pt 1): p. 4429-34.
19. Troester, M.A., et al., *Gene expression patterns associated with p53 status in breast cancer.* BMC Cancer, 2006. **6**: p. 276.
20. Hess, K.R., et al., *Metastatic patterns in adenocarcinoma.* Cancer, 2006. **106**(7): p. 1624-33.
21. Nguyen, D.X., P.D. Bos, and J. Massague, *Metastasis: from dissemination to organ-specific colonization.* Nat Rev Cancer, 2009. **9**(4): p. 274-84.

22. Clezardin, P., *Therapeutic targets for bone metastases in breast cancer.* Breast Cancer Res, 2011. **13**(2): p. 207.
23. Zhang, X.H., et al., *Latent bone metastasis in breast cancer tied to Src-dependent survival signals.* Cancer Cell, 2009. **16**(1): p. 67-78.
24. Roodman, G.D., *Mechanisms of bone metastasis.* Discov Med, 2004. **4**(22): p. 144-8.
25. Suva, L.J., R.J. Griffin, and I. Makhoul, *Mechanisms of bone metastases of breast cancer.* Endocr Relat Cancer, 2009. **16**(3): p. 703-13.
26. Coleman, R.E., *Metastatic bone disease: clinical features, pathophysiology and treatment strategies.* Cancer Treat Rev, 2001. **27**(3): p. 165-76.
27. Roodman, G.D., *Mechanisms of bone metastasis.* N Engl J Med, 2004. **350**(16): p. 1655-64.
28. Mohan, S. and D.J. Baylink, *Bone growth factors.* Clin Orthop Relat Res, 1991(263): p. 30-48.
29. Minn, A.J., et al., *Distinct organ-specific metastatic potential of individual breast cancer cells and primary tumors.* J Clin Invest, 2005. **115**(1): p. 44-55.
30. Yu, H.H., Y.Y. Tsai, and S.E. Hoffe, *Overview of diagnosis and management of metastatic disease to bone.* Cancer Control, 2012. **19**(2): p. 84-91.
31. Bock, O. and D. Felsenberg, *Bisphosphonates in the management of postmenopausal osteoporosis--optimizing efficacy in clinical practice.* Clin Interv Aging, 2008. **3**(2): p. 279-97.
32. Casimiro, S., T.A. Guise, and J. Chirgwin, *The critical role of the bone microenvironment in cancer metastases.* Mol Cell Endocrinol, 2009. **310**(1-2): p. 71-81.
33. Tonyali, O., C. Arslan, and K. Altundag, *The role of zoledronic acid in the adjuvant treatment of breast cancer: current perspectives.* Expert Opin Pharmacother, 2010. **11**(16): p. 2715-25.
34. Hussein, O. and S.V. Komarova, *Breast cancer at bone metastatic sites: recent discoveries and treatment targets.* J Cell Commun Signal, 2011. **5**(2): p. 85-99.
35. Onishi, T., et al., *Future directions of bone-targeted therapy for metastatic breast cancer.* Nat Rev Clin Oncol, 2010. **7**(11): p. 641-51.
36. Hussein, O., K. Tiedemann, and S.V. Komarova, *Breast cancer cells inhibit spontaneous and bisphosphonate-induced osteoclast apoptosis.* Bone, 2011. **48**(2): p. 202-11.
37. Roodman, G.D., *Regulation of osteoclast differentiation.* Ann N Y Acad Sci, 2006. **1068**: p. 100-9.
38. Boyle, W.J., W.S. Simonet, and D.L. Lacey, *Osteoclast differentiation and activation.* Nature, 2003. **423**(6937): p. 337-42.
39. Bendre, M.S., et al., *Tumor-derived interleukin-8 stimulates osteolysis independent of the receptor activator of nuclear factor-kappaB ligand pathway.* Cancer Res, 2005. **65**(23): p. 11001-9.
40. Sims, N.A., et al., *Interleukin-11 receptor signaling is required for normal bone remodeling.* J Bone Miner Res, 2005. **20**(7): p. 1093-102.
41. McHugh, K.P., et al., *Mice lacking beta3 integrins are osteosclerotic because of dysfunctional osteoclasts.* J Clin Invest, 2000. **105**(4): p. 433-40.
42. Teitelbaum, S.L. and F.P. Ross, *Genetic regulation of osteoclast development and function.* Nat Rev Genet, 2003. **4**(8): p. 638-49.

43. Wilson, S.R., et al., *Cathepsin K activity-dependent regulation of osteoclast actin ring formation and bone resorption.* J Biol Chem, 2009. **284**(4): p. 2584-92.
44. van der, P., et al., *Attachment characteristics and involvement of integrins in adhesion of breast cancer cell lines to extracellular bone matrix components.* Lab Invest, 1997. **77**(6): p. 665-75.
45. Kawa-Uchi, T., et al., *Messenger RNA expression of the genes encoding receptors for bone morphogenetic protein (BMP) and transforming growth factor-beta (TGF-beta) in the cells from the posterior longitudinal ligament in cervical spine.* Endocrine, 1996. **5**(3): p. 307-14.
46. Watson, P.H., et al., *Enhanced osteoblast development after continuous infusion of hPTH(1-84) in the rat.* Bone, 1999. **24**(2): p. 89-94.
47. Komori, T., et al., *Targeted disruption of Cbfa1 results in a complete lack of bone formation owing to maturational arrest of osteoblasts.* Cell, 1997. **89**(5): p. 755-64.
48. Weitzmann, M.N., et al., *T cell activation induces human osteoclast formation via receptor activator of nuclear factor kappaB ligand-dependent and -independent mechanisms.* J Bone Miner Res, 2001. **16**(2): p. 328-37.
49. Phadke, P.A., et al., *Kinetics of metastatic breast cancer cell trafficking in bone.* Clin Cancer Res, 2006. **12**(5): p. 1431-40.
50. Kozlow, W. and T.A. Guise, *Breast cancer metastasis to bone: mechanisms of osteolysis and implications for therapy.* J Mammary Gland Biol Neoplasia, 2005. **10**(2): p. 169-80.
51. Park, B.K., et al., *NF-kappaB in breast cancer cells promotes osteolytic bone metastasis by inducing osteoclastogenesis via GM-CSF.* Nat Med, 2007. **13**(1): p. 62-9.
52. Lieschke, G.J., et al., *Mice lacking both macrophage- and granulocyte-macrophage colony-stimulating factor have macrophages and coexistent osteopetrosis and severe lung disease.* Blood, 1994. **84**(1): p. 27-35.
53. Lei, S.F., et al., *An in vivo genome wide gene expression study of circulating monocytes suggested GBP1, STAT1 and CXCL10 as novel risk genes for the differentiation of peak bone mass.* Bone, 2009. **44**(5): p. 1010-4.
54. Gallet, M., et al., *Breast cancer cell line MDA-MB 231 exerts a potent and direct anti-apoptotic effect on mature osteoclasts.* Biochem Biophys Res Commun, 2004. **319**(2): p. 690-6.
55. Yin, J.J., et al., *TGF-beta signaling blockade inhibits PTHrP secretion by breast cancer cells and bone metastases development.* J Clin Invest, 1999. **103**(2): p. 197-206.
56. Courtney, K.D., R.B. Corcoran, and J.A. Engelman, *The PI3K pathway as drug target in human cancer.* J Clin Oncol, 2010. **28**(6): p. 1075-83.
57. van der Heijden, M.S. and R. Bernards, *Inhibition of the PI3K pathway: hope we can believe in?* Clin Cancer Res, 2010. **16**(12): p. 3094-9.
58. Brugge, J., M.C. Hung, and G.B. Mills, *A new mutational AKTivation in the PI3K pathway.* Cancer Cell, 2007. **12**(2): p. 104-7.
59. Reis-Filho, J.S., et al., *Metaplastic breast carcinomas exhibit EGFR, but not HER2, gene amplification and overexpression: immunohistochemical and chromogenic in situ hybridization analysis.* Breast Cancer Res, 2005. **7**(6): p. R1028-35.
60. von Lintig, F.C., et al., *Ras activation in human breast cancer.* Breast Cancer Res Treat, 2000. **62**(1): p. 51-62.

61. Toyama, S., et al., *Inhibitory effects of ZSTK474, a novel phosphoinositide 3-kinase inhibitor, on osteoclasts and collagen-induced arthritis in mice.* Arthritis Res Ther, 2010. **12**(3): p. R92.
62. Omerovic, J., A.J. Laude, and I.A. Prior, *Ras proteins: paradigms for compartmentalised and isoform-specific signalling.* Cell Mol Life Sci, 2007. **64**(19-20): p. 2575-89.
63. Keller, J.W., et al., *Oncogenic KRAS provides a uniquely powerful and variable oncogenic contribution among RAS family members in the colonic epithelium.* J Cell Physiol, 2007. **210**(3): p. 740-9.
64. Chang, F., et al., *Signal transduction mediated by the Ras/Raf/MEK/ERK pathway from cytokine receptors to transcription factors: potential targeting for therapeutic intervention.* Leukemia, 2003. **17**(7): p. 1263-93.
65. Thompson, N. and J. Lyons, *Recent progress in targeting the Raf/MEK/ERK pathway with inhibitors in cancer drug discovery.* Curr Opin Pharmacol, 2005. **5**(4): p. 350-6.
66. McCubrey, J.A., et al., *Roles of the Raf/MEK/ERK pathway in cell growth, malignant transformation and drug resistance.* Biochim Biophys Acta, 2007. **1773**(8): p. 1263-84.
67. Steelman, L.S., et al., *Roles of the Raf/MEK/ERK and PI3K/PTEN/Akt/mTOR pathways in controlling growth and sensitivity to therapy-implications for cancer and aging.* Aging (Albany NY), 2011. **3**(3): p. 192-222.
68. Karnoub, A.E. and R.A. Weinberg, *Ras oncogenes: split personalities.* Nat Rev Mol Cell Biol, 2008. **9**(7): p. 517-31.
69. McCubrey, J.A., et al., *Roles of the RAF/MEK/ERK and PI3K/PTEN/AKT pathways in malignant transformation and drug resistance.* Adv Enzyme Regul, 2006. **46**: p. 249-79.
70. Patsialou, A., et al., *Invasion of human breast cancer cells in vivo requires both paracrine and autocrine loops involving the colony-stimulating factor-1 receptor.* Cancer Res, 2009. **69**(24): p. 9498-506.
71. Nickerson, N.K., et al., *Decreased autocrine EGFR signaling in metastatic breast cancer cells inhibits tumor growth in bone and mammary fat pad.* PLoS One, 2012. **7**(1): p. e30255.
72. Breitkreutz, I., et al., *Targeting MEK1/2 blocks osteoclast differentiation, function and cytokine secretion in multiple myeloma.* Br J Haematol, 2007. **139**(1): p. 55-63.
73. Bradley, E.W., et al., *Pathway crosstalk between Ras/Raf and PI3K in promotion of M-CSF-induced MEK/ERK-mediated osteoclast survival.* J Cell Biochem, 2008. **104**(4): p. 1439-51.
74. Chappell, W.H., et al., *Ras/Raf/MEK/ERK and PI3K/PTEN/Akt/mTOR inhibitors: rationale and importance to inhibiting these pathways in human health.* Oncotarget, 2011. **2**(3): p. 135-64.
75. Pacold, M.E., et al., *Crystal structure and functional analysis of Ras binding to its effector phosphoinositide 3-kinase gamma.* Cell, 2000. **103**(6): p. 931-43.
76. Moelling, K., et al., *Regulation of Raf-Akt Cross-talk.* J Biol Chem, 2002. **277**(34): p. 31099-106.
77. Wan, X., et al., *Rapamycin induces feedback activation of Akt signaling through an IGF-1R-dependent mechanism.* Oncogene, 2007. **26**(13): p. 1932-40.
78. Chen, X.G., et al., *Rapamycin regulates Akt and ERK phosphorylation through mTORC1 and mTORC2 signaling pathways.* Mol Carcinog, 2010. **49**(6): p. 603-10.

79. Mirzoeva, O.K., et al., *Basal subtype and MAPK/ERK kinase (MEK)-phosphoinositide 3-kinase feedback signaling determine susceptibility of breast cancer cells to MEK inhibition.* Cancer Res, 2009. **69**(2): p. 565-72.
80. Hoeflich, K.P., et al., *In vivo antitumor activity of MEK and phosphatidylinositol 3-kinase inhibitors in basal-like breast cancer models.* Clin Cancer Res, 2009. **15**(14): p. 4649-64.
81. Maira, S.M., et al., *Identification and characterization of NVP-BEZ235, a new orally available dual phosphatidylinositol 3-kinase/mammalian target of rapamycin inhibitor with potent in vivo antitumor activity.* Mol Cancer Ther, 2008. **7**(7): p. 1851-63.
82. Wagner, A.J., et al., *A first-in-human phase I study to evaluate the pan-PI3K inhibitor GDC-0941 administered QD or BID in patients with advanced solid tumors.* Journal of Clinical Oncology, 2009. **27**(15).
83. Jimeno, A., et al., *Phase I trial of PX-866, a novel phosphoinositide-3-kinase (PI-3K) inhibitor.* Journal of Clinical Oncology, 2009. **27**(15).
84. Tolcher, A.W., et al., *A phase I study of MK-2206, an oral potent allosteric Akt inhibitor (Akti), in patients (pts) with advanced solid tumor (ST).* Journal of Clinical Oncology, 2009. **27**(15).
85. Wipf, P., et al., *Synthesis and biological evaluation of synthetic viridins derived from C(20)-heteroalkylation of the steroidal PI-3-kinase inhibitor wortmannin.* Organic & Biomolecular Chemistry, 2004. **2**(13): p. 1911-1920.
86. Ihle, N.T., et al., *Molecular pharmacology and antitumor activity of PX-866, a novel inhibitor of phosphoinositide-3-kinase signaling.* Mol Cancer Ther, 2004. **3**(7): p. 763-72.
87. Koul, D., et al., *Cellular and in vivo activity of a novel PI3K inhibitor, PX-866, against human glioblastoma.* Neuro Oncol, 2010. **12**(6): p. 559-69.
88. Ihle, N.T., et al., *The phosphatidylinositol-3-kinase inhibitor PX-866 overcomes resistance to the epidermal growth factor receptor inhibitor gefitinib in A-549 human non-small cell lung cancer xenografts.* Mol Cancer Ther, 2005. **4**(9): p. 1349-57.
89. Hong, D.S., et al., *A Multicenter Phase I Trial of PX-866, an Oral Irreversible Phosphatidylinositol 3-Kinase Inhibitor, in Patients with Advanced Solid Tumors.* Clin Cancer Res, 2012. **18**(15): p. 4173-82.
90. Rinehart, J., et al., *Multicenter phase II study of the oral MEK inhibitor, CI-1040, in patients with advanced non-small-cell lung, breast, colon, and pancreatic cancer.* J Clin Oncol, 2004. **22**(22): p. 4456-62.
91. Wang, D., et al., *Clinical experience of MEK inhibitors in cancer therapy.* Biochim Biophys Acta, 2007. **1773**(8): p. 1248-55.
92. Yeh, T.C., et al., *Biological characterization of ARRY-142886 (AZD6244), a potent, highly selective mitogen-activated protein kinase kinase 1/2 inhibitor.* Clin Cancer Res, 2007. **13**(5): p. 1576-83.
93. Denton, C.L. and D.L. Gustafson, *Pharmacokinetics and pharmacodynamics of AZD6244 (ARRY-142886) in tumor-bearing nude mice.* Cancer Chemother Pharmacol, 2011. **67**(2): p. 349-60.
94. Davies, B.R., et al., *AZD6244 (ARRY-142886), a potent inhibitor of mitogen-activated protein kinase/extracellular signal-regulated kinase kinase 1/2 kinases: mechanism of action in vivo, pharmacokinetic/pharmacodynamic relationship, and potential for combination in preclinical models.* Mol Cancer Ther, 2007. **6**(8): p. 2209-19.

95. Meng, J., et al., *Apoptosis induction by MEK inhibition in human lung cancer cells is mediated by Bim.* PLoS One, 2010. **5**(9): p. e13026.
96. Garon, E.B., et al., *Identification of Common Predictive Markers of In vitro Response to the Mek Inhibitor Selumetinib (AZD6244; ARRY-142886) in Human Breast Cancer and Non-Small Cell Lung Cancer Cell Lines.* Molecular Cancer Therapeutics, 2010. **9**(7): p. 1985-1994.
97. Bondareva, A., et al., *The lysyl oxidase inhibitor, beta-aminopropionitrile, diminishes the metastatic colonization potential of circulating breast cancer cells.* PLoS One, 2009. **4**(5): p. e5620.
98. Chambers, A.F., A.C. Groom, and I.C. MacDonald, *Dissemination and growth of cancer cells in metastatic sites.* Nat Rev Cancer, 2002. **2**(8): p. 563-72.
99. Lu, X. and Y. Kang, *Organotropism of breast cancer metastasis.* J Mammary Gland Biol Neoplasia, 2007. **12**(2-3): p. 153-62.
100. Gupta, G.P. and J. Massague, *Cancer metastasis: building a framework.* Cell, 2006. **127**(4): p. 679-95.
101. Lopez-Knowles, E., et al., *PI3K pathway activation in breast cancer is associated with the basal-like phenotype and cancer-specific mortality.* Int J Cancer, 2010. **126**(5): p. 1121-31.
102. Howes, A.L., et al., *The phosphatidylinositol 3-kinase inhibitor, PX-866, is a potent inhibitor of cancer cell motility and growth in three-dimensional cultures.* Mol Cancer Ther, 2007. **6**(9): p. 2505-14.
103. Ihle, N.T., et al., *Mutations in the phosphatidylinositol-3-kinase pathway predict for antitumor activity of the inhibitor PX-866 whereas oncogenic Ras is a dominant predictor for resistance.* Cancer Res, 2009. **69**(1): p. 143-50.
104. Eckert, L.B., et al., *Involvement of Ras activation in human breast cancer cell signaling, invasion, and anoikis.* Cancer Res, 2004. **64**(13): p. 4585-92.
105. Li, R. and J.A. Stafford, *Kinase inhibitor drugs*. Wiley series in drug discovery and development. 2009, Hoboken, N.J.: Wiley. xv, 510 p., 16 p. of plates.
106. Adjei, A.A., et al., *Phase I pharmacokinetic and pharmacodynamic study of the oral, small-molecule mitogen-activated protein kinase kinase 1/2 inhibitor AZD6244 (ARRY-142886) in patients with advanced cancers.* J Clin Oncol, 2008. **26**(13): p. 2139-46.
107. Wee, S., et al., *PI3K pathway activation mediates resistance to MEK inhibitors in KRAS mutant cancers.* Cancer Res, 2009. **69**(10): p. 4286-93.
108. Moon, J.B., et al., *Akt induces osteoclast differentiation through regulating the GSK3beta/NFATc1 signaling cascade.* J Immunol, 2012. **188**(1): p. 163-9.
109. Lee, S.E., et al., *The phosphatidylinositol 3-kinase, p38, and extracellular signal-regulated kinase pathways are involved in osteoclast differentiation.* Bone, 2002. **30**(1): p. 71-7.
110. Gingery, A., et al., *Phosphatidylinositol 3-kinase coordinately activates the MEK/ERK and AKT/NFkappaB pathways to maintain osteoclast survival.* J Cell Biochem, 2003. **89**(1): p. 165-79.
111. Hiraga, T., et al., *Suppression of IGF signaling propagation and NF-kappa B activation reduces bone metastases in breast cancer.* Journal of Bone and Mineral Research, 2001. **16**: p. S200-S200.

112. Meloche, S. and J. Pouyssegur, *The ERK1/2 mitogen-activated protein kinase pathway as a master regulator of the G1- to S-phase transition.* Oncogene, 2007. **26**(22): p. 3227-39.
113. Bratton, D.L., et al., *Appearance of phosphatidylserine on apoptotic cells requires calcium-mediated nonspecific flip-flop and is enhanced by loss of the aminophospholipid translocase.* J Biol Chem, 1997. **272**(42): p. 26159-65.
114. Sawai, H. and N. Domae, *Discrimination between primary necrosis and apoptosis by necrostatin-1 in Annexin V-positive/propidium iodide-negative cells.* Biochem Biophys Res Commun, 2011. **411**(3): p. 569-73.
115. Hirbe, A.C., et al., *Granulocyte colony-stimulating factor enhances bone tumor growth in mice in an osteoclast-dependent manner.* Blood, 2007. **109**(8): p. 3424-31.
116. Craig, M.J. and R.D. Loberg, *CCL2 (Monocyte Chemoattractant Protein-1) in cancer bone metastases.* Cancer Metastasis Rev, 2006. **25**(4): p. 611-9.
117. Bendre, M.S., et al., *Interleukin-8 stimulation of osteoclastogenesis and bone resorption is a mechanism for the increased osteolysis of metastatic bone disease.* Bone, 2003. **33**(1): p. 28-37.
118. Singh, B., et al., *Involvement of IL-8 in COX-2-mediated bone metastases from breast cancer.* J Surg Res, 2006. **134**(1): p. 44-51.
119. Benoy, I.H., et al., *Increased serum interleukin-8 in patients with early and metastatic breast cancer correlates with early dissemination and survival.* Clin Cancer Res, 2004. **10**(21): p. 7157-62.
120. Foley, J., et al., *EGFR signaling in breast cancer: bad to the bone.* Semin Cell Dev Biol, 2010. **21**(9): p. 951-60.
121. Fritz, V., et al., *Micro-CT combined with bioluminescence imaging: a dynamic approach to detect early tumor-bone interaction in a tumor osteolysis murine model.* Bone, 2007. **40**(4): p. 1032-40.
122. Haba, Y., et al., *Relationship between mechanical properties and bone mineral density of human femoral bone retrieved from patients with osteoarthritis.* Open Orthop J, 2012. **6**: p. 458-63.
123. Gundersen, H.J., et al., *The Conneulor: unbiased estimation of connectivity using physical disectors under projection.* Bone, 1993. **14**(3): p. 217-22.
124. Feldkamp, L.A., et al., *The direct examination of three-dimensional bone architecture in vitro by computed tomography.* J Bone Miner Res, 1989. **4**(1): p. 3-11.
125. Kim, D.G., et al., *The effect of microcomputed tomography scanning and reconstruction voxel size on the accuracy of stereological measurements in human cancellous bone.* Bone, 2004. **35**(6): p. 1375-82.
126. Odgaard, A., *Three-dimensional methods for quantification of cancellous bone architecture.* Bone, 1997. **20**(4): p. 315-28.
127. Zheng, Y., et al., *Phospholipase D couples survival and migration signals in stress response of human cancer cells.* J Biol Chem, 2006. **281**(23): p. 15862-8.
128. Porter, A.G. and R.U. Janicke, *Emerging roles of caspase-3 in apoptosis.* Cell Death Differ, 1999. **6**(2): p. 99-104.
129. Elmore, S., *Apoptosis: a review of programmed cell death.* Toxicol Pathol, 2007. **35**(4): p. 495-516.

130. Lakkakorpi, P.T., et al., *Phosphatidylinositol 3-kinase association with the osteoclast cytoskeleton, and its involvement in osteoclast attachment and spreading.* Exp Cell Res, 1997. **237**(2): p. 296-306.
131. Pilkington, M.F., S.M. Sims, and S.J. Dixon, *Wortmannin inhibits spreading and chemotaxis of rat osteoclasts in vitro.* J Bone Miner Res, 1998. **13**(4): p. 688-94.
132. Nakamura, I., et al., *Wortmannin, a specific inhibitor of phosphatidylinositol-3 kinase, blocks osteoclastic bone resorption.* FEBS Lett, 1995. **361**(1): p. 79-84.
133. Lee, S.E., et al., *The phosphatidylinositol 3-kinase, p38, and extracellular signal-regulated kinase pathways are involved in osteoclast differentiation.* Bone, 2002. **30**(1): p. 71-77.
134. Nakamura, H., et al., *Role of osteoclast extracellular signal-regulated kinase (ERK) in cell survival and maintenance of cell polarity.* J Bone Miner Res, 2003. **18**(7): p. 1198-205.
135. Singer, C.F., et al., *HER2 overexpression and activation, and tamoxifen efficacy in receptor-positive early breast cancer.* J Cancer Res Clin Oncol, 2009. **135**(6): p. 807-13.
136. Datta, D., et al., *Ras-induced modulation of CXCL10 and its receptor splice variant CXCR3-B in MDA-MB-435 and MCF-7 cells: relevance for the development of human breast cancer.* Cancer Res, 2006. **66**(19): p. 9509-18.
137. Hui, L., et al., *Mutant p53 in MDA-MB-231 breast cancer cells is stabilized by elevated phospholipase D activity and contributes to survival signals generated by phospholipase D.* Oncogene, 2006. **25**(55): p. 7305-10.
138. Strano, S., et al., *Mutant p53 proteins: between loss and gain of function.* Head Neck, 2007. **29**(5): p. 488-96.
139. Mazars, R., et al., *p53 mutations occur in aggressive breast cancer.* Cancer Res, 1992. **52**(14): p. 3918-23.
140. Kang, D.W., et al., *Autoregulation of phospholipase D activity is coupled to selective induction of phospholipase D1 expression to promote invasion of breast cancer cells.* Int J Cancer, 2011. **128**(4): p. 805-16.
141. Hendrickson, A.W., X.W. Meng, and S.H. Kaufmann, *Anticancer therapy: boosting the bang of Bim.* J Clin Invest, 2008. **118**(11): p. 3582-4.
142. Oakes, S.R., et al., *Sensitization of BCL-2-expressing breast tumors to chemotherapy by the BH3 mimetic ABT-737.* Proc Natl Acad Sci U S A, 2012. **109**(8): p. 2766-71.
143. Cragg, M.S., et al., *Treatment of B-RAF mutant human tumor cells with a MEK inhibitor requires Bim and is enhanced by a BH3 mimetic.* J Clin Invest, 2008. **118**(11): p. 3651-9.
144. Muranen, T., et al., *Inhibition of PI3K/mTOR leads to adaptive resistance in matrix-attached cancer cells.* Cancer Cell, 2012. **21**(2): p. 227-39.
145. Hemann, M.T. and S.W. Lowe, *The p53-Bcl-2 connection.* Cell Death Differ, 2006. **13**(8): p. 1256-9.
146. Pratt, M.A., et al., *Cytoplasmic mutant p53 increases Bcl-2 expression in estrogen receptor-positive breast cancer cells.* Apoptosis, 2007. **12**(4): p. 657-69.
147. Kim, H.S., et al., *Clinical significance of a serum CA15-3 surge and the usefulness of CA15-3 kinetics in monitoring chemotherapy response in patients with metastatic breast cancer.* Breast Cancer Res Treat, 2009. **118**(1): p. 89-97.
148. De La Lande, B., et al., *Prognostic value of CA 15.3 kinetics for metastatic breast cancer.* Int J Biol Markers, 2002. **17**(4): p. 231-8.

149. Kiang, D.T., et al., *Alternating chemotherapy regimens for patients with metastatic breast cancer. A pilot study based on tumor marker kinetics. Cancer and Leukemia Group B.* Cancer, 1995. **75**(3): p. 826-30.
150. Robinson, R.G., et al., *Strontium-89: treatment results and kinetics in patients with painful metastatic prostate and breast cancer in bone.* Radiographics, 1989. **9**(2): p. 271-81.
151. Matsushita, T., et al., *Extracellular signal-regulated kinase 1 (ERK1) and ERK2 play essential roles in osteoblast differentiation and in supporting osteoclastogenesis.* Mol Cell Biol, 2009. **29**(21): p. 5843-57.
152. Kawamura, N., et al., *Akt1 in osteoblasts and osteoclasts controls bone remodeling.* PLoS One, 2007. **2**(10): p. e1058.
153. Mukherjee, A. and P. Rotwein, *Selective signaling by Akt1 controls osteoblast differentiation and osteoblast-mediated osteoclast development.* Mol Cell Biol, 2012. **32**(2): p. 490-500.
154. Glantschnig, H., et al., *M-CSF, TNFalpha and RANK ligand promote osteoclast survival by signaling through mTOR/S6 kinase.* Cell Death Differ, 2003. **10**(10): p. 1165-77.
155. Ulici, V., et al., *The PI3K pathway regulates endochondral bone growth through control of hypertrophic chondrocyte differentiation.* BMC Dev Biol, 2008. **8**: p. 40.
156. Bobick, B.E. and W.M. Kulyk, *The MEK-ERK signaling pathway is a negative regulator of cartilage-specific gene expression in embryonic limb mesenchyme.* J Biol Chem, 2004. **279**(6): p. 4588-95.
157. Redlich, K., et al., *Osteoclasts are essential for TNF-alpha-mediated joint destruction.* J Clin Invest, 2002. **110**(10): p. 1419-27.
158. Farhana, L., et al., *Apoptosis signaling by the novel compound 3-Cl-AHPC involves increased EGFR proteolysis and accompanying decreased phosphatidylinositol 3-kinase and AKT kinase activities.* Oncogene, 2004. **23**(10): p. 1874-84.
159. Ford-Hutchinson, A.F., et al., *Inactivation of Pten in osteo-chondroprogenitor cells leads to epiphyseal growth plate abnormalities and skeletal overgrowth.* J Bone Miner Res, 2007. **22**(8): p. 1245-59.
160. Murakami, S., et al., *Constitutive activation of MEK1 in chondrocytes causes Stat1-independent achondroplasia-like dwarfism and rescues the Fgfr3-deficient mouse phenotype.* Genes Dev, 2004. **18**(3): p. 290-305.
161. Pelleitier, M. and S. Montplaisir, *The nude mouse: a model of deficient T-cell function.* Methods Achiev Exp Pathol, 1975. **7**: p. 149-66.
162. Helliwell, P.A., et al., *Regulation of GLUT5, GLUT2 and intestinal brush-border fructose absorption by the extracellular signal-regulated kinase, p38 mitogen-activated kinase and phosphatidylinositol 3-kinase intracellular signalling pathways: implications for adaptation to diabetes.* Biochem J, 2000. **350 Pt 1**: p. 163-9.
163. Rexer, B.N., R. Ghosh, and C.L. Arteaga, *Inhibition of PI3K and MEK: it is all about combinations and biomarkers.* Clin Cancer Res, 2009. **15**(14): p. 4518-20.
164. Pelicano, H., et al., *Glycolysis inhibition for anticancer treatment.* Oncogene, 2006. **25**(34): p. 4633-46.
165. Strano, S., et al., *Mutant p53: an oncogenic transcription factor.* Oncogene, 2007. **26**(15): p. 2212-9.

166. Shan, G., *RNA interference as a gene knockdown technique.* Int J Biochem Cell Biol, 2010. **42**(8): p. 1243-51.
167. Isalan, M., *Zinc-finger nucleases: how to play two good hands.* Nat Methods, 2012. **9**(1): p. 32-4.
168. Herrmann, F., et al., *p53 Gene repair with zinc finger nucleases optimised by yeast 1-hybrid and validated by Solexa sequencing.* PLoS One, 2011. **6**(6): p. e20913.
169. Tiwary, R., et al., *alpha-TEA cooperates with chemotherapeutic agents to induce apoptosis of p53 mutant, triple-negative human breast cancer cells via activating p73.* Breast Cancer Res, 2011. **13**(1): p. R1.
170. Kravchenko, J.E., et al., *Small-molecule RETRA suppresses mutant p53-bearing cancer cells through a p73-dependent salvage pathway.* Proc Natl Acad Sci U S A, 2008. **105**(17): p. 6302-7.
171. Sauer, B., *Inducible gene targeting in mice using the Cre/lox system.* Methods, 1998. **14**(4): p. 381-92.